PARTS OF THE ORIGINAL DOCUMENT

ARE OF POOR REPRODUCTIVE QUALITY

CERTAINES PARTIES DU DOCUMENT ORIGINAL

SONT DE PIÈTRE QUALITÉ DE REPRODUCTION

TP 7508E

MAGNETOENCEPHALOGRAPHIC SIGNALS: Source Localization

Prepared for the
Transportation
Development Centre
Transport Canada

by

H. Weinberg

Brain Behavior Laboratory
Simon Fraser University
Burnaby, British Columbia
V5A 1S6

February 1987

1987

The contents of this report reflect the opinions of the authors and not necessarily the official views or opinions of the Transportation Development Centre.

Un sommaire en français de ce document est inclus avant la table des matières.

PROJECT TEAM

H. Weinberg, Ph.D., Professor and Director,
Brain Behaviour Laboratory, Simon Fraser University
Professor, Imaging Centre, University of British Columbia
Adjunct Professor, University of British Columbia

A. Robertson, Ph.D., Visiting Fellow
Brian Behavior Laboratory Simon Fraser University

P. Brickett, Ph.D., Adjunct Professor
Brain Behaviour Laboratory, Simon Fraser University

D. Cheyne, M.A., Graduate Assistant
Brain Behaviour Laboratory, Simon Fraser University

R. Harrop, Ph.D., Professor
Brain Behaviour Laboratory, Simon Fraser University
Dpt. Computing Sciences, Simon Fraser University
Dpt. Mathematics, Simon Fraser University
Imaging Centre, University of British Columbia

C. Dykstra, B.A.
Brain Behaviour Laboratory, Simon Fraser University

M. Baff, B.S.
Brain Behaviour Laboratory, Simon Fraser University

Transport Canada / Transports Canada

Development / Developpement

REPORT DOCUMENTATION FORM

1. Transport Canada Report No.	2. TDC Project No.	3. Recipient's Catalogue No.
TP 7508E	6016	

4. Title and Subtitle	5. Report Date
Magnetoencephalographic Signals: Source Localization	February 1987
	6. Performing Organization Report No.

7. Author(s)	8. Transport Canada File No.
Dr. H. Weinberg	D1450-146-2

9. Performing Organization Name and Address	10. DSS File No.
Brain Behavior Laboratory Department of Psychology Simon Fraser University Burnaby, British Columbia V5A 1S5	T8200-3-3601
	11. DSS or Transport Canada Contract No
	1ST83-00196

12. Sponsoring Agency Name and Address	13. Type of Report and Period Covered
Transportation Development Centre (TDC) 200 Dorchester Blvd. West Suite 601, West Tower Montreal, Quebec H2Z 1X4	14. Sponsoring Agency Code 6016

15. Supplementary Notes	16. TDC Project Officer
	Dr. R. Heron/ J.E. Laframboise

17. Abstract

Simultaneous Electroencephalographic (EEG) and Magnetoencephalographic (MEG) recordings were made of brain bioelectric and biomagnetic fields with subjects performing visual discrimination and categorization of moving targets having different probabilities of occurrence, as happens during air controller operations.

Magnetic field distributions were used to estimate the most probable location of intracranial dipole sources responsible for observed differences in response between images identified as targets and non-targets.

The outcome of the experiment showed that the EEG indicated a bioelectric event 600 ms after a target stimulus but none following a non-target, while the MEG indicated the existence of a different set of simultaneous intracranial current dipole sources associated with each of the two target conditions.

18. Key Words	19. Distribution Statement
Air traffic control, brain response, visual discrimination, electroencephalographic, magnetoencephalographic, EEG, MEG	A limited number of copies are available from the Transportation Development Centre.

20. Security Classification (of this report)	21. Security Classification (of this page)	22. No. of Pages	23. Price
Unclassified	Unclassified	-	-

Canada v

Transports Canada Transport Canada

Développement Development

FORMULE DOCUMENTAIRE DU RAPPORT

1. N° du rapport Transports Canada	2. N° de l'étude — CDT	3. N° de catalogue du destinataire
4. Titre et sous-titre		5. Date du rapport
		6. N° du rapport de l'organisme exécutant
7. Auteur(s)		8. N° de dossier Transports Canada
9. Nom et adresse de l'organisme exécutant		10. N° de dossier — ASC
		11. N° de contrat — ASC ou Transports Canada
12. Nom et adresse de l'organisme parrain		13. Genre de rapport et période visée
		14. Code de l'organisme parrain
15. Remarques additionnelles		16. Agent de projet — CDT

17. Résumé

18. Mots-clés	19. Diffusion

20. Classification de sécurité (de ce rapport)	21. Classification de sécurité (de cette page)	22. Nombre de pages	23. Prix

CDT/TDC 79-005
Rev 86

Canada

Transport Canada / Transports Canada

Development / Développement

REPORT DOCUMENTATION FORM

1. Transport Canada Report No.	2. TDC Project No.	3. Recipient's Catalogue No.
TP 7508E	6016	

4. Title and Subtitle	5. Report Date
Magnetoencephalographic Signals: Source Localization	Février 1987
	6. Performing Organization Report No.
7. Author(s)	8. Transport Canada File No.
Dr. H. Weinberg	D1450-146-2
9. Performing Organization Name and Address	10. DSS File No.
Brain Behavior Laboratory Department of Psychology Simon Fraser University Burnaby (Colombie-Britannique) V5A 1S5	T8200-3-3601
	11. DSS or Transport Canada Contract No.
	1ST83-00196
12. Sponsoring Agency Name and Address	13. Type of Report and Period Covered
Centre de développement des transports (CDT) 200 ouest, boul. Dorchester Suite 601, tour ouest Montréal (Québec) H2Z 1X4	
	14. Sponsoring Agency Code 6016
15. Supplementary Notes	16. TDC Project Officer Dr. R. Heron/ J.E. Laframboise

17. Abstract

Des enregistrements ont été faits simultanément par électroencéphalographie (EEG) et par magnétoencéphalographie (MEG) relativement aux champs bioélectriques et biomagnétiques du cerveau de sujets tentant de faire une discrimination visuelle et d'identifier des cibles en mouvement apparaissant à intervalles différents, comme cela se produit dans les opérations de contrôle de la circulation aérienne.

La répartition du champ magnétique a été utilisée pour calculer la situation la plus probable dans le cerveau des sources de dipôles responsables des réponses différentes suivant que l'image identifiée est une cible ou non.

Les résultats de l'expérience montrent que l'EEG indique un événement bioélectrique 600 ms après un stimulus provoqué par une cible et aucun événement lorsque le stimulus n'est pas provoqué par une cible. Le MEG indique l'existence de sources différentes de dipôles se produisant simultanément dans le cerveau et qui sont associés à chacun des deux types de cible.

18. Key Words	19. Distribution Statement
Contrôle de la circulation aérienne, réponse cérébrale, discrimination visuelle, électroencéphalographie, magnétoencéphalographie, EEG, MEG.	Le Centre de développement des transports dispose d'un nombre limité d'exemplaires.

20. Security Classification (of this report)	21. Security Classification (of this page)	22. No. of Pages	23. Price
non classifié	non classifiée	-	-

TDC CDT 79-005
Rev 86

Transports Canada / Transport Canada

Développement / Development

FORMULE DOCUMENTAIRE DU RAPPORT

1. N° du rapport Transports Canada	2. N° de l'étude — CDT	3. N° de catalogue du destinataire
4. Titre et sous-titre		5. Date du rapport
		6. N° du rapport de l'organisme exécutant
7. Auteur(s)		8. N° de dossier Transports Canada
9. Nom et adresse de l'organisme exécutant		10. N° de dossier — ASC
		11. N° de contrat — ASC ou Transports Canada
12. Nom et adresse de l'organisme parrain		13. Genre de rapport et période visée
		14. Code de l'organisme parrain
15. Remarques additionnelles		16. Agent de projet — CDT

17. Résumé

18. Mots-clés	19. Diffusion		
20. Classification de sécurité (de ce rapport)	21. Classification de sécurité (de cette page)	22. Nombre de pages	23. Prix

CDT/TDC 79-005
Rev 86

Canada

SUMMARY

As the result of a new technology developed in the 1970's, the first magnetic fields of the brain were measured in 1972. This technology continued to develop and in 1980 C.T.F. Systems, Inc., of British Columbia, constructed the first third-order gradiometer. This instrument was capable of discriminating very small magnetic signals of biological origin from magnetic noise of much higher levels within the normal environments of laboratories and hospitals.

The advancement of this technology resulted in the real possibility that electrical current sources of the brain could be imaged with greater accuracy than was possible previously. The location and identification of current sources in the brain is important for several theoretical reasons and has important implications for the application of the technology to human-factors.

For many years there has been developing a large body of research into the ways in which electrical potentials recorded from the scalp index memory processes and performance. However, a critical link was missing in the understanding of the genesis of these electrical potentials. It is necessary to know how brain physiology and anatomy generate these electrical potentials. A knowledge of precisely which structures in the brain are responsible for memory, information processing and the programming of movements has widespread implications for assessment, prediction and control of behaviour.

In 1983 the Brain Behavior Laboratory under the direction of H. Weinberg and C.T.F. Systems Inc. approached the Provincial Government of British Columbia, the National Research Council and the Transportation Development Centre with a proposal (a) to build a computerized robotics system for scanning magnetic fields of biological origin, (b) to develop mapping and analytic procedures for locating the brain sources of electrical potentials known to be indices of information processing and memory, and (c) to initiate studies using (a) and (b) to determine the feasibility of applying the technology for assessments of the capability to individuals to make the kind of judgements critical in flying aircraft.

The Transportation Development Centre of Transport Canada expressed an interest in (c), the NRC an interest in (b) and the Science Council of British Columbia an interest in both (a) and (b). The cooperation of these three agencies was combined to fund, in conjunction with Bridge Funding from the Department of Supply and Services, a series of studies and the development of an integrated biomagnetic system. The components of the research and development programme included:

I. The development, testing and evaluation of the scanning gantry robotics used in the study of magnetic fields of the brain.

II. Theoretical studies of methods of mapping magnetic fields of the brain and the use of that data to locate systems of sources in the brain.

III. Initial studies of the location in the brain of electrical sources associated with visual information processing of moving targets on radar screens.

The interest of the Transportation Development Centre was primarily in III, therefore I and II are summarised somewhat more briefly than III.

I. The scanning gantry system and associated techniques have been essential for the accurate location in the brain of magnetic field sources. The gantry system is constructed with special non-magnetic materials and with computer controlled stepping motors. Each step of each motor is monitored by the computer system in order to insure orderly coordination of the movement along five different axes. Several safety devices are built into the system, including the requirement that all steps of the motors be precisely phased relative to a starting position and a capacitance device located on the end of the dewar. The dewar contains liquid helium maintaining the sensing coils and the Superconducting Quantum Interference Device (SQUID) at supercooled temperatures (-269^{o}C). If the capacitance device is closer than a predefined distance from the scalp, the entire control system halts. The gantry system is able to move with five degrees of freedom with an accuracy of less than 5 mm. This means that the exact location of the sensing coils and their orientation with respect to the normal of the skull is available for computation of source location. For accurate source location it is essential to know each position of the sensing coils relative to an origin at the centre of the head. The origin is determined by a digitizing system which is part of the gantry design. This allows the gantry computer to know the exact position of both the origin and each point on the head relative to the position of the coils in the three-dimensional space of its search limits. By digitizing the head, the exact configuration of the head can be modeled, and the exact distance from each point on the head (and hence from the sensing coil) to the origin can be computed. With this knowledge the location of the source can be estimated. Furthermore, the gantry system makes it possible to automate the acquisition of data and send the sensing coils to any sequence of predefined positions over the head.

II. Current dipoles energised by isolated sources were located in known positions inside a human skull filled with an electrically conductive medium. Maps of the measured electrical and magnetic fields confirmed the predicted relationships between those fields for both single and multiple dipoles. Two methods of dipole localisation were compared: the peak-location method which used only the locations of the maximum and minimum recorded values, and a least-squares iterative method which found the parameters for a dipole such that the sum of squared differences between the recorded and predicted data was minimised.

Also, in an attempt to account for some of the error due to the non-sphericity of the head, the measured distance from the centre of the skull to each recording position was used in the dipole calculations. This last technique resulted in the smallest three-dimensional location error (averaging 3.5 mm) for the least-squares method, even when no recording positions were near the actual field extrema and the peak-location method therefore produced much greater error. Also investigated were combinations of two dipoles for which the magnetic field maps appeared similar to those for a single dipole and comparisons were made to determine how well single and double models could account for the recorded data.

III. There have been many reports of Event Related Potentials (ERP) associated with the perception and categorization of static visual stimuli where one stimulus class ("oddball" stimuli) occurs less frequently than another. When these "oddball" stimuli were designated as response targets, they were commonly associated with a late (300 to 600 ms) vertex-positive ERP. In the present study, dynamic visual stimuli, simulating those on a radar screen, were employed to elicit ERPs and Event Related (magnetic) Fields (ERF) using an "oddball" paradigm. The stimuli were computer generated circular and square shapes (0.4 degrees at the subject's eye) that moved across a stimulus display (4.0 degrees at the subject's eye) every one to two seconds. The shape of the stimulus for each sweep (circle or square) was chosen randomly but each shape occurred with a fixed probability during each trial of 300 sweeps (circles + squares). The stimuli entered from randomly selected points around the perimeter of the mask and moved at a constant velocity along trajectories that intersected the central fixation point which the subject fixated throughout the trial. At the beginning of "no target" trials the subject was instructed to: "fixate the centre and observe the circles and squares"; and on "target" trials to: "fixate the centre, count the circles and ignore the squares" (or vice-versa).

The Electroencephalogram (EEG) was recorded from various scalp locations from the International 10-20 System. Simultaneous MEG recordings were made with the third-order scanning gradiometer described above. The head was digitized using the procedures described in I and II and a digitized model of the subject's head was computed and stored in the computer system for control of the automated gantry system. EEG and MEG signals were amplified and digitized over 1 sec. epochs starting with the appearance of a circle or square on the stimulus monitor. On-line sweep rejection occurred when eye movements were detected.

The EEG results showed little difference in a comparison of the "no target" responses for squares and circles. However, in the two "target" conditions (target probability = .5; target probability = .3), the target responses showed substantially higher amplitudes than did the nontarget responses at frontal and midline scalp locations. Having the subject count one stimulus (target) while ignoring the other resulted in increased late (400-600 ms) positive activity for both stimuli (targets and nontargets) but lowering the probability of target appearance only resulted in marked response amplitude changes for target stimuli (Fig. 1b).

The EEG results comparing target (p=.3) and nontarget responses at frontal, midline and temporal sites showed target-versus-nontarget amplitude differences at latencies between 350 and 700 ms. Such response differences between 350 and 450 ms were most pronounced at frontal locations whereas the 600 ms response differences were approximately equal at all three recording sites. Although the subject differences were large, the MEG bears the same relationship to the conditions as does the EEG. The strong correspondences among these EEG and MEG responses at 600 ms responses suggest that the polarity reversal seen in the ERPs and the magnetic field reversal in the ERFs was related to common sources that have homologous intracranial locations.

Isocontour maps of the ERFs were constructed for 50 ms intervals following presentation of each stimulus type. The most notable differences between the target and nontarget maps for each subject were that target response magnitudes were larger and that target ERFs have a more complex distribution.

Preliminary estimates of current dipole sources for the 600 ms target and nontarget MEG scalp distributions, generated with the above procedure, suggest the existence of a different set of multiple simultaneous dipoles for each stimulus condition.

For nontarget stimuli, where the stimuli were not counted, dipole sources have been tentatively localized in the vicinities of the anterior calcarine fissures, the inferior temporal lobes and deep within the brain near the optic chiasm. Since current theories of functional brain localization would associate these approximate anatomical locations with peripheral vision, movement in the visual field and oculomotor activity (respectively), these pituitive cortical dipoles might be considered as being appropriate from a functional standpoint.

For target stimuli, where stimuli were counted covertly, dipole sources have been localized in the vicinities of the left inferior frontal gyrus (pars triangularis), the left supramarginal gyrus of the parietal lobe, deep within the right Sylvian fissure near the inferior parietal lobe and in the superior right parietal lobe posterior to the postcentral gyrus. Once again, these dipole sources are consistent with theories of functional brain localization that would associate these anatomical locations with (respectively) speech, processing sequential information (eg. counting) and performing special tasks. While these preliminary source localizations are interesting, relative to the neuroanatomical substrates expected to be involved in tasks such as these, it must be emphasised that this procedure is just under development and that the number of MEG recording positions (25) for subject TR is probably not adequate for localising four dipoles with 5 parameters each.

These initial results suggest that the temporal lobe may be the structure to monitor for the purpose of assessing the capability for discrimination of moving targets, and the judgement of temporal intervals.

SOMMAIRE

Une nouvelle technologie imaginée en 1970 a permis en 1972 de mesurer les premiers champs magnétiques du cerveau. Grâce aux perfectionnements apportés à cette technologie, C.T.F. Systems Inc. de Colombie-Britannique fabriquait en 1980 le premier gradiomètre de troisième ordre, instrument dont le pouvoir de séparation permet de reconnaître les très faibles signaux magnétiques d'origine biologique au travers du bruit magnétique, de plus forte intensité, qui parasite normalement les laboratoires et les hôpitaux.

Cette technologie améliorée a vraiment rendu possible la visualisation des sources de courant électrique du cerveau, et cela avec une précision jamais égalée. La localisation et la détermination des sources de courant dans le cerveau revêtent une grande importance pour diverses considérations théoriques et sont essentielles à l'adaptation de cette nouvelle technologie à l'étude des facteurs humains.

Pendant de nombreuses années, beaucoup de travaux ont cherché à élucider les rapports entre les potentiels électriques du cuir chevelu et les mécanismes de mémorisation et de fonctionnement. Toutefois, un chaînon essentiel manquait: la compréhension de la genèse de ces potentiels électriques. Car il faut absolument savoir, à partir de la physiologie et de l'anatomie du cerveau, comment apparaissent ces potentiels. La reconnaissance des structures responsables de la mémoire, du traitement de l'information et de la programmation des mouvements jettera un nouvel éclairage sur l'évaluation, la prévision et le contrôle du comportement.

En 1983, le laboratoire du comportement du cerveau de l'Université Simon Fraser, sous la direction de H. Weinberg et C.T.F. Systems Inc., présentait une proposition au Gouvernement provincial de la Colombie-Britannique, au Conseil national de recherches (CNR) et au Centre de développement des transports (CDT) en vue:

a) de construire un système de robotique informatisé permettant l'analyse des champs magnétiques d'origine biologique;

b) d'élaborer des procédures de cartographie et d'analyse pour la localisation des sources cérébrales de potentiels électriques reconnues comme associées au traitement de l'information et à la mémorisation; et

c) de mettre en marche des études à l'aide du système de robotique et des procédures élaborées, afin d'établir la possibilité d'appliquer ces connaissances à l'évaluation de la capacité des personnes à prendre des décisions critiques concernant la navigation aérienne.

Le Centre de développement des transports de Transports Canada s'est montré intéressé par la partie c) de la proposition, le CNR par la partie b) et le Conseil des sciences de la Colombie-Britannique par les parties a) et b). L'action concertée de ces trois organismes a permis de subventionner, conjointement avec le Fonds d'Appoint du ministère des Approvisionnements et Services, une série d'études et le développement d'un système biomagnétique intégré. Voici les composantes de ce programme de recherche et de développement:

I. La mise au point, la vérification et l'évaluation d'un portique robot à balayage pour l'étude des champs magnétiques du cerveau.

II. La poursuite d'études théoriques sur la cartographie des champs magnétiques du cerveau et le recours aux résultats de ces études pour la localisation de groupes de sources dans le cerveau.

III. L'amorce d'études sur la localisation dans le cerveau des sources de potentiels électriques qui seraient associées au traitement de l'information visuelle des mouvements de cibles sur écran radar.

Comme le Centre de développement des transports s'intéresse avant tout à la composante III, il est normal que les composantes I et II soient exposées plus succinctement que la composante III.

I. Le portique à balayage et les techniques de son utilisation sont essentiels à la localisation précise de sources de champ magnétique. Ce portique, fabriqué à partir de matériaux non magnétiques, est doté de moteurs pas à pas commandés par ordinateur. Chaque pas d'un moteur est surveillé par un système informatique afin d'assurer une coordination harmonieuse du déplacement suivant cinq axes. Plusieurs aspects sécuritaires ont été intégrés à ce système, notamment un dispositif condensateur à l'extrémité du tube dewar et la consigne que tous les pas des moteurs soient calibrés par rapport à une position de départ. Le tube dewar est plein d'hélium liquide qui garde les capteurs bobines et le dispositif d'interférence quantique supraconducteur (SQUID) à des températures près du zéro absolu (-269 degrés C). Si la distance entre le dispositif condensateur et le cuir chevelu est inférieure à une distance fixée à l'avance, tout le système de contrôle s'arrête. Le portique se déplace avec cinq degrés de liberté et se place avec une précision inférieure à 5 mm. Ainsi est-il possible de calculer la position des sources d'après l'emplacement exact des capteurs bobines et de leur orientation par rapport à la normale au crâne. Pour connaître précisément la position d'une source, il faut déterminer chaque position des capteurs bobines en fonction d'une origine ou du centre de la tête. C'est un système numériseur faisant partie intégrante du portique qui établit l'origine. De cette façon, l'ordinateur du portique connaît les positions exactes de l'origine et de chacun des points de la tête relativement à la position des capteurs dans le volume tridimensionnel délimité par ses limites de recherche. La numérisation de la tête rend possible la modélisation de la configuration exacte de la tête et, de ce fait, permet de calculer la distance précise séparant chaque point de la tête (donc des capteurs) et l'origine.

À partir de tout cela, il est possible d'estimer la position de la source. De plus, avec ce portique, on peut automatiser la saisie des données et diriger les capteurs vers n'importe quelle suite de positions fixées à l'avance au-dessus de la tête.

II. Des dipôles de courant alimentés par des sources isolées sont placés à des endroits connus à l'intérieur d'un crâne humain rempli d'un milieu conducteur d'électricité. Les cartes des champs électriques et magnétiques mesurés confirment les relations prévues entre ces champs pour les dipôles simples et les dipôles multiples. On a comparé deux méthodes de localisation de dipôles: la méthode de localisation des extremums où seules les valeurs minimales et maximales sont utilisées, et une méthode d'itération par les moindres carrés avec laquelle on trouve les paramètres du dipôle en effectuant la minimisation de la somme des carrés des différences entre les données relevées et celles prévues. De plus, en vue de tenir compte d'une partie de l'erreur consécutive à la non-sphéricité de la tête, on a eu recours dans les calculs du dipôle à la distance mesurée entre le centre du crâne et chacune des positions enregistrées. Cette dernière technique donne lieu à l'erreur de position tridimensionnelle la plus faible pour la méthode des moindres carrés (3,5 mm en moyenne), et cela malgré l'absence de mesure de la position près des extremums réels du champ.

D'ailleurs, la méthode de localisation des extremums produit une erreur beaucoup plus grande. On a en outre étudié des combinations de deux dipôles pour lesquelles les cartes de champs magnétiques semblaient analogues à celles d'un dipôle; des comparaisons ont été faites dans le but de voir comment des modèles à un et deux dipôles pouvaient expliquer les données enregistrées.

III. Il existe de nombreux rapports sur les potentiels liés à des phénomènes (PLP), notamment des rapports sur les potentiels associés à la perception et à la catégorisation de stimulus visuels statiques dans le cas où une classe de stimulus (stimulus "excentrique") est moins fréquente que les autres. Généralement, quand la cible était le stimulus "excentrique", on a relevé des PLP lents à sommet positif (300 à 600 ms). Dans la présente étude, on a simulé les échos sur des écrans radar par des stimulus visuels dynamiques, exploitant le paradigme excentrique, afin de mettre en évidence les PLP et les champs liés à des phénomènes (CLP). Comme stimulus, on a employé des cercles et des carrés générés par ordinateur (0,4 degré au niveau de l'oeil du sujet) passant devant un affichage de stimulation (4 degrés au niveau de l'oeil du sujet) à toutes les une ou deux secondes. La forme du stimulus durant chaque balayage (cercle ou carré) était choisie au hasard, avec une probabilité fixe de reproduction durant chaque essai de 300 balayages (cercle + carrés). Les stimulus apparaissaient à partir de points choisis au hasard autour du périmètre du masque et se déplaçaient à vitesse constante le long de trajectoires qui coupaient le point de fixation central visé par le regard du sujet durant tout l'essai. Au début des essais "sans cible", le sujet avait la consigne de "fixer le centre et d'observer les cercles et les carrés"; lors des essais "avec cible", la consigne était de "fixer le centre, de dénombrer les cercles et d'ignorer les carrés" (ou vice versa).

À divers endroits du cuir chevelu du sujet, on a obtenu des électro-encéphalogrammes (EEG) au moyen de l'International 10-20 System, et des magnétoencéphalogrammes (MEG) à l'aide du gradiomètre à balayage de troisième ordre déjà mentionné. Ainsi a-t-il été possible de numériser la tête du sujet, en faisant appel aux procédures I et II, et de calculer un modèle numérisé de la tête, puis de le stocker dans l'ordinateur à des fins de contrôle du portique automatisé. Les signaux des EEG et MEG étaient amplifiés et numérisés sur des périodes de 1 seconde commençant avec l'apparition d'un cercle ou d'un carré sur le moniteur de stimulus. Le rejet automatique d'un balayage avait lieu lorsqu'on décelait des mouvements d'yeux.

Les EEG n'ont mis en évidence qu'une petite différence entre les réponses aux essais "sans cible" et celles aux essais avec cercles et carrés. Toutefois, dans la situation des deux cibles (probabilité de cible 0,5 et 0,3), les réponses obtenues manifestaient des amplitudes sensiblement supérieures à celles des réponses aux essais "sans cible" pour les endroits frontaux et médians du cuir chevelu. En demandant au sujet de ne compter qu'un stimulus (cible) sur deux, on a remarqué une augmentation d'activité positive avec retards (400 à 600 ms) pour les deux stimulus (essais avec cible et sans cible), alors qu'en abaissant la probabilité d'apparition de la cible, il en est résulté seulement des changements marqués de l'amplitude de la réponse pour les stimulus essais avec cible (figure 1b). Les résultats d'EEG obtenus en comparant les réponses aux essais avec cible ($p = 0,3$) à celles aux essais sans cible, aux emplacements frontaux, médians et temporaux, démontrent des différences d'amplitude cible-sans cible avec retards de 350 à 700 ms. Ces différences, pour les temps de retard entre 350 et 450ms, sont moins prononcées aux endroits frontaux, tandis que celles associées au temps de 600 ms sont approximativement égales aux trois emplacements d'enregistrement. Quoique les écarts entre sujets étaient importants, les MEG dépendent des conditions de la même manière que les EEG.

La forte correspondance entre les réponses EEG et MEG au temps de latence de 600 ms semble indiquer que l'inversion de polarité et l'inversion de champs magnétiques observées dans les PLP sont imputables à des sources communes situées à des endroits intercrâniens homologues.

Des cartes d'isolignes du champ lié aux phénomènes ont été tracées pour des intervalles de 50 ms après la présentation de chaque type de stimulus. Les principales différences entre les cartes avec cible et celles sans cible, pour chaque sujet, sont les amplitudes plus grandes des réponses aux essais avec cible et la répartition plus complexe des CLP dans les expériences avec cible.

Les premières estimations des sources de dipôles de courant pour les répartitions MEG avec cible et sans cible, avec retard de 600 ms, établies selon la procédure ci-dessus, semblent corroborer l'existence d'un ensemble différent de dipôles multiples simultanés pour chaque condition de stimulus.

Dans le cas des stimulus sans cible (pas de dénombrement des stimulus), on a provisoirement localisé les sources de dipôles au voisinage des scissures calcarines antérieures, des lobes temporaux inférieurs et en profondeur dans le cerveau près du chiasma optique. Étant donné que les théories courantes sur les aires fonctionnelles du cerveau placent respectivement à ces endroits anatomiques la vision périphérique, le mouvement dans le champ visuel et l'activité oculomotrice, ces dipôles corticaux pituitaires devraient être appropriés du point de vue fonctionnel.

Pour les stimulus avec cible qui sont dénombrés indirectement, on a localisé les sources de dipôles au voisinage du gyrus frontal inférieur gauche (pars triangularis), du gyrus supramarginal gauche du lobe pariétal, en profondeur dans la scissure de Sylvius droite près du lobe pariétal inférieur et dans le lobe pariétal droit supérieur derrière le gyrus postcentral. De nouveau, cette localisation des dipôles est conforme aux théories sur les aires fonctionnelles du cerveau qui associent respectivement ces emplacements anatomiques aux sièges de la parole, du traitement séquentiel des informations (par ex. dénombrement) et de l'exécution des tâches spatiales.

Quoique ces localisations provisoires de sources soient intéressantes pour ce qui concerne les structures neuroanatomiques où semblent siéger de telles tâches, il importe de rappeler que cette procédure en est encore au stade du développement et que le nombre de positions d'enregistrement MEG (25) pour le sujet TR est probablement insuffisant pour la localisation de quatre dipôles ayant chacun cinq paramètres.

Les premiers résultats semblent indiquer que la structure à étudier pour évaluer la capacité de séparation des objets en mouvement et de jugement des intervalles de temps devrait être le lobe temporal.

Table Of Contents

Introduction		1
I	Conceptual Overview of Issues	2
	Introduction to Magnetoencephalography	4
	Location and Identification of Current Sources	5
II	Evaluation of Gantry System	9
III	Theoretical Studies of Sources Location	11
IV	Studies of the Contingent Negative Variation	12
V	Sources Associated With Judgements of Moving Targets	14
VI	New Developments Resulting From Research	23
VII	Bibliography	25

Appendix 1
Magnetic Localization of Intracranial Dipoles

Appendix 2
MEG in the Evaluation of Complex Neural Systems

INTRODUCTION

Recent developments of technology have made it possible to measure small magnetic fields in the brain. Magnetic fields of the brain are the result of electrical currents in the brain. Electrical currents arise from the patterns of electrophysiological and biochemical activity of the brain which are responsible for all brain functions.

Because the tissues of the brain, the membranes of the brain and the skull are all transparent to magnetic fields, the measurement of magnetic fields allows a more accurate estimate of the sources of currents in the brain than is now possible through only the measurement of electrical potentials arising from those currents. Identification of the location of the pattern of sources responsible for currents in the brain allows the investigation of the activity of those sources which are responsible for visual and auditory perception, the processing of information of different kinds and the programming of motor output (movements). Accurtate identification and measurement of sources has the potential for accurate prediction of capabilities for different kinds of performance through the measurement of brain activity. It has long been recognised that measures of performance do not always accurately assess capabilities of memory, perception and performance.

The studies carried out under TP7508E were the first step in establishing a method of assessing capability for performance from a measurement of brain activity through the analysis of magnetic fields of the brain. The ultimate goal of this research is to be able to assess pilots, and other personnel, with respect to their capability for processing the type of information which is critical to their performance.

The following report comprises of six sections:

(I) A conceptual overview of issues related to the study of information processing in the brain and an introduction to Magnetoencephalography.

(II) Testing and evaluation of the scanning gantry system used in the study of magnetic fields of the brain.

(III) Theoretical studies regarding source localisation and associated mapping techniques in preperation for the studies of sources associated information processing of visual information.

(IV) Studies of early and late components of slow electrical potential shifts in the brain (e.g., the Contingent Negative Variation and Readiness Potential).

(V) Development of procedures for estimating current sources in the brain associated with visual information

processing of moving targets on a radar screen.

(VI) New developments resulting from this work.

np

I

Conceptual Overview of Issues Related to Information Processing In The Brain

It is probably not true that memories, especially complex memories are stored in single cells. It is much more likely, and the evidence certainly suggests, that memories are stored as networks of intercommunicating cells. There are advantages to networks. One is that networks are distributed in space and the loss of a small part of the network would leave the memory partially entact. Networks also give the brain a much greater capacity for storage, since the same cells can be part of different networks. Of course, networks are not only spatial but temporal. The same group of cells activated in a different order, or even in the same order but in a different rhythm could store different information. Networks also allow for immediate and dynamic changes in memories depending on experience. This notion of networks fits with the evidence which shows that memories are never static, that accuracy of memory depends very much on what transpires between what happened and what is remembered. Unlike a telephone system in which the meaning of a message depends on the sender, in the brain the meaning of the message depends on the receiver, because all inputs interact with existing memories.

Insofar as brains are concerned no two inputs are identical, regardless of the identity of their physical characteristics. Each and every input modifies the brain such that each subsequent input impacts a different physiology. Furthermore, each output, each response or behaviour, by virtue of unavoidable sensory feedback modifies storage and processing systems. If we could read those storage and processing systems of the brain we would see them updated by each and every input, and each and every output.

The concept of a brain as a system in which the amalysis of input depends on the moment to moment state of the brain, rather than solely on what is coming in, the physical characteristics of what is coming in, has serious implications. One implication is that information processing of the brain determines the meaning of any input and determines the output. Since information processing also occurs independently of immediate input it means that behaviour cannot always be predicted solely on the basis of past behaviour or past experience. One has to know how the brain is processing information. Furthermore, different brains may process the same information differently,

consequently the updates will be different for different brains given the same input. This means the brain cannot be treated as a black box. It is not possible to know everything going on in the brain by observation of the relationship between stimuli (input) and responses (output). Nor is it possible to generalize from the behaviour of one individual to that of another without knowing how each is processing information.

What obviously is needed is a method for directly reading memories, directly accessing the information processing occurring within a brain, when it is occurring.

In the past ten years a great deal of evidence has converged on the conclusion that the measurement of performance may not be the best indicator of capability to perform. The reason is twofold.

In some contexts performance may not fail because additional resources are mobilize to meet the requirements of the task, whereas in other contexts this may not occur. The degree to which this mobilization occurs may vary widely from individual to individual and is very much determined by both the subjective and objective consequences of failure, or of success. Normally the motivating context is very difficult to control, or to measure.

Secondly, in order to achieve a reasonable index of capability to perform in different contexts performance must fail. The performance required must become too difficult or too arduous such that significant errors occur. If the performance is of the type which is modified by success or failure, failure which occurs in the process of performance evaluation may itself modify the probability of subsequent performance.

It is not that measures of performance are not useful or important in the evaluation of the success or accuracy of behaviour. However, measures of performance may not be the best independent predictor of an individuals capability to perform at a defined level.

In the past 60 years there has been an evolution of workload methodology from one that has been based on a rate-of-task-completion approach to one which emphasize the nature of information processing and the interaction of man with machine. With respect to the latter a good deal of research was directed toward making the machine compatible with human capabilities and limitations. However there is a body of research in which the studies were directed toward making the human more compatible with what the machine was required to do.
Attempts to better interface machines and humans led to the so-called system analysis approach. This approach is exemplified by the definition of a system as an "assemblage of elements engaged in the accomplishment of some common

purpose and tied together by a common information network, the output being a function not only of the characteristics of the elements but also their interactions". Engineering biology and psychology are thought of as those parts of the information which can be used by design and systems engineers in the solution of specific design problems that involve the behaviour of people. Human factors however is presumably the application of information from the biological and behavioural sciences in the design of components of the system.

Introduction To Magnetoencephalography

The first measurements of magnetic fields identified with electrical activity of the brain was recorded by Cohen (1). He observed spontaneous rhythms in the MEG which were of alpha (8-12 Hz) frequency by averaging 8 second records, each collected by triggering from the same phase of alpha waves in the EEG (electroencephalograph). Following those initial observations the field has grown rapidly. Several recent reviews have documented the field of Biomagnetism (2, 3, 4). Brain research using MEG has focused, almost exclusively, on attempts to localize current sources responsible for components of spontaneous EEG rhythms and components of Evoked Potentials (EP), and Evoked magnetic Fields (EF). A components of an EP or EF is an electrical or magnetic field change defined by its latency after sensory stimulation or preceding muscle movement. Components are sometimes said to overlap in time if it can be shown that the demand characteristics of different stimuli, or motor response, differentially modify the component. Two broad categories of components are discussed in the literature, (a) those which reflect the properties of the stimulus energy, called Sensory Evoked Potentials below, and (b) those which index the nature of information processing in the brain resulting from stimuli or preceding response output, called Event Related Potentials below (ERP). It is generally assumed that components of type (a) are localized to a much greater extent than type (b). A component in category B which has probably received the most attention from "cognitive-psychophysiology" is P300. The design of the experiment reported below was developed to utilise P300 as an index of information processing. P300 is a positive component of an evoked (event related) potential that occurs at approximately 300 msec in adults and is delayed by about 90 to 100 msec in children. P300 is modality unspecific and is influenced greatly by the degree of novelty in the evoking stimulus. It has been called an endogenous or emitted potential because it occurrence is clearly influenced by the set a subject has established with respect to previous occurrence of the eliciting stimuli. This interpretation is supported by the observation that variations in P300, due to a stimulus which requires a differential manual response, can be seen at latencies greater than the response time. In other words, the differential response occurs before P300, therefore P300 is

apparently more related to an update of memory rather than being solely a reaction to stimulus input. The construct most frequently associated with P300 is that of orienting to a novel stimulus. Novelty in most experiments has been defined by the frequency of occurrence of a stimulus, in a stimulus context. If a stimulus occurs only rarely in the context of sequential repetition of another stimulus, or stimuli, the rare stimulus will elicit a large P300. In this respect the amplitude of P300 is associated with rarity of the stimulus; the more rare the stimulus the larger is P300.

Because the thrust of MEG research is to investigate the location of components of EPs and EFs issues related to the inverse solution (prediction of sources from observed fields) and assumptions about localization of function in the brain have had significant impacts on MEG research.

The Location and Identification of Current Sources In The Brain

Accurate location of sources is theoretically made possible because magnetic fields are not attenuated or distorted by tissues of the head. Until now estimates of source location make use of the simplifying assumption that neural generators can be modelled as current dipoles and that the head can be approximated as a sphere. The implication of this assumption is that the component of the magnetic field which is radial to the surface of the sphere (the skull) is die to the component of the primary component of the current dipole tangential to the skull (6). The radial components of the primary current dipole does not contribute to the tangential (or radial) component of the magnetic field observed outside the head. Theoretically, this is because the field due to the radial current dipole is cancelled by the field due to the secondary sources (volume currents). The current dipole which best accounts for the observed data can be computed (5). However, given that it is impossible to know the total pattern of current flow in the intact, functioning brain at any instant, it is also impossible to determine the amount of error in the location of sources. Several attempts have been made to use computer modelling but the accuracy of locations in these studies is determined by the assumptions used to develop the models (7, 8). An important problem in estimates of source location is how to accommodate the actual shape of the head in the dipole localization procedure. The spherical approximation has in some cases caused significant errors. Physical models have been used to study the problem of source location (9) in which current dipoles emplanted in known positions within a human skull, in vitro. Using a least-squares iterative method which found the parameters for a dipole such that the sum of squared differences between the recorded and predicted data were minimized, the smallest three dimensional location error computed was 3.5 mm. Romani (5) has pointed out that it is important to distinguish between

attempts to identify the individual and specific neural currents which are active at any instant in time from the estimates of sources of components of EPs or EFs. The sources or the latter are actually source-systems, i.e., the magnetic fields measured depend on the spatial and temporal configuration of cells and synapses. The properties of the magnetic fields in the electrically conductive media, particularly the summation of fields arising from a distribution of current flow in the brain at any instant of time, means that the source identified is an aggregate of all those currents systematically related in time to components of EPs and EFs, this is particularly true of ERPs.

Studies of visual, auditory and somatosenosry systems have comprised the largest body of MEG research. One reason for this is that there is known neuroanatomy and neurophysiology associated with sensory function. Therefore, initial attempts to localise sources associated with components of sensory evoked potentials used known neuroanatomy to validate methods of estimating source location.

Retinotopic organisation is mapped on the striate cortex. Brenner (14) estimated sources associated with full field, and right and left hemifield stimulation. The stimulus was a vertical grating whose luminance varied sinusoidally across an oscilloscope with a partial frequency of 5 cycles per degree. He estimated equivalent dipoles contralateral to hemifield stimulation oriented horizontally and symmetrically, in agreement with the Cruciform model. The equivalent dipole for full field stimulation was a linear sum of those estimated for the hemifield stimulation. Okada (15) using essentially the same technique showed that the phase lag between VEP and VEF was a function of spatial frequency of the stimulus and argued that the VEP was attributable in part to a different source than that measured by the VEF. Other studies of sinusoidally modulated gratings report sources in the Rolandic Fissure near the sites from which efferent fibres influence eye movements (16). Weinberg, et al. (17) recorded EF resulting from stereopsis of a random-dot binocular display. Their data suggested that the source of an early component of the EF associated with fusion was located in striate area and the source of a later component associated with fusion in the right temporal lobe.

EEG Auditory evoked potentials have been studied for many years and have distinguished between sources in brain stem and cortex. MEG studies have been, almost exclusively, concerned with cortical sources. However, Cohen (18) did report that attempts to record 6 10 msec brain-stem EF were unsuccessful. He explained the failure to record brain-stem MEG as attributable to the possible combination of excessive depth with respect to the location of his sensing coil and sources which were primarily radial dipoles. It is however unlikely that the assumptions of a spherical model apply to

sources as deep as cochlear nucleus. The question of whether MEG is capable of locating brain stem sources is still open. Reite (19) first detected the auditory evoked field using brief clicks. They reported fields which were maximal in central and parietal regions but did not sample sufficiently to establish reversals. Hari (20) recorded auditory evoked fields elicited by a continuous tone of 800 msec duration. She distinguished between the sources of N100 (msec) and the slow field which immediately preceded off-set of the stimulus. Both these sources were estimated to be in the superior surface of the temporal lobe in the primary auditory cortex. She postulated that the sources were sheets of dipoles consistent with assumption that they were produced by apical depolarization of pyramidal cells with extracellular sinks in the superficial cortex. Romani (21) reported responses to single frequencies that were modulated at 32 Hz. He used steady state averaging techniques in which the samples were time locked to the modulation. He recorded averaged fields resulting from 200, 600, 2000 and 5000 Hz stimulation. The estimated sources were located in the primary auditory cortex and increased in depth from 2.2 to 3.2 cm below the scalp as the frequency of the tone increased from 100 to 5000 Hz.

Many MEG studies have utilised somatosensory stimulation because there is reasonable agreement about the anatomy of afferent somatosensory projections to the cortex. Brenner (22), Kaufman (23) and Okada (24) did the early experiments in which they showed that in steady state stimulation of the median nerve produced magnetic fields that suggested dipolar sources in the contralateral somatosensory cortex. Hari (25) studied both both median nerve and peroneal nerve stimulation in the same experiment Two different types of magnetic responses were reported, one type (SI) with sources near the primary projection areas of somatosensory cortex (30-80msec and 150-180msec latencies) and a second type (SII) near Sylvian fissure (90-125msec latencies). The (SI) response was lateralised with respect to contralateral stimulation. The (SII) response occurred after both ipsilateral and contralateral stimulation. Previous studies of these two cortical sites (somatosensory cortex and Sylvian fissure) suggest that they are not heirarchically organized anatomically, or functionally, but that the Sylvian cortex functions to integrate somatosensory input with input from other sensory modalities and with memories. Magnetic field distributions differentiated between equivalent dipoles active in SI and SII whereas electrical field distributions did not (26).

The search for sources of motor function using MEG has been primarily confined to study of the Bereitschaftspotential (BP) of Kornhuber and Deecke. The BP is a slow negative electrical cerebral potential which occurs preceding a voluntary movement and has been shown to be sensitive to both cortical and brain-stem lesions of the motor system. Deecke (27) recorded magnetic and electric fields preceding

finger movement and localised the source to the precentral gyrus in the contralateral area of the motor homunculus consistent with known anatomy. In electrical recordings the BP is not lateralized to contralateral hemisphere but is widely distributed over both hemispheres. The MEG appears to allow much sharper localization to the contralateral hemisphere and is therefore more consistent with known anatomy and physiology. Deecke (28) also reported evidence for the location of systems associated with the control and programing of complex patterns of finger movements in the supplementary motor area of the mesial frontal cortex. Okada (29) also localised two sources active preceding finger movements to the precentral gyrus which were anatomically separated for 75 msec and 110 msec components of the BP (preceding movement), and Hari (30) sources in the motor cortex preceding foot movements.

It is in the study of cognitive function that the concept of an "equivalent dipole" has met its most serious resistance. The issue is whether the strategy of defining a single (equivalent) dipole as a source of components of electrical potential that are known to index information processing is useful or misleading. Components of ERPs which are not modality specific and which are responsive to a variety of complex cognitive conditions are probably not localized within small regions of the brain. However, as a first approximation to a description of sources estimates of equivalent single diplole sources have been applied to P300, N100 and CNV data. P300 is an electrical potential elicited by stimuli which require discrimination and judgement about the probability of their occurrence. One of the first reports of P300 observed by MEG was by Weinberg (31) who reported a similar morphology of MEG and EEG responses; however the MEG response, unlike the EEG response showed reversed polarity over posterior hemispheres, suggesting deep midline sources, although no isocontour mapping was done. Okada (32) reported MEG data which was interpreted as evidence for the source of P300 being located in the hippocampal formation. There have however been reports that P300 can be observed without temporal lobes in humans and that it can be see by intracranial electrodes widely distributed in the Frontal and Limbic brain of monkeys. Another electrical potential which is known to index attention and information processing is the Contingent Negative Variation, a slow increase in cortical negativity occurring between two stimuli one of which is a warning stimulus and the second of which requires a decision or response. Some of the issues as yet unresolved includes the nature of the distribution of sources underlying the shift, whether the shift is composed of overlapping components, each of which has different sources, and others. It is clear from all MEG studies of the CNV that the maps of field distributions are not dipolar and designation of equivalent sources should be done with caution. Weinberg (33) reported studies in which the CNV was studied preceding the same movement that produced a BP. They reported two components

of the CNV an early component whose source was widely distributed associated with attention and a later component whose source was localized to motor cortex, associated with response preperation. Fiumara (34) however reported data suggesting the source of the later component of the CNV was in frontal lobes. They comment on the complexity of the distributions of the fields and point out that the subject requires further study. Several laboratories are now in the process of investigating other components of ERPs which are associated with selective attention and information processing.

II
Evaluation of Gantry System:

1. The gradiometer gantry was designed with five degrees of freedom; x, y, z and rotations through the spherical polar angles theta and phi (longitude and latitude). This allows the gantry to be positioned in 3-dimensional space within the limits of each coordinate variable.

2. As far as we were able to determine all materials were selected and magnetically screened to minimize effects of magnetic interference which could h
ave produced magnetic noise in biomagnetic measurements. The noise levels after installation of the gantry in the Brain Behaviour Laboratory (BBL) were substantially unchanged from those existing in the previous suspension system.

3. The positioning of the gantry system in the laboratory allows easy access to the patients from three sides. The volume of the scanning domain of the gantry system was designed to cover all those areas of the head which could be accessed with not more than a 30 degree tilt of the dewar. The scanning volume could be extended through software to include scanning of other parts of the body but this capability was not tested. However the limitation of 30 degree tilt requires that the patient be moved if all points on the head are to be samples with a normal angle of the dewar. The instrument is not able to move to any point on the head without moving the subject and establishing a new origin for subsequent measurement.

4. The drive elements were selected to minimize the magnitude of the magnetic signal. However the noise of the drive systems is loud enough to be uncomfortable to patients. This was not anticipated in the original specifications of the gantry.

5. A spatial digitizer was constructed for the purpose of establishing a computer model of the subject's head. A commercial digitizer was purchased and incorporated into a positioning plate which could be removed from the dewar after the subject's head had been digitized. The project

called for the development of an algorithm which constructed a head shape that best fit the measured points. This aspect of the project, the hardware for digitizing and the associated software were extremely important because the data enters into computation of polar coordinates for estimation of dipole locations and vectors. The data from the digitizer is also used to define an origin from which normal angles are determined to establish the orientation of the dewar at each recording position; this is called the zeroing procedure. The zeroing procedure consists of digitizing known positions at pre-auricular, nasion and inion positions. From this data the projected position of the dewar in five degrees of freedom for any point on the subject's head can be computed. In addition the origin is used in computation of the parameters necessary to estimate dipole location.

Unfortunately digitizer errors due to the inferior quality of the digitizer introduces errors which make accurate dipole estimates problematic. Therefore additional software was developed by C.T.F. Systems Inc. (CTF) to smooth the data for the purpose of reducing the average error. These smoothing routines use a significant amount of time and the procedure has forced us into reserving a seperate day for digitizing the head of the subject before recording can begin. Furthermore, although smoothing is helpful in defining the true head shape, such smoothing cannot be used for determination of the origin. Therefore errors in the origin can also lead to significant difficulties. If the polar coordinates of dewar position and normal angles are in error the maps of distributions of the magnetic fields cannot be accurately constructed. With the help of Dr. Ronald Harrop of the Computing Science and Mathematics department, the BBL has been in the process of developing the software necessary to take into account these errors in the estimates of dipoles.

6. The speed of gantry movement is about 4 times slower than estimated originally.

7. There were several hardware problems which emerged after delivery but which were dealt with through a mutual interaction between CTF and the BBL. They included:

   a. Occasional movement past the limit switches and jamming at the extremes of travel.
   b. Unpredictable breakdown in joystick-to-computer interface.
   c. Failsafe mechanism occasionally failing.
   d. Differential movement of two ends of the gantry during homing.

8. In addition it has become obvious that it is necessary to have software for the manual adjustment of normal angles, such that the angle of the dewar and its position are known. This is now being implemented by CTF.

Summary: The following summary has been agreed by CTF and the BBL. "Consistent with the goals of our mutual interaction on this project (and within the broader teaming effort towards MEG instrumentation and technique developments in general) we (CTF) are committed to an ongoing collaboration with your labe toward achievement to this end. As part of this effort (and consistent with the needs of a prototype system of the Gantry's complexity) we will continue to provide "fine tuning" support to assure that the system meets the fullest level of operational performance possible. From CTF System's point of view, we are eager to see that the Gantry System be used to its fullest potential and to learn from this use with regard to subsequent innovations which will further increase its utility and commercial value."

III

Theoretical Studies of Source Localisation.

The objective of MEG is to locate the distribution of current sources in the brain. The purpose of this is to use the knowledge of that location to observe the activity of those sources during memory and information processing which were necessary for pilot performance and related human-factors. In order to locate the sources of electrical currents in the brain, an "inverse solution" must be developed. The inverse solution is the computation of sources responsible for the magnetic fields which were measured. Maps, i.e., distributions of magnetic fields over the head, were constructed . The data of field distribution over the head were used to estimate the location of current fields. In order to test the accuracy of the theory, a physical model of the brain wa constructed. The model contained current sources (dipoles) in known positions within the model. These dipoles were energised with known currents and the fields were measured from outside the model.

Included in this report is the paper entitled "Magnetic localisation of intracranial dipoles: simulation with a physical model" by H. Weinberg, P. Brickett, F. Coolsma and M. Baff (1986). This paper has been accepted for publication by the Journal of Electroencephalography and Clinical Neurophysiology.

Note: See Appendix 1 for copy of the paper published on this subject:

Weinberg, H., Brickett, P., Coolsma, F., and Baff, M. (in

press, 1986) Magnetic localisation of intracranial dipoles: Simulation with a physical model.
Electroecnceph
. and Clin. Neurophysiol.

A summary of the paper is the following: Current dipoles energised by isolated sources are located in known positions inside a human skull filled with an electrically conductive medium. Maps of the measured electrical and magnetic fields confirmed the predicted relationships between those fields for both single and multiple dipoles. Two methods of dipole localisation were compared: the peak-location method which used only the locations of the maximum and minimum recorded values, and a least-squares iterative method which found the parameters for a dipole such that the sum of squared differences between the recorded and predicted data was minimised. Also, in an attempt to account for some of the error due to the non-sphericity of the head, the measured distance from the centre of the skull to each recording position was used in the dipole calculations. This last technique resulted in the smallest three-dimensional location error (averaging 3.5 mm) for the least-squares method, even when no recording positions were near the actual field extrema and the peak-location method therefore produced much greater error. Also investigated were combinations of two dipoles for which the magnetic field maps appeared similar to those for a single dipole and comparisons were made to determine how well single and double dipole models could account for the recorded data.

IV

Studies of the Contingent Negative Variation.

Studies by Weinberg, et al., (1983, 1984, 1985a, Brickett, et al. (1982, 1983) of the Contingent Negative Variation (CNV) demonstrated that slow fields which change in intervals of 1/4 Hz or less can be measured with the 3rd order gradiometer. The CNV is an electrical potential show shift which is surface negative on the surface of the cortex with respect to indifferent electrodes. Like the Bereitschaftspotential (BP) the CNV is found prior to a movement, but in the case of the CNV it occurs between a warning stimulus and the movement. There has been considerable controversy over whether the two potentials preceding movement are produced by the same cerebral generators. The studies carried out under RC-7 were designed to investigate this problem, in addition to demonstrating that these slow shifts could be measured. The findings indicated that two components of the CNV could be distinguished, an early component associated with response to the warning signal and a later response associated with response preperation. The later component, just preceding

the motor response had the same morphology as the BP. Furthermore the later component showed a reversal of the field direction as the probe was moved over the Rolandic fissure. This reversal was not seen in measures of concurrent electrical potentials. Therefore it was concluded that the the later component of the CNV was the same as the BP and generated in the Rolandic fissure, in those locations associated with the control of the response used in the CNV and BP paradigm.

See appendix 2 for copy of the published paper:

Weinberg, H., Brickett, P., Baff, M., and Coolsma, F. (in press). The MEG in the evaluation of complex neural systems that generate event related slow potentials. In C. McCallum (ed.) **Proceedings of the Seventh International Conference on Event Related Potentials of the Brain (EPIC VII).**

V

Sources Associated with Judgments of Moving Targets

INTRODUCTION

Dynamic visual stimuli, employed in recent studies (35,36,37), have intuitive appeal due to their apparent ecological validity. There have been many reports of Event Related Potentials (ERP) associated with the perception and categorization of static visual stimuli (reviewed in 38) where one stimulus class ("oddball" stimuli) occurs less frequently than another. When these "oddball" stimuli are designated as response targets, they are commonly associated with a late (300 to 600 ms) vertex-positive ERP. In the present study, dynamic visual stimuli, simulating those on a radar screen, were employed to elicit ERPs and Event RElated (magnetic) Fields (ERF) using an "oddball" paradigm.

Experimental method

Subjects

Two right-handed males (aged 26 and 35 years), with normal uncorrected vision, served as subjects. Both were associated with the laboratory and had previous experience as subjects in vision studies.

Stimuli

The stimuli for these studies were produced with a "Commodore 64" computer and software written for this purpose. They were presented on a Zenith High Resolution Monitor (monochrome, orange phosphor). A Fresnel lens was employed to magnify the monitor screen so that the monitor could be sufficiently removed from the recording equipment that electrical artifacts were eliminated. In some instances the stimuli were viewed with the aid of a first-surface mirror when the monitor had to be positioned perpendicularly to the subject's line of sight.

The stimulus field appeared as a homogeniously bright, circular area (subtending 4 degrees of visual angle at the subject's eyes) with a dark fixation point at its centre (subtending 0.1 degrees) and a dark mask surrounding it. The stimuli were two geometric shapes (a circle and a square) defined by single dark lines (subtending 0.4 degrees). These are illustrated in Figure 1.

The geometric shapes entered the circular stimulus field one at a time from random positions about the perimeter defined by the dark mask. Each shape moved across the screen at a constant velocity on a trajectory that intersected the central fixation point (duration = approximately 1 sec.). Although the shape of the stimulus crossing the screen at

any one time was chosen randomly, the probability of one shape or the other (circle or square) appearing could be varied. The inter-stimulus interval was always greater than 1 second but varied as the initiation of stimulus movement had to be coordinated with the screen refresh rate to minimize distortion. A different digital pulse was associated with th appearance of each stimulus shape and occurred as the stimulus appeared from behind the dark mask.

Recording System

Electrical responses were recorded from the scalp with 1.0 cm. Beckman electrodes (Ag Ag-Cl) that were attached with Grass electrode paste at various positions from the International 10-20 EEG System (impedence 5 Kohm). Linked mastoids were used as the reference and a ground electrode was atta ched to the forehead. Eye movements were monitored with electrodes applied to the suborbital bone and the superior orbit of one eye and large signals from this derivation (Electrooculogram or EOG) were employed for on-line sweep rejection.

The electroencephalographic (EEG) signals were amplified and filtered (time constant=1.2 sec., 30 Hz.), digitized (dwell= 2msec.) and averaged (sweep= 1000msec.) with a Nova IV computer and appropriate software. Employing the unique digital trigger pulse associated with each stimulus shape, separate average evoked potentials (EP) were calculated; one EP related to the circular stimulus and one EP related to the square stimulus. A total of 100 sweeps (circle EP + square EP) were averaged in each trial. All averages were stored on computer disk for subsequent analysis and display.

Magnetic responses were recorded over the scalp with a 3rd order spatial gradiometer (loop diameter= 28mm) manufactured by CTF Systems Inc. (Vrba et al. 1982, Weinberg et al. 1985). The dewar containing the superconducting quantum interference device (SQUID) was moved to selected scalp locations and oriented appropriately to the scalp surface with a computerized gantry system (see Figure 2) and computer software that contained a digitized three-dimensional model of each subject's head (described in Vrba et al. 1985). The magnetoencephalograghic (MEG) data were amplified, filtered, digitized and averaged in the same way as the EEG data described above.

In some of the studies only EEG and EOG responses were recorded, but whenever MEG recordings were made, the EOG and at least one EEG channel were recorded simultaneously. This allowed for monitoring of response consistency and on-line sweep rejection using the same criteria (eg. gross eye movements during stimulus movement).

Procedure

a) EEG studies: The EEG was recorded from 10-20 electrode positions F7, Pz, F8, C3, Cz, C4, T5, Pz and T6 referred to

linked mastoids. During EEG recordings the subject sat comfortably in a semi-reclining position within a dimmly lit room. The stimulus monitor was located at eye level some 4 meters from the subject. When a trial was to begin the stimulus monitor was turned on and the subject was instructed to "fixate the fixation point on the display," and : Study 1 - "observe the moving shapes" (probability = 50:50 circles:squares); Study 2 - "count silently the circles and ignore the squares" (probability = 50:50); Study 3 - "count silently the circles and ignore the squares" (probability = 30:70). There were 5 trials recorded in each study.

b) MEG (+EEG) Study: The subject reclined in various positions on a specially designed couch that allowed easy access to all scalp locations with the tip of the SQUID dewar. All recordings were made in a dimmly lit room that was not electrically or magnetically shielded. After the subject was positioned comfortably, such that the stimulus monitor was in clear view, his head position was stabilized and maintained with a "vacuum cast" pillow. The head location and orientation within the room were digitized such that recording positions could be chosen on the digitized head model that was part of the computer software that moved the gantry system supporting the SQUID dewar. With these head position data and the software head model the tip of the SQUID dewar was positioned over the selected areas of the subject's scalp in an orientation that was tangentially normal to the scalp surface at each location. Fine adjustments to the location and orientation of the dewar tip were made maually when neccessary.

When the position of the SQUID dewar tip was satisfactory with respect to the subject's scalp, the stimulus monitor was turned on and the subject was instructed to "fixate the fixation point on the display , count (silently) the circles and ignore the squares" (subject MB counted the squares and ignored the circles). The probability of the target stimulus appearing was 30%. During MEG recording the EOG and the EEG from Cz or from Fz, Cz, Pz and Oz (referred to linked mastoids) were recorded simultaneously. As was the case in the EEG studies, the MEG and EEG responses associated with each stimulus shape were averaged separately. Three trials of 100 sweeps (target responses + nontarget responses) were made at each scalp location.

Data Analysis

EEG data: The EPs were averaged across trials within each stimulus condition. In the EEG studies the composition of these averages was as follows: Study 1 (no target counted) = 50 sweeps for each stimulus shape X 5 trials at each electrode site; Study 2 (circles counted, probability= .5) = 50 sweeps for each stimulus shape X 5 trials at each electrode site; Study 3 (circles counted, probability= .3) = 30 sweeps for circles and 70 sweeps for squares X 5 trials at each electrode site. The resulting averages were filtered (brickwall = 25 points), adjusted about a mean baseline of

the responses during the first 100 msec. following stimulus presentation and plotted as waveforms for amplitude and latency analysis.

MEG data: The MEG responses were averaged across trials within each recording position. The composition of these averages was as follows: Subject MB (squares counted, probability = .3) = 30 sweeps for squares and 70 sweeps for circles X 3 trials X 45 scalp recording positions; Subject TR (circles counted, probability = .3) = 30 sweeps for circles and 70 sweeps for squares X 3 trials X 25 scalp recording positions. The resulting averages were filtered (brickwall = 25 points), adjusted about a mean baselined of the responses during the first 100msec. following stimulus presentation and either plotted as waveforms (for amplitude and latency analysis) or plotted as isocontour maps of magnetic field intensity over the scalp surface. These MEG data were also analysed by Simplex Curve Fitting (Weinberg et al., in press) to estimate the locations of intracranial current dipoles that accounted for the obtained spatial distribution of magnetic flux density over the scalp.

RESULTS

EEG Studies

The EEG responses from subject TR are displayed in Figures 3a and 3b for three experimental conditions: (a) no designated target(solid lines); (b) circle stimulus = target (probability of appearance =.5) counted silently(broken line); circle stimulus = target (p=.3) counted silently (dotted line). The responses in Figure 3a were evoked by square stimuli and those in Figure 3b by circle stimuli.

In the first condition (no target counted, solid line) the major EEG event is a positivity at approximately 320 msec. that is largest at posterior recording positions (T5,Pz,T6) and at the vertex (Cz,) for both stimuli (Fig3aand 3b). At the frontal recording positions (F7,Fz,F8) the 320 msec. positivity is much smaller but there is a somewhat larger sustained negativity over the 600 to 700 msec. epoch than there is at central and posterior positions. Both ofthese responses show left-right symmetry in their distribution.

In the second condition (circle = target p=.5, dashed line) the 320 msec. positivity is similar in magnitude and distribution to condition one but there is considerably higher amplitude late-activity.

For the square stimulus (nontarget, Fig.3a) there is a small positivity at approximately 600 msec. observed at the frontal positions and at Cz. However, at the posterior positions there is a sustained positivity between 300 and 600 msec.

For the circle stimulus (target, Fig.3b) the frontal and vertex responses are of much higher amplitude and all responses contain a positive peak at approximately 470 msec. (P470). In addition, there is evidence of a small positivity at 600 msec. at the three midline positions. Once again all responses show left-right symmetry in their distribution for both stimuli but anterior-posterior differences in distribution are evident. There are also marked amplitude differences between the target responses(Fig. 3b) and the nontarget responses (Fig.3a. target, nontarget) between 400 and 600 msec., at all recording positions.

In the third condition (circle = target p=.3, dotted lines), the nontarget (square) responses (Fig.3a) are very similar to those obtained in the second condition (p=.5 dashed line) but the P470 amplitude is slightly larger. However, the target (circle) responses (Fig.3b) show considerably higher amplitude for the P470 (F7,Fz,F8,Cz) and a well developed positive peak at 600 msec. (P600 at Fz,Cz,Pz,T5,T6) that is not evident in the nontarget responses (Fig.3a). This wave feature (P600) and the overallhigher amplitude in the target responses are the main findings in this condition (dotted lines in Fig.3a compared to Fig.3b). There is a smallleft-right amplitude assymetry between the two posterior target responses (T5 vs T6 Fig.3b) but it is not as large as the anterior-posterior differences already noted.

In summary, the findings in these three studies were that:

1. The effect of designating one stimulus as target, and having the subject count the target resulted in increased late (400-600 msec) positive activity for both the target and nontarget MEG responses (p=.5);

2. lowering the probability of target appearance (p=.5to p=.3) resulted in little change to the nontarget responses but significant changes in the target responses (P470 higher in amplitude at all recording sites, except T5 and T6; appearance of P600 at all recording sites, except F7 and F8.

3. there was little evidence of left-right assymetry in any of the response distributions but there was considerable anterior-posterior asymmetry in the distributions of the P470 (largest frontally and at Cz) and the P600 (largest posteriorly and at Cz).

4. there were no polarity reversals within any of the EEG distributions that would allow estimation of the intracranial source of any of the putative EP components described for any of the three experimental conditions.

Discussion of EEG data:

Figure 4 shows a comparison target (p=.3) versus nontarget (p=.7) EPs at three electrode sites (Fz,Cz,Pz) for two subjects. The waveforms on the right were shown earlier in Figures 3a and 3b (subject TR). It was noted that a positivity at 470 msec.(P470) was largest at anterior and central electrode sites for target stimuli and that a later positivity (P600), that was only present for target stimuli, was slightly larger at posterior and central recording sites. In the waveforms on the right of Figure 4 (subject MB) it can be seen that there is a larger positivity at approximately 350 msec.at Fz for target stimuli (dotted line). However, the later portions of these waveforms are opposite in polarity to those of subject TR. The data from MB show a large negativity at 600 msec.(N600) that is largest for target stimuli (dotted lines) rather than a positivity (P600) as in the data from TR. Although this putative component at 600 msec. is opposite in polarity for the two subjects, the existence of such a clear difference between target and nontarget responses at the same latency was considered as evidence that these two events (P600 and N600) might reflect a common underlying brain process in these two subjects that is related to some aspect of task performance (visually detect and count rarely occurring target stimuli).

The scalp distribution of the 600 msec. event provided no clues as to its intracranial source in either subject. Figure 5 shows target versus nontarget responses recorded from lateral electrode sites (subject TR). The midline responses from TR (Fig 4) showed the P600 to be slightlylargerat Pz than at Cz or Fz while the N600 (subject MB) was similar at all three midline sites. The lateral responses from TR (Fig 5) show the largest target versus nontarget differences in the P600 at the central recording sites C3 and C4. These two sites also show a large P470 difference as do F7 and F8. It was noted earlier that the responses were left-right symmetrical in all conditions.Therefore it is not surprising that the target versus nontarget differences are also distributed left-right symetrically. Without any polarity reversals within the response distribution of either subject, no estimates of intracranial sources can be made. However, the scalp distributions of both the early positivity (P350 for MB and P470 for TR) and the later peak at 600 msec.(N600) for MB and P600 for (TR) were similar for these two subjects. On the basis of these EEG results it was concluded that there was are reliable difference between the electrical brain events evoked by the stimulus designated as target (and counted) and those evoked by the stimulus designated as nontarget (and ignored). This difference was manifest mainly as a target versus nontarget difference in the EP waveforms at 600 msec.following stimulus presentation in both subjects. Although the polarity of this 600 msec event was opposite for the two subjects, it was suggested that the identical latencies of the P600 and N600 and their similar scalp distributions may be evidence of a task-related brain

event that is common in both subjects.

In order that some estimate of the intracranial source(s) of the 600 msec event might be made, MEG was recorded from each of the subjects while they performed the same task (ie. detect and count target stimuli that appear with a probability of .3). Since both the early positivity (P350:MB, P470:TR) and the 600 msec peak(N600:MB, P600:TR) were reliably recorded at the vertex (Cz), and together they characterize the target versus nontarget respose differences for both subjects, it was decided that a simultaneous EEG recording from Cz would serve as an adequate control during MEG recording.107

Discussion MEG data:

In Figures 6 and 7 MEG data are presented as waveforms depicting changes in magnetic flux density as a function of time at selected scalp recording locations. In Figures 8 and 9 the MEG data are presented as colour enhanced isocontour maps that illustrate the distribution of magnetic flux density over each subject's scalp at 50 msec intervals following the appearance of target (p=.3) or nontarget (p=.7) stimuli.

Owing to the fact that subject MB was the first to be tested with new apparatus, the scalp positions sampled in his recordings were not ideally distributed. As a result, there was not an exact correspondence between the MEG recording distributions for the two subjects. Although this means that the MEG response waveforms from the two subjects could only be compared for a few scalp locations, it does not prevent comparisons of the overall scalp distribution of magnetic flux (isocontour maps) between the them. At the top of Figure 6 the target (p=.3) EEG responses from Cz for the two subjects are superimposed so that their polarity difference at 600 msec can be observed. Plotted directly below are MEG waveforms (target) for the two subjects recorded from the scalp locations indicated on the head figure. At both of these recording positions, the subjects' MEG responses are also opposite at 600 msec., suggesting magnetic fields moving in opposite directions (ie. into the head for one subject and out of the head for the other) at these locations 600 msec following target stimulus appearance.

When each subject's MEG waveforms are viewed in isolation from the rest of their recording distribution, they suggest MEG extrema at these two scalp locations that peak in amplitude 600 msec following stimulation. If these were the only extrema in each subject's recording distribution, they could be interpreted as evidence of an intracranial current dipole source that is located between the two scalp positions. However, the direction of current flow in this dipole would be opposite for the two subjects, even though its intracranial location would be very similar in both

subjects (ie.the source would be in the same brain structure). Such a situation would be consistent with the polarity difference shown in their EEG responses at the top of Figure 6.

An interpretation (though no doubt oversimplified) of the distribution of brain activity at 600 msec. following stimulation, it that these MEG and EEG responses are manifestations of one or more common intracranial sources. In Figure 7 there are further examples of MEG waveforms from subject TR that show magnetic field extrema that peak at the same point in time (approximately 600 msec.) following target stimulation. The existence of this many extrema is consistant with multiple simultaneous current dipole sources in various parts of the brain which peak in intesity at 600msec.

Figures 8 and 9 show the three dimesional head models, MEG recording positions and colour enhanced isocontour MEG maps for subjects TR and MB (respectively). These maps illustrate regions of inward going magnetic flux (red/yellow/white) and outward going magnetic flux (blue/light blue/white) at 50 msec. intervals following stimulus appearance (target p=.3, nontaret p=.7). The waveforms at the bottom of each map are the simultaneous Cz EEG responses for nontarget stimuli (blue) and target stimuli (red) at the latencies indicated by the white time cursor. The nontarget MEG maps (right side of each pair) for both subjects show very stable distributions of ingoing and outgoing magnetic fields after 350 msec. It also appears to be the case that these distributions are similar for both TR (Fig 8) and MB (Fig 9); that is, both sets of nontarget maps show regions of ingoing fields (red) along a diagonal line extending from the left occipital scalp (lower left on map) to the right frontal scalp (upper right on map) with regions of outgoing fields (blue) on either side of this diagonal. The main changes across time in these nontarget maps are in the magnitude of the extrema rather than their distribution.

One major difference between the two subjects nontarget maps is in the size of homogenious isofield areas. In TR's maps such areas are relatively largerthan in MB's maps. This difference is probably due to the differences in their recording distributions and methodological differences rather than response differences. The target maps (left side of each pair) from MB are also more fragmented in appearance than those from TR and the reasons for these difference are probably also methodological. The target maps from MB (Fig 9) are quite similar in distribution to his nontarget maps after 250 msec. but there are some notable differences in the magnitudes of their extrema (target nontarget) and the specific centres of these extrema (eg. Fig 9 : 500 msec to 700 msec). It can be seen when comparing the target maps from TR to his nontarget maps (Fig 8) between 400 and 500 msec. that the distributions of

extrema are similar for the two conditions. However, there are significant differencesin the magnitudes of these extrema (target nontarget).

A similar comparison of the target and nontarget maps between 600 and 700 msec. reveals differences in the distributions of extrema between the two conditions as well as large differences in their magnitudes (target nontarget). Although some similarities were noted between the nontarget maps ofTR (Fig. 8) and those of MB(Fig. 9), there are some distinct differences in their nontarget maps. A comparison of their 600 msec target maps reveals that, with the exception of the right temporal scalp region (right side of figure), these maps show several large extrema that have opposite directions of field for the two subjects (ie. ingoing field for one subject at ascalp location where the other has an outgoing field). This is consistent with the MEG waveform analysis and with the EEG findings presented earlier.

A more general analysis of the MEG maps reveals important differences between the MEG and EEG recordings. Whereas the EEG recordings consistently showed a left-right symmetrical distribution of electrical brain activity. Subject TR performed the target detection task, the MEG maps revealseveralleft-right asymmetries in the distribution of magnetic brain activity duringthis task. In addition, the MEG maps reveal several distributed brain sources at each point in the recoding epoch whereas this was not obvious in the EEG data. It may be the case that the multiple simultaneous current dipole sources that are suggested by the MEG maps are oriented such that their current spreads optimally toward the vertex of the head, thus accounting for the EEG findings reported here (ie. the 600 msec peak for target stimuli).

It is clear from the data that from observations of only EEG, even from best electrode site(Cz) would not be adequate for monitoring performance in this task. Although TR had a P600 peak that was only present in target EEG responses, it's amplitude was small. MB had a N600 peak for target stimuli but it was only marginally larger than the N600 response for nontarget stimuli. Furthermore, polarity reversal in EEG target responses of TR (P600) and MB (N600) could not be identified as same component (ie as having same source) on the basis of EEG alone, but corroborating evidence was obtained from MEG recordings.

Dipole Location Procedures:

In the course of these experiments developments of procedures for the location of multiple dipoles has been proceeding as an extension of those reported above. In the earlier procedures discussed above the localisation of a single dipole position corresponding to observed magnetic

field data recorded from current dipoles of known position and orientation in a model of the brain.

A number of extensions to the method were attempted wwith the MEG data for nontaget stimuli, since that data was least variable. The procedure is considerably more flexibile than the procedure for the location of single equivalent dipoles and utilises refinements of the techniques used for field calculations which make it possible to simultaneously fit two dipoles to an observed field. This procedure is appropriate in a number of contexts, like the MEG data reported in which a single dipole approximation is obviously inappropriate due to the clearly nondipolar character of the data and where two dipole approximations are more appropriate. Furthermore, we have attempted to fit four dipoles to the data by fitting addition dipoles to the residual of the data after the initial two dipole fit had been established.

In addition, mathematical extensions to the procedure have permitted gradiometer corrections to be introduced into the calculations. These corrections take into account the number, size and position of the gradiometer coils and are more effective in source localisation than if calculations are made using the assumption that the fields measured are at the centre of a single sensing coil. This work has also enabled the direction of the gradiometer axis to be more precisely taken into account, a factor which is of particular importance in contexts where the direction of the normal to the head rapidly changes with the position of the sensing coil over the head.

The introduction of the possibility of considering two dipole localisation required the solution of several computational problems, in particular those relating to the choice of inital estimates of positions, and those for determining whether two dipole approximations to the data are appropriate.

Use of this procedure resulted in the fit of four multiple simultaneous dipole sources at 600 msec.components of non target MEG data recorded from TR.

Dipole 1 was located in the occipital cortex, anterior calcarine fissure.

Dipole 2 was located in the left inferior temporal lobe.

Dipole 3 was located in the right inferior temporal lobe.

Dipole 4 was located in vacinity of optic chiasm

VI

<u>New Developments Resulting From This Work</u>'

I. A proposal to NSERC is a direct extention of the work carried on under the DSS grant. The proposal is for: **The Measurement And Study Of Current Sources In The Human Brain With SQUID and MRI**

The research programme is one which was proposed for the next three years and included three components, all of which are complementary. They include:

1. The combination of SQUID data with MRI data (Nuclear Magnetic Resonance images) for the purpose of locating dipoles in anatomical structures.

2. Studies of physical models in which comparisons can be made between the effectiveness of SQUID data (Superconducting Quantum Interference Device) and EEG data (Electroencephalographic) to estimate locations and vectors of dipole sources. The purpose is to develop procedures for estimating the locations of distributed current sources from the measurements of EEG and MEG fields.

3. The study of sensory evoked electrical and magnetic responses for the purpose of determining if sources active in seperate stimulation of sensory modalities interact during simultaneous stimulation of those modalities.

A brief description of these studies are as follows:

Combinations of MRI and SQUID data for the study of epilepsy: The Brain Behaviour Laboratory of Simon Fraser University is now formally part of the University of British Columbia Imaging Centre. Decisions by the Scientific Advisory Committee and the Board of Management of the Imaging Centre have approved the use of MRI for studies of the combination of those images with SQUID data. The P.I. is a member of these bodies and has an adjunct appointment in UBC.

One of the important goals of both EEG and MEG technology is to make accurate estimates of the location of neurophysiological sources that are active in normal and pathological processes of the brain. To accomplish this there must be a method of relating estimates of dipole location to real anatomical structures. Therefore it is desirable to combine SQUID and EEG data with the data from other scanning techniques such that the estimates of dipole locations are related to the detailed anatomy of the brain from which magnetic and electric fields were measured. If the electrical and magnetic fields observed result from known anatomical pathology, that can be seen with available tomographic images, the accurate location of dipoles in those anatomical structures would be an important method of confirming the degree to which methods of locating dipoles are correct.

We propose to develop techniques for combining SQUID and MRI

data. To do this we will use data collected from some of the epileptic patients of Dr. Jun Wada and Dr. S. Purves. We now have approval for the use of these patients. Dr. Li, director of MRI and of the Department of Radiology at the Health Sciences Centre at U.B.C., will be responsible for collection and interpretation of the MRI data. Techniques for the transfer of MRI data from U.B.C to S.F.U. computers are now established.

Initially, methods of combining data will begin with those epilepsy patients for which the EEG indicates a well defined focus. MRI will be followed by SQUID measurements. A second MRI scan will be completed after SQUID data has been collected. The purpose of the first MRI scan will be to determine if there are clearly defined anatomical pathologies which could be associated with the seizures. We wish to use some patients with and some without anatomical pathologies.

Bibliography

1. D. Cohen, "Magnetoencephalography: detection of the brain's electrical activity with a superconducting magnetometer", Science, 175:664-666, 1972.

2. S.J. Williamson, G.L. Romani, L. Kaufman and I. Modena (Eds.) Biomagnetism: An Interdisciplinary Approach. Nato ASI Series A: 66: Plenum Press, New York, 1983.

3. G.L. Romani and S.J. Williamson (Eds.) Proceedings of the Fourth International Workshop on Biomagnetism. Il Nuovo Cimento, 2D, 2, 123-664, 1983.

4. H. Weinberg, G. Stroink and T. Katila (Eds.) Biomagnetism: Applications and Theory., Pergamon Press, New York, 1985.

5. G.L. Romani and R. Leoni. Localization of cerebral courses by neuromagnetic measurements. In H. Weinberg, G. Stroink and T. Katila (Eds.), Biomagnetism: Applications and Theory. Pergamon Press, New York, 205-220, 1985.

6. D.B. Geselowitz On bioelectric potentials in an inhomogeneous volume conductor. J. Biophys., 7:1-11, 1967.

7. N.B. Cuffin, Effects of inhomogeneous regions on electric potentials and magnetic fields: Two special cases. J. Appl. Phys., 53:9192-9197, 1982.

8. Y.C. Okada Discrimination of localized and distributed current dipole sources and localized single and multiple sources. In: H. Weinberg, G. Stroink and T. Katila (Eds.), Biomagnetism: Applications and Theory. Pergamon Press, New York, 266-272, 1985.

9. H. Weinberg, P. Brickett, F. Coolsma and Mr. Baff. Magnetic localisation of intracranial dipoles. J. EEG and Clin. Neurophysiol., 1986.

10. M. Reite, J.E. Zimmerman, J. Edrich and J.T. Zimmerman The human magnetoencephalograph: Some EEG and related correlations. EEG Clin. Neurophysiol. 40:59-66, 1976.

11. P. Carelli, I. Modena, G.B. Ricci and G.L. Romani. Magnetoencephalography. In Biomagnetism An Interdiciplinary Approach. S.J. Williamson, G.L. Romani, L. Kaufman and I. Modena (Eds.). NATO ASI Series A, Plenum Press, New York, 1983.

12. R.M. Chapman, R.J. Ilmoniemi, S. Barbanera and G.L. Romani Selective localization of alpha brain activity with neuromagnetic measurements. EEG Clin. Neurophysiol. 58:569-572, 1984.

13. V.L. Vvedensky, R.J. Ilmoniemi and M.J. Kajola Study of the alpha rhythm with a 4 channel squid magnetometer. Med. and Biol. Engineering and Computing 23:Supp. Part 1, 11-12, 1985.

14. D. Brenner, Y. Okada, E. Maclin, S.J. Williamson and L. Kaufman Evoked magnetic fields reveal different visual areas in the human cortex. In Biomagnetism S.N. Erne', H-D. Hahlbohm and H. Lubbig (Eds.) Walter de Gruyter, Berlin, 1981.

15. Y. Okada, L. Kaufman, D. Brenner and S.J. Williamson Modulation transfer functions of the human visual system revealed by magnetic field measurements. Vision Res. 22:319-333, 1982.

16. O.V. Lounasmaa, S.J. Williamson, L. Kaufman and R. Tanenbaum Visually evoked responses from non-occipital areas of the human cortex. In Biomagnetism: Applications and Theory H. Weinberg, G. Stroink and T. Katila (Eds.), 348-353, Pergamon Press, New York, 1985.

17. H. Weinberg, P. Brickett, R. A. Neill, B. PEnelon and M. Baff. Magnetic fields evoked by random-dot stereograms. In Biomagnetism: Applications and Theory H. Weinberg, G. Stroink and T. Katila (Eds.), 354 -359, Pergamon Press, New York, 1985.

18. D. Cohen and B.N. Cuffin Search for MEG signals due to auditory brain-stem stimulation. In Biomagnetism: Applications and Theory H. Weinberg, G. Stroink and T. Katila (Eds.), 316 - 320. Pergamon Press, New York, 1985.

19. M. Reite, J. Edrich, J.T. Zimmerman and J.E. Zimmerman Human magneti auditory evoked fields. EEG Clin Neurophysiol., 45:114-117, 1978.

20. R. Hari, K. Aittoniemi, M.L. Jarvinen, T. Katila and T. Varpula Auditory evoked transient and sustained magnetic fields of the human brain. Localization of neural generators. Exp. Brain Res., 40:237-240, 1980.

21. G.L. Romani, S.J. Williamson and L. Kaufman Tonotopic organization of the human auditory cortex. Science, 216:1339-1340, 1982.

22. D. Brenner, J. Kaufman and S.J. Williamson. Somatically evoked fields of the human brain. Science, 199:81-83, 1978.

23. L. Kaufman, Y. Okada, D. Brenner and S.J. Williamson On the relation between somatic evoked potentials and fields. Int. J. Neurosci. 15:223-239, 1981.

24. Y.C. Okada, L. Kaufman, D. Brenner and S.J. Williamson Application of a SQUID to measurement of somatically evoked fields: transient responses to electrical stimulation of the median nerve: In Biomagnetism, S.N.

Erne', H.D. Hahlmohm and H. Lubbig (Eds.), Walter de Gruyter, Berlin 445-461, 1981.

25. R. Hari, K. Reinkainen, E. Kaukoranta, M. Hamalainen, R. Ilmoniemi, A. Penttinen, J. Salminen and D. Teszner Somatosensory evoked cerebral magnetic fields from SI and SII in man. EEG Clin. Neurophysiol. 57:254-263, 1984.

26. R. Hari Somatically evoked magnetic fields. Med. and Biol. Engineering and Computing 22: (Supp. 1)29-31, 1985.

27. L. Deecke, H. Weinberg and P. Brickett Magnetic fields of the human brain accompanying voluntary movement: Bereitschaftsmagnetfeld. Exp. Brain Res., 48:144-148, 1982.

28. L. Deecke, J. Boschert, P. Brickett and H. Weinberg Magnetoencephalographic evidence for possible supplementary motor area participation in human voluntary movement. In Biomagnetism: Applications and Theory H. Weinberg, G. Stroink and T. Katila (Eds.), pergamon Press, New York, 369-372, 1985.

29. Y. Okada, S.J. Williamson and L. Kaufman Magnetic field of the human sensorimotor cortex. Intl. J. Neurosciences, 17:33-38, 1982.

30. R. Hari, A. Antervo, T. Katila, T. Poutanen, M. Seppanen, T. Tuomisto, and T. Varpula Cerebral magnetic fields associated with voluntary limb movements in man. Il Nuovo Cimento 2D, 1:484-495, 1983.

31. H. Weinberg, P.A. Brickett, J. Vrba, A.A. Fife and M.B. Burbank. The use of a SQUID third order spatial gradiometer to measure magnetic fields of the brain. In Brain and Information: Event Related Potentials. R. Karrer, J. Cohen and P. Teuting (Eds.) New York Acad. Sci. 42:743-752, 1984.

32. Y.C. Okada, L. Kaufman and s.J. Williamson The Hippocampal Formation as a source of the slow endogenous potentials. EEG Clin. Neurophysiol. 55:417-426, 1982.

33. H. Weinberg, P.A. Brickett, L. Deecke and J. Boschert Slow magnetic fields preceding movement and speech. IL Nuovo Cimento 2D 1:495-504, 1983.

34. R. Fiumara, F. Campitelli, G.L. Romani, R. Leoni, M. Caporali, M. Zanasi, A. Cappiello, G. Fioriti and I. Modena Neuromagnetic study of endogenous fields related to the contingent negative variation. Biomagnetism: Applications and Theory H. Weinberg, G. Stroink, T. Katila (Eds.) Pergamon Press, New York 336-342, 1985.

23. L. Kaufman, Y. Okada, D. Brenner and S.J. Williamson On the relation between somatic evoked potentials and fields. Int. J. Neurosci. 15:223-239, 1981.

24. Y.C. Okada, L. Kaufman, D. Brenner and S.J. Williamson Application of a SQUID to measurement of somatically evoked fields: transient responses to electrical stimulation of the median nerve: In Biomagnetism, S.N. Erne', H.D. Hahlmohm and H. Lubbig (Eds.), Walter de Gruyter, Berlin 445-461, 1981.

25. R. Hari, K. Reinkainen, E. Kaukoranta, M. Hamalainen, R. Ilmoniemi, A. Penttinen, J. Salminen and D. Teszner Somatosensory evoked cerebral magnetic fields from SI and SII in man. EEG Clin. Neurophysiol. 57:254-263, 1984.

26. R. Hari Somatically evoked magnetic fields. Med. and Biol. Engineering and Computing 22: (Supp. 1)29-31, 1985.

27. L. Deecke, H. Weinberg and P. Brickett Magnetic fields of the human brain accompanying voluntary movement: Bereitschaftsmagnetfeld. Exp. Brain Res., 48:144-148, 1982.

28. L. Deecke, J. Boschert, P. Brickett and H. Weinberg Magnetoencephalographic evidence for possible supplementary motor area participation in human voluntary movement. In Biomagnetism: Applications and Theory H. Weinberg, G. Stroink and T. Katila (Eds.), pergamon Press, New York, 369-372, 1985.

29. Y. Okada, S.J. Williamson and L. Kaufman Magnetic field of the human sensorimotor cortex. Intl. J. Neurosciences, 17:33-38, 1982.

30. R. Hari, A. Antervo, T. Katila, T. Poutanen, M. Seppanen, T. Tuomisto

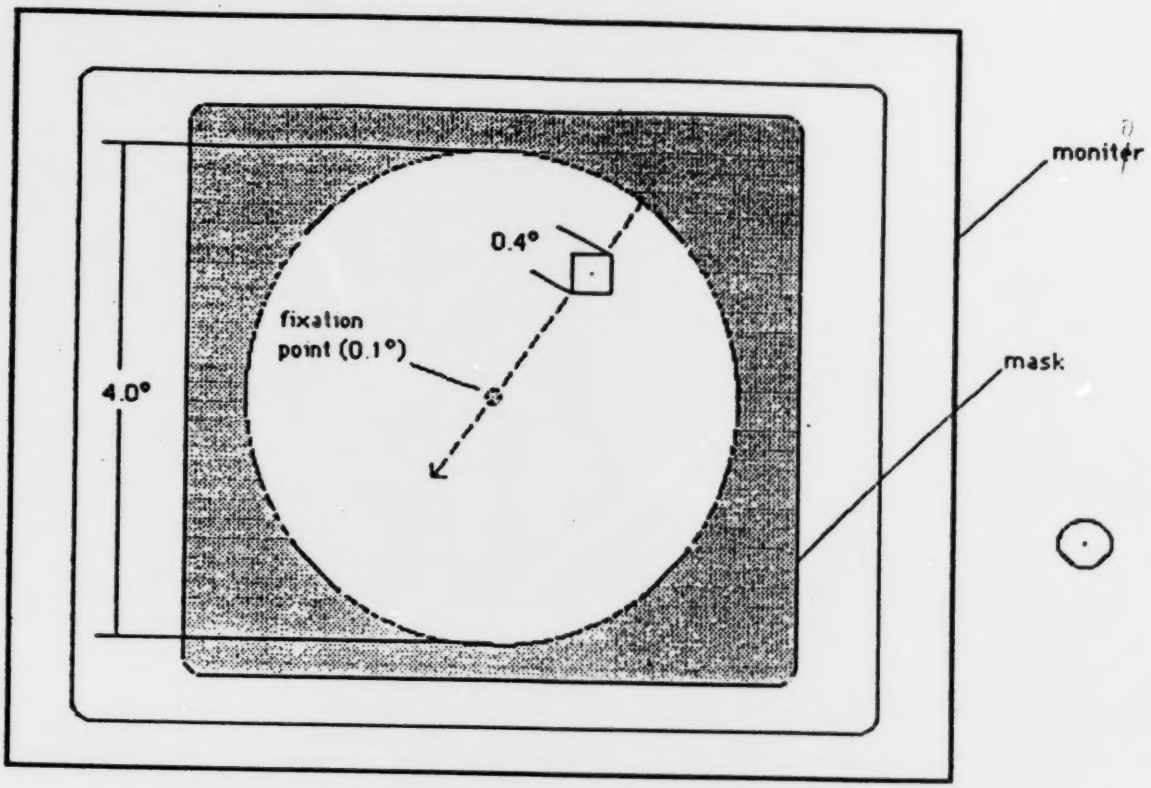

Figure 1. Stimulus Display. Circular stimulus field (as displayed on the monochrome CRT) is shown above with a square image moving across the screen. The other image used was a circle (shown at the side of the diagram). During each trial, one image at a time would appear from behind the black mask (border of circular field) and move across the stimulus field in a straight line intersecting the fixation point in the center. The starting point for each image trajectory occured randomly from any point around the circumference of the circle and the duration of the movement across the field was approximately one second. The interstimulus interval was variable but always less than or equal to one second. Dimensions of the display are given in degrees of angular subtense at the subject's eyes.

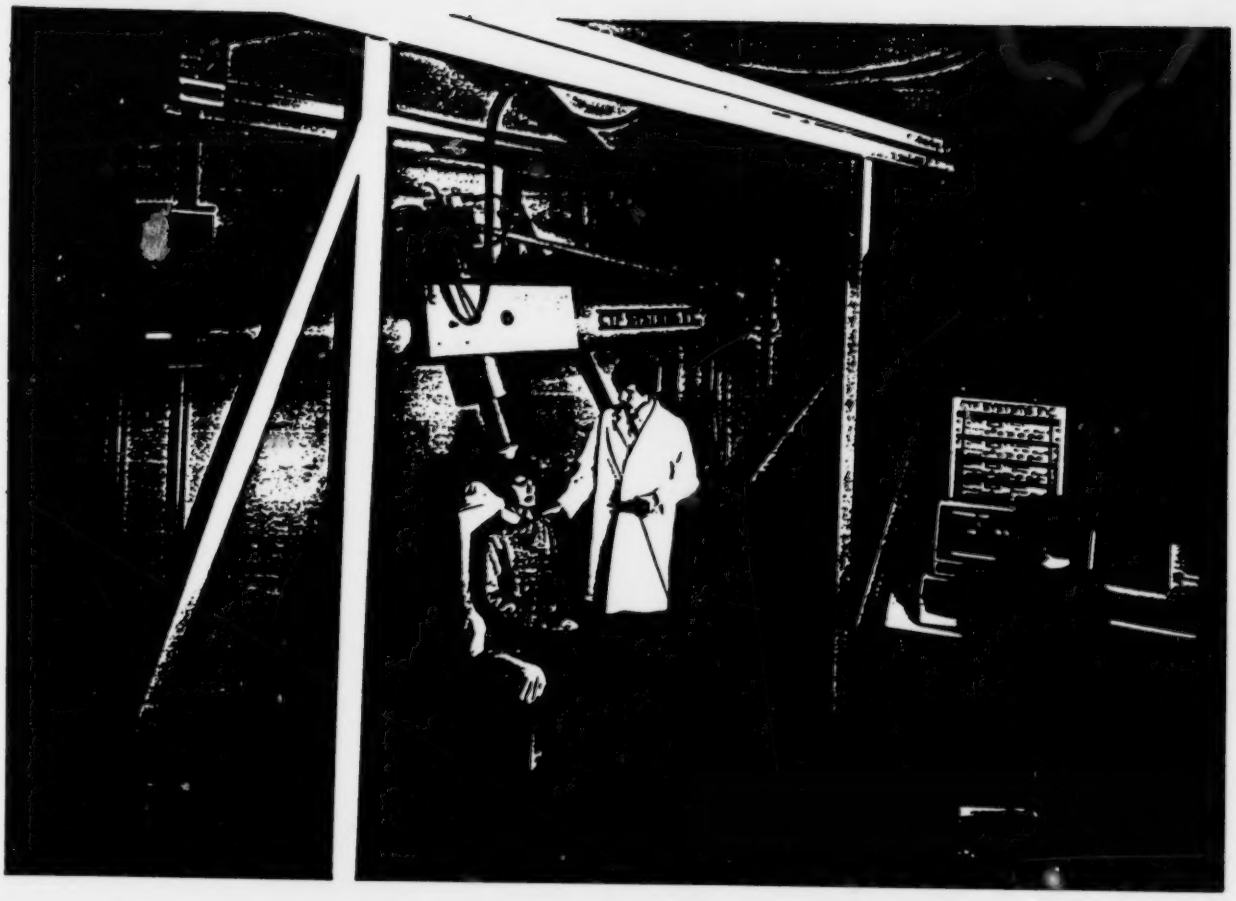

Figure 2. Photograph of the mechanical gantry used for the manipulation of the biogradiometer around the subject's head.

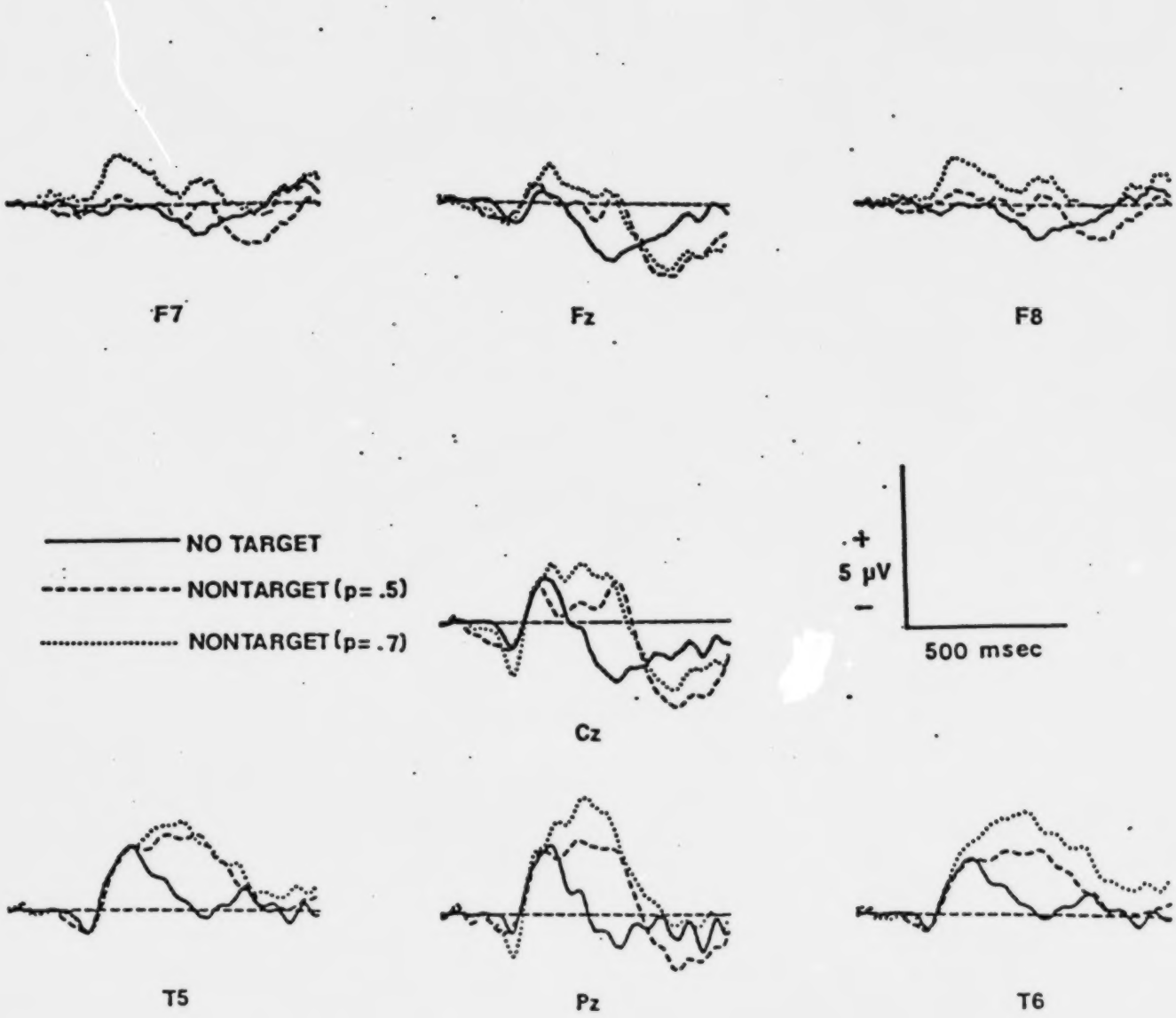

Figure 3 (a). EEG responses to square stimuli for subject T.R. . Superimposed waveforms show responses to non-target stimuli (p=.5, p=.7) and square stimuli when no target was specified (p=.5).

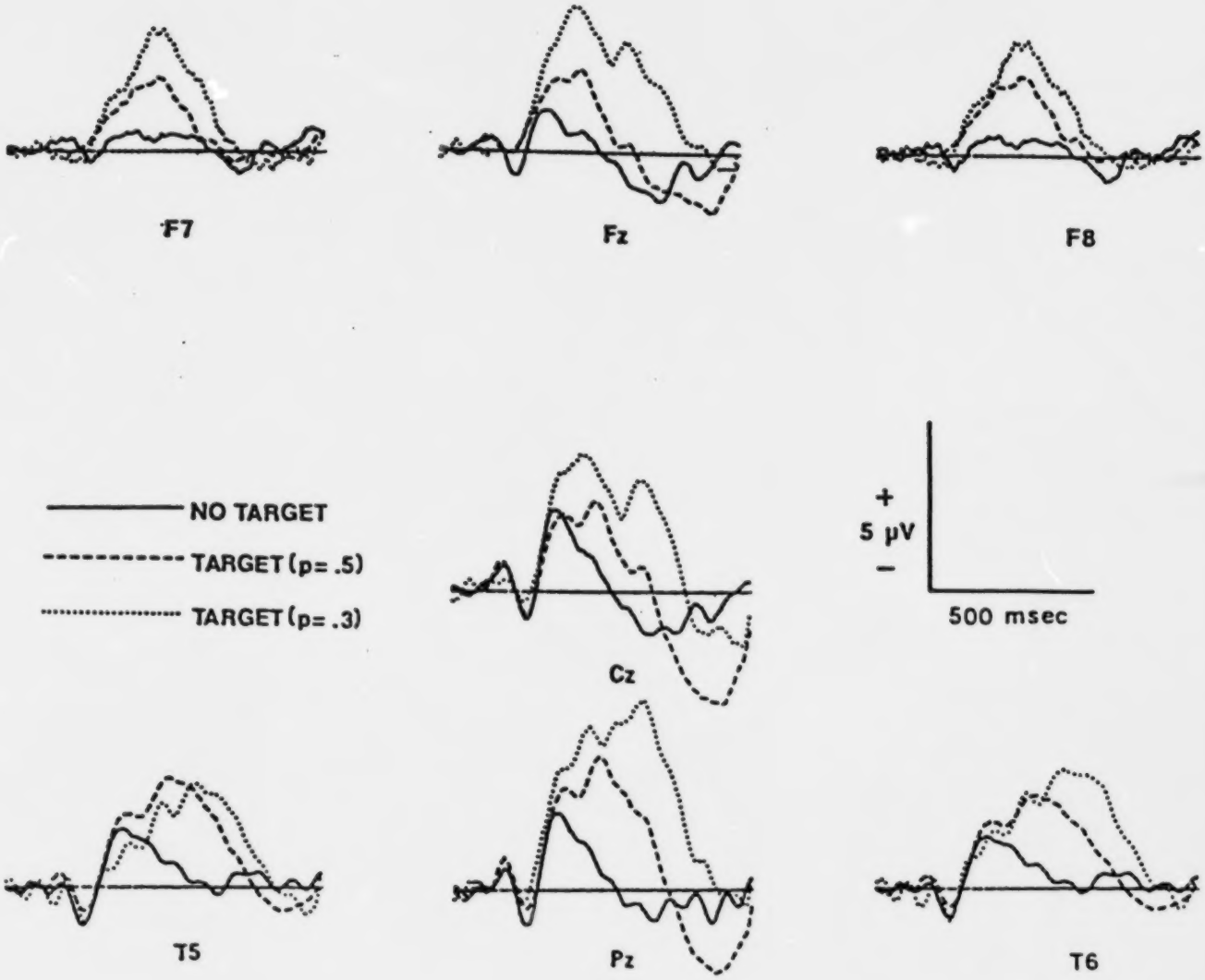

Figure 3 (b). EEG responses to circle stimuli for subject T.R. . Superimposed waveforms show responses to target stimuli (p=.5, p=.3) and circle stimuli when no target was specified (p=.5).

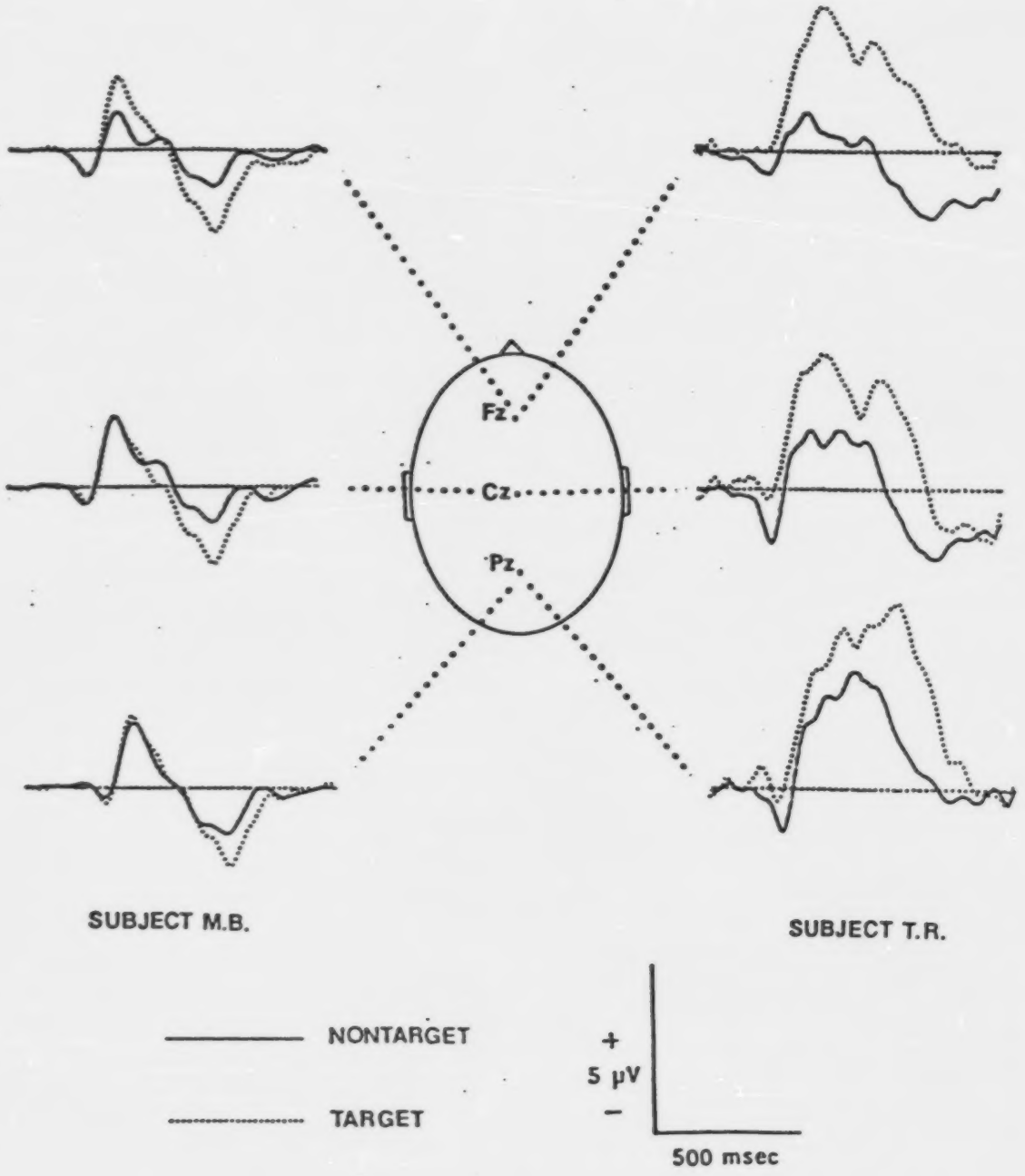

Figure 4. Comparison of EEG responses from midline positions to target and non-target stimuli for subjects T.R. and M.B. .

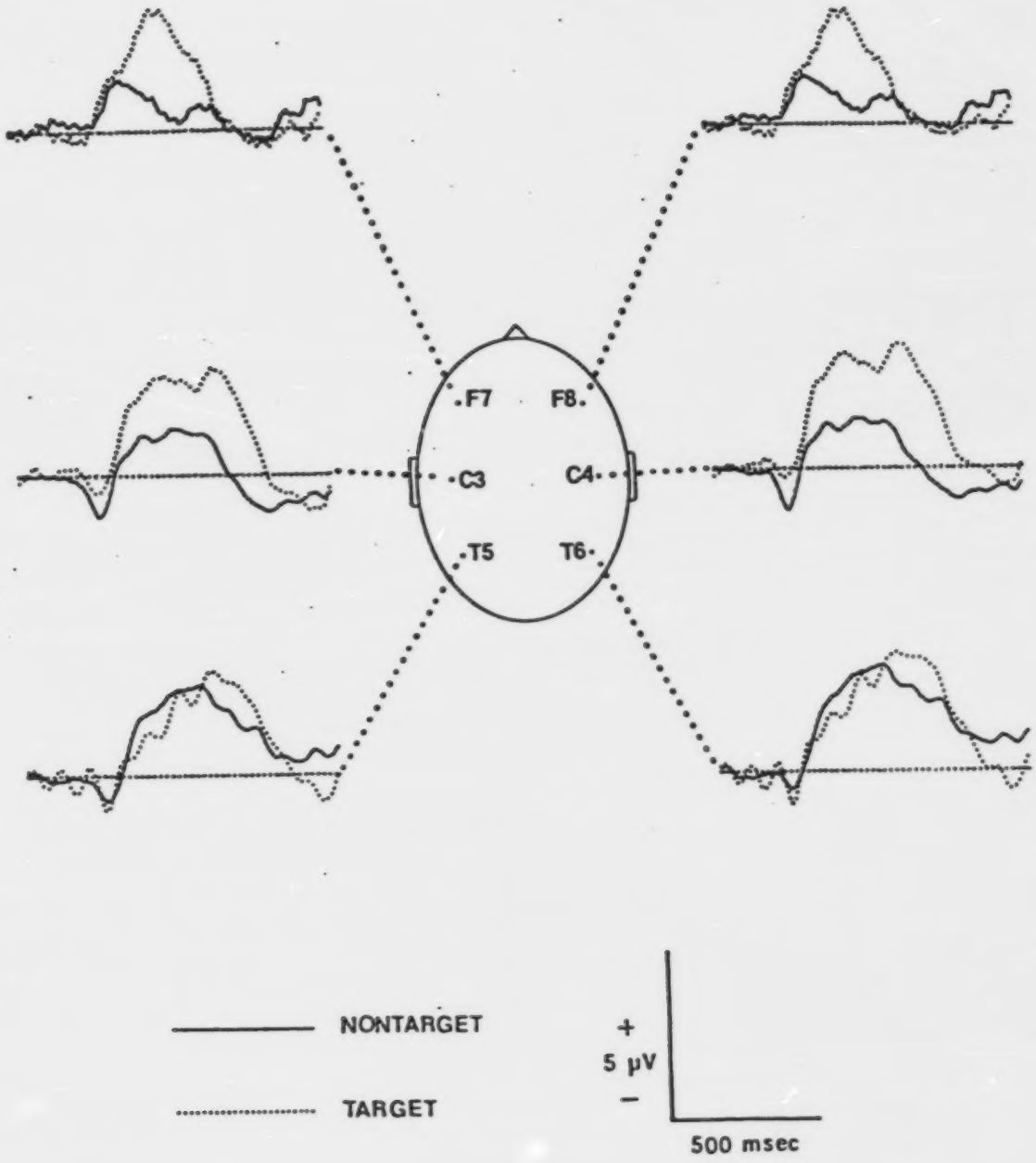

Figure 5. EEG responses from lateral positions to target and non-target stimuli for subject T.R. .

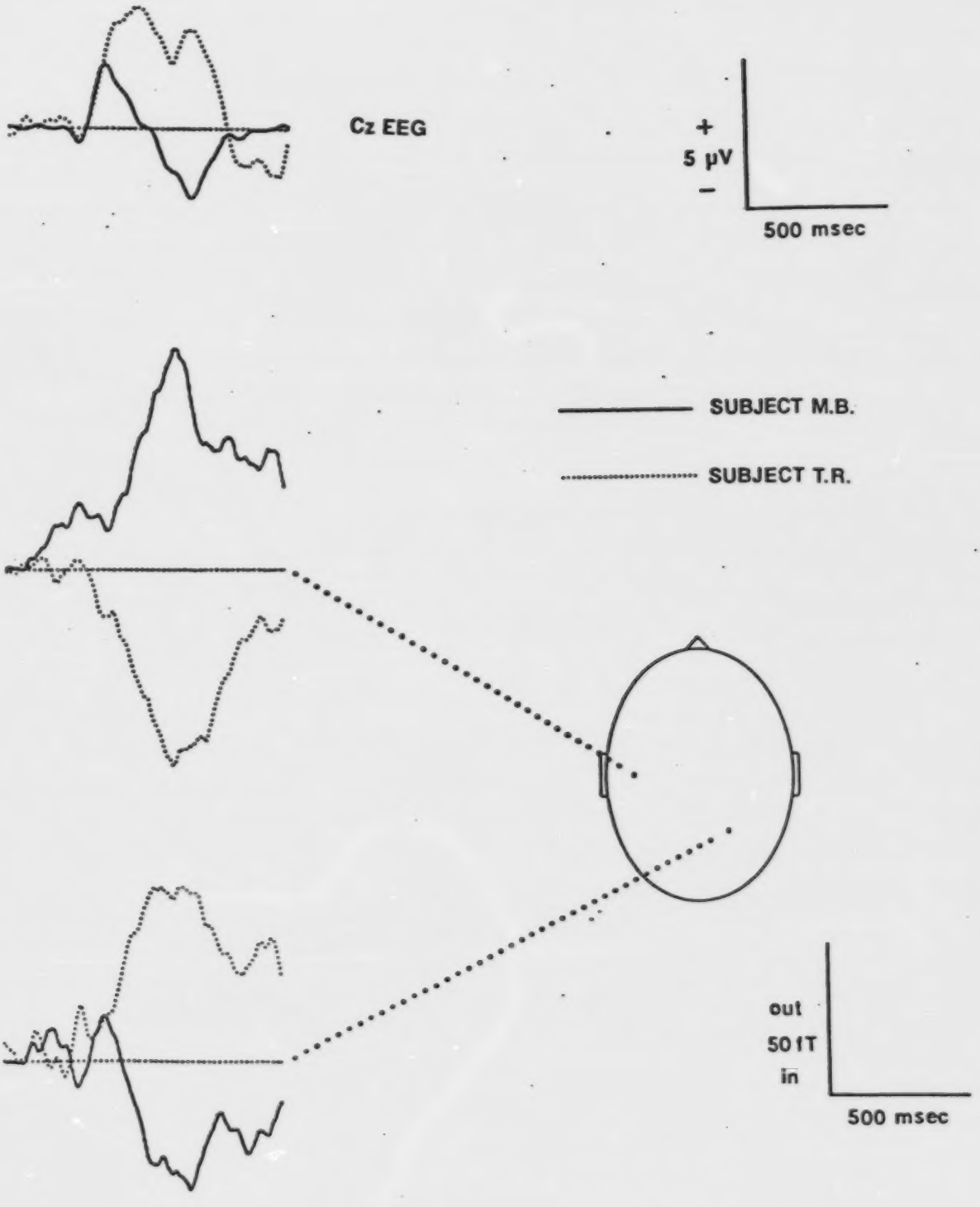

Figure 6. Comparison of MEG responses to target stimuli at two recording positions for subjects T.R. and M.B. showing fields of opposite direction. Upward deflections represent fields coming out of the head.

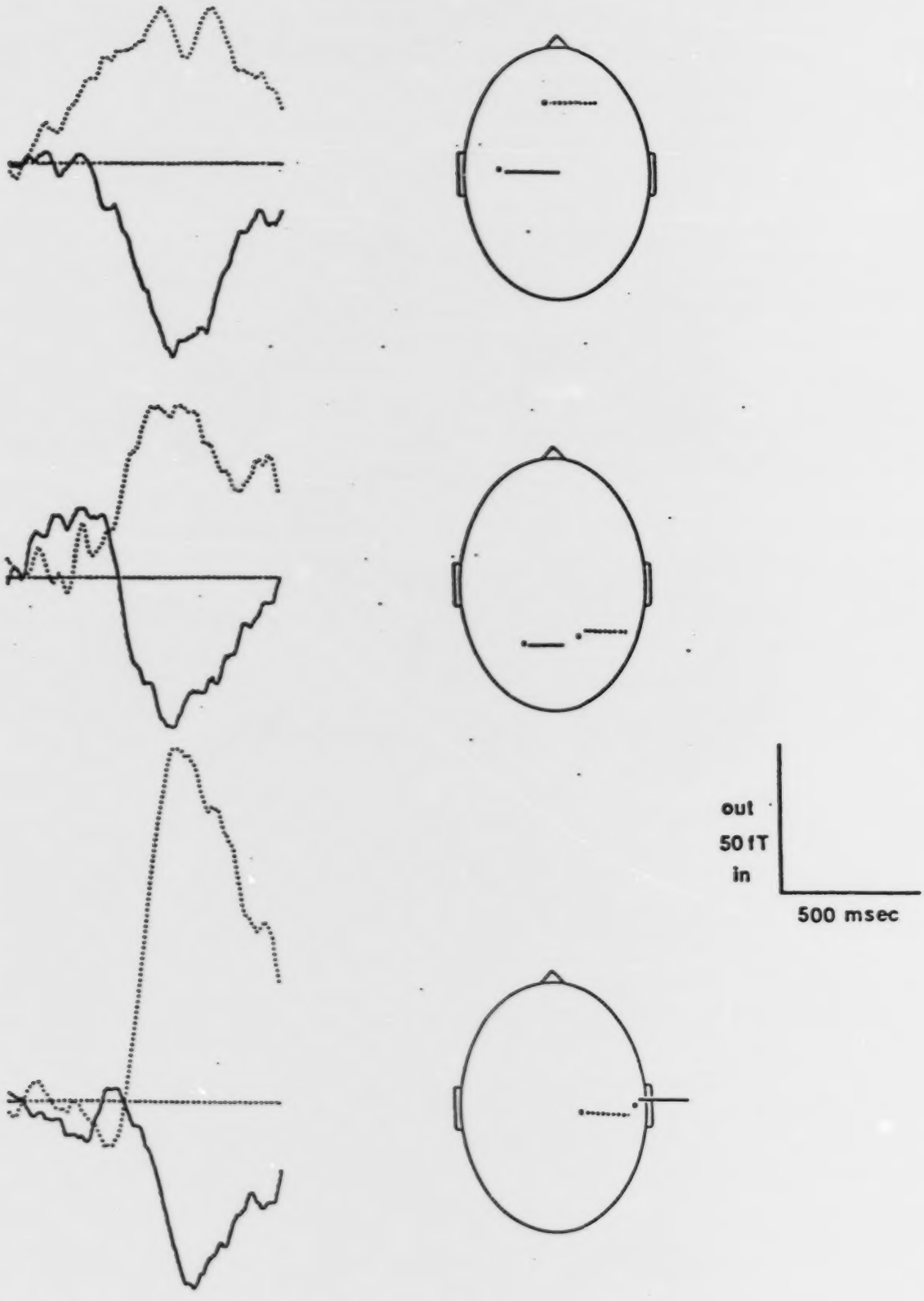

Figure 7. MEG responses for subject T.R. showing maxima of fields entering or leaving the head. Recording positions suggest three possible dipole sources occurring at a latency of approximately 600 milliseconds.

Figure 8. The following photographs show colour-coded isofield contour maps of MEG activity during the 1 second trial for target and non-target stimuli. Blue shades indicate fields coming out of the head and red shades indicate fields entering the head. The maps are shown as equidistant projections of the head surface with the vertex as the center of the map and recording positions indicated by white dots. Maps are shown for each 50 millisecond interval of the 1 second epoch. Below each map is the EEG (Cz) grand average for target (red) and non-target (blue) stimuli with the cursor bar at the corresponding point in time.
Colour images of the 3-dimensional head model used to position the biogradiometer (first page, upper left) are shown from three perspectives: top view (left), posterior view (upper right), and left lateral view (lower right).
Subject T. R. .

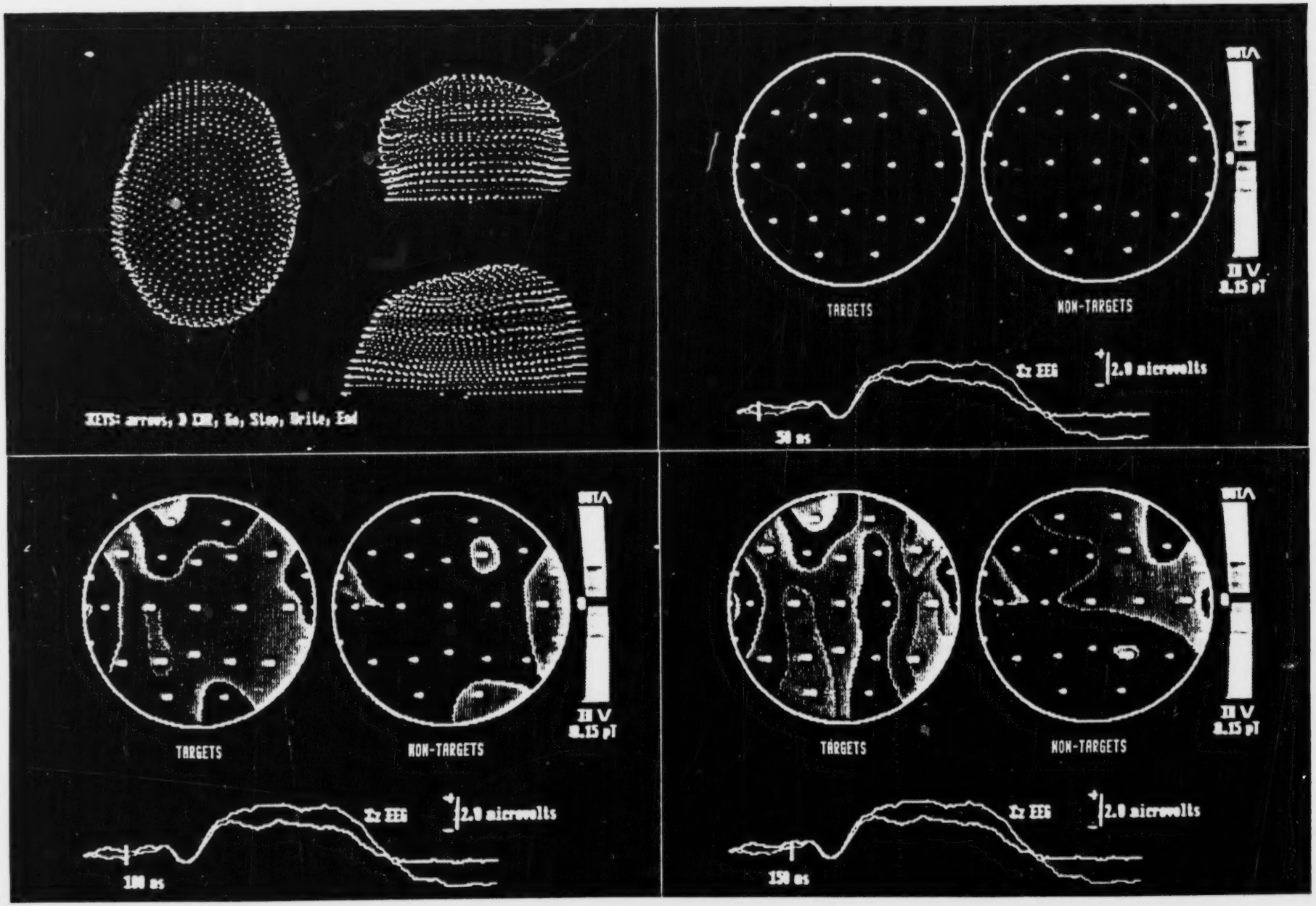
TARGETS
NON-TARGETS
2.0 microvolts
50 ms
TARGETS
NON-TARGETS
2.0 microvolts
100 ms
TARGETS
NON-TARGETS
2.0 microvolts
150 ms

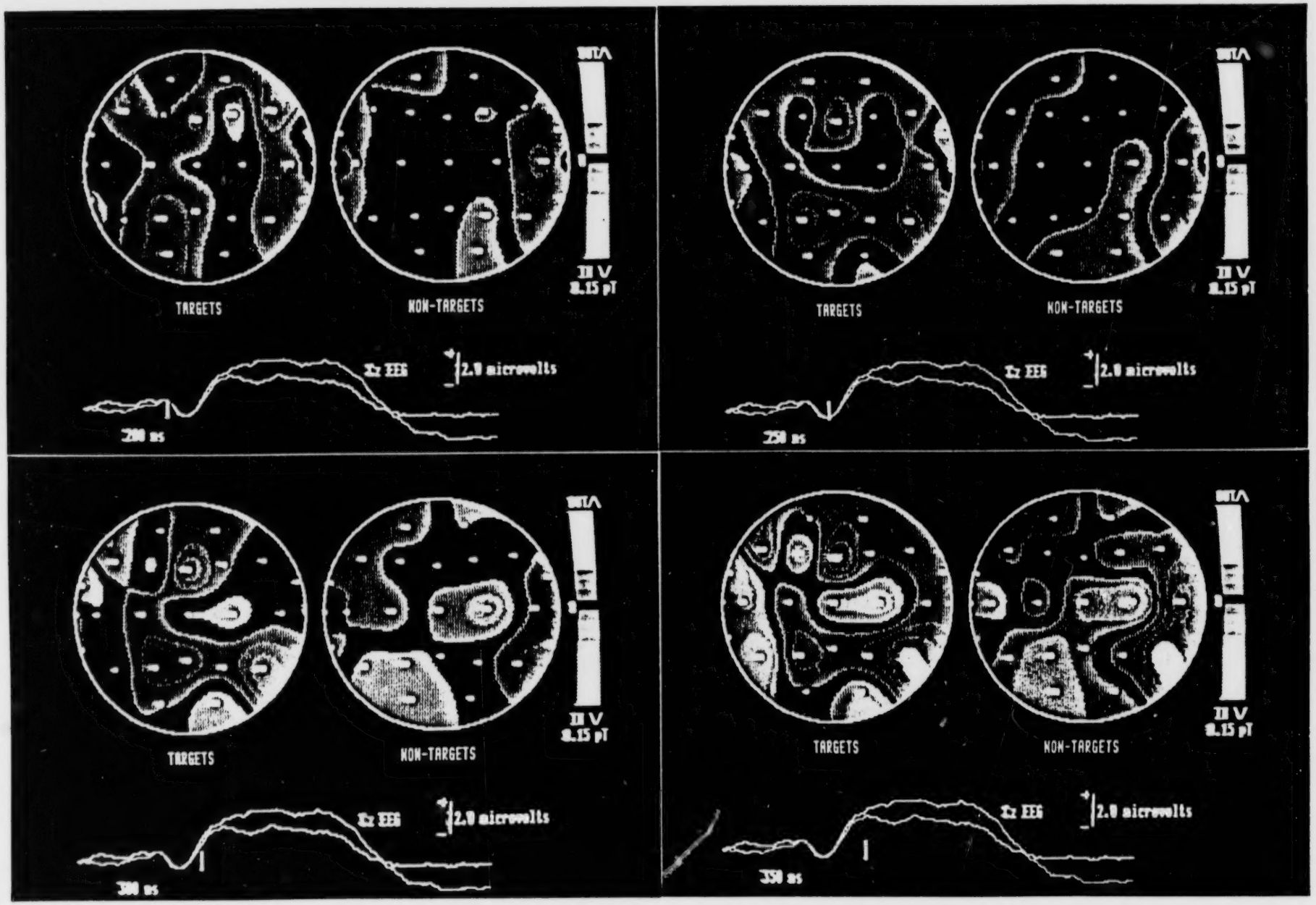
TARGETS
NON-TARGETS
Fz EEG
2.0 microvolts
200 ms
TARGETS
NON-TARGETS
Fz EEG
2.0 microvolts
250 ms
TARGETS
NON-TARGETS
Fz EEG
2.0 microvolts
300 ms
TARGETS
NON-TARGETS
Fz EEG
2.0 microvolts
350 ms

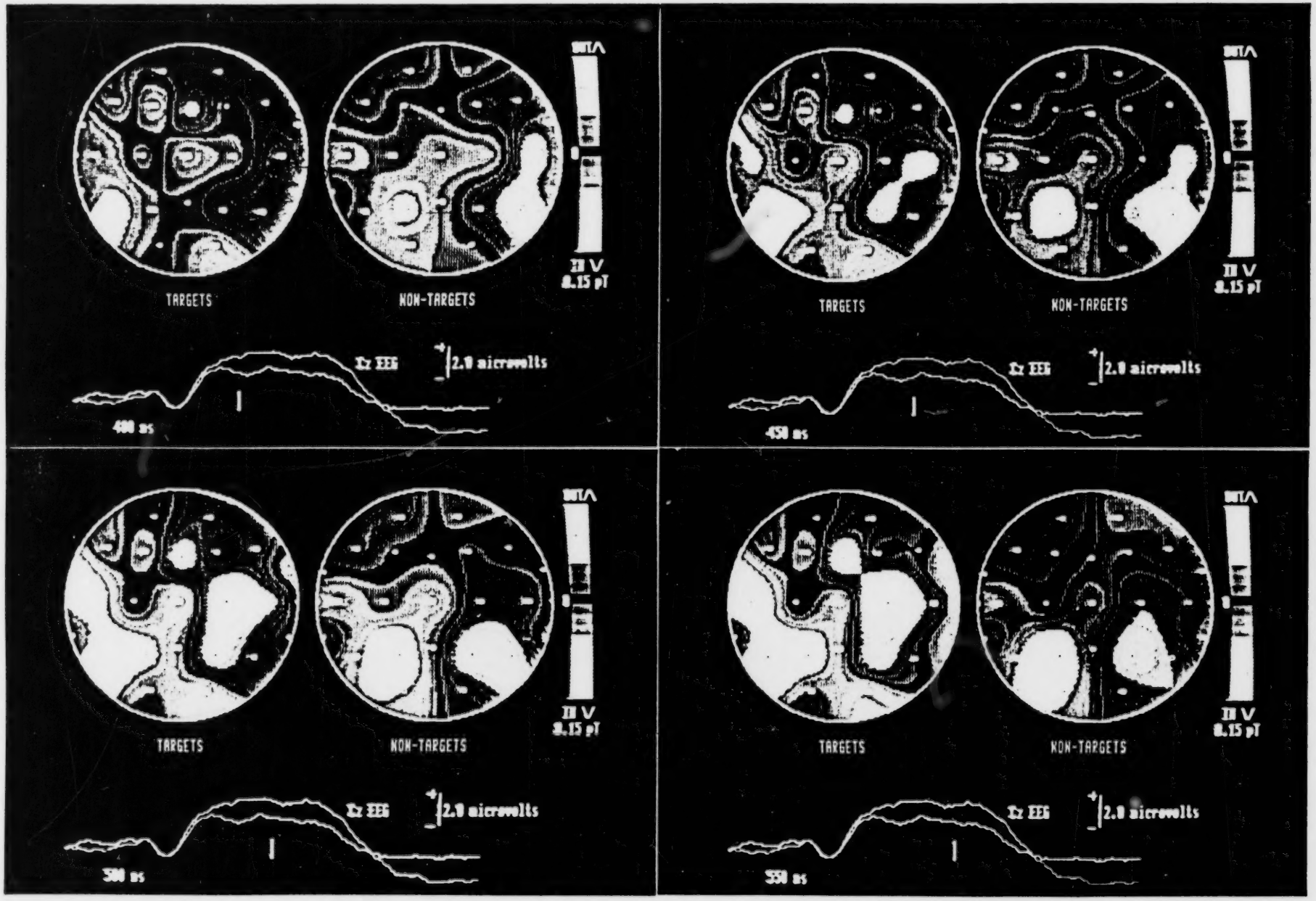
TARGETS
NON-TARGETS
11 V
8.15 pT
Cz EEG
2.0 microvolts
400 ms
TARGETS
NON-TARGETS
11 V
8.15 pT
Cz EEG
2.0 microvolts
450 ms
TARGETS
NON-TARGETS
11 V
8.15 pT
Cz EEG
2.0 microvolts
500 ms
TARGETS
NON-TARGETS
11 V
8.15 pT
Cz EEG
2.0 microvolts
550 ms

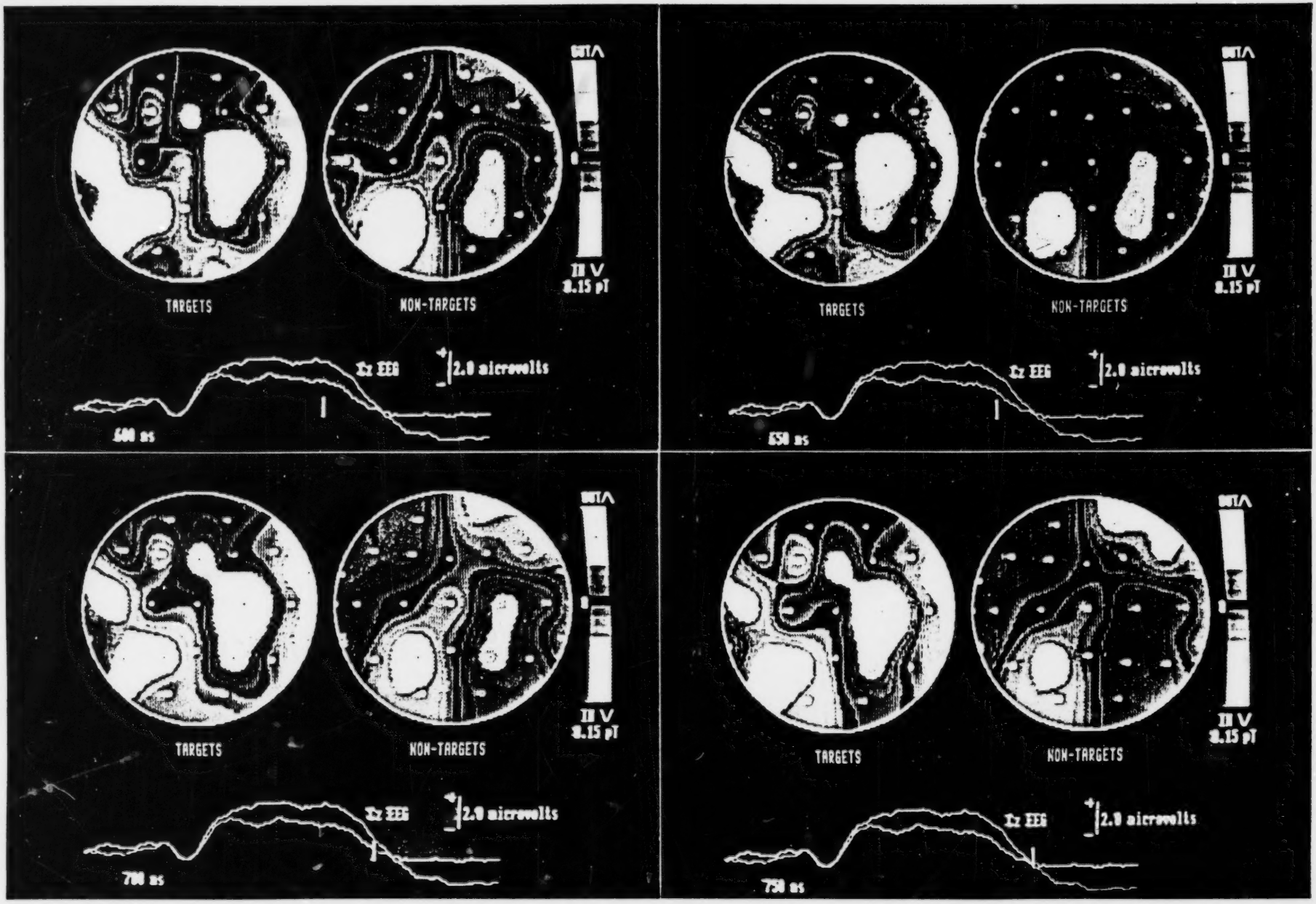
TARGETS
NON-TARGETS
8.15 pT
Iz EEG
2.0 microvolts
500 ms
TARGETS
NON-TARGETS
8.15 pT
Iz EEG
2.0 microvolts
650 ms
TARGETS
NON-TARGETS
8.15 pT
Iz EEG
2.0 microvolts
700 ms
TARGETS
NON-TARGETS
8.15 pT
Iz EEG
2.0 microvolts
750 ms

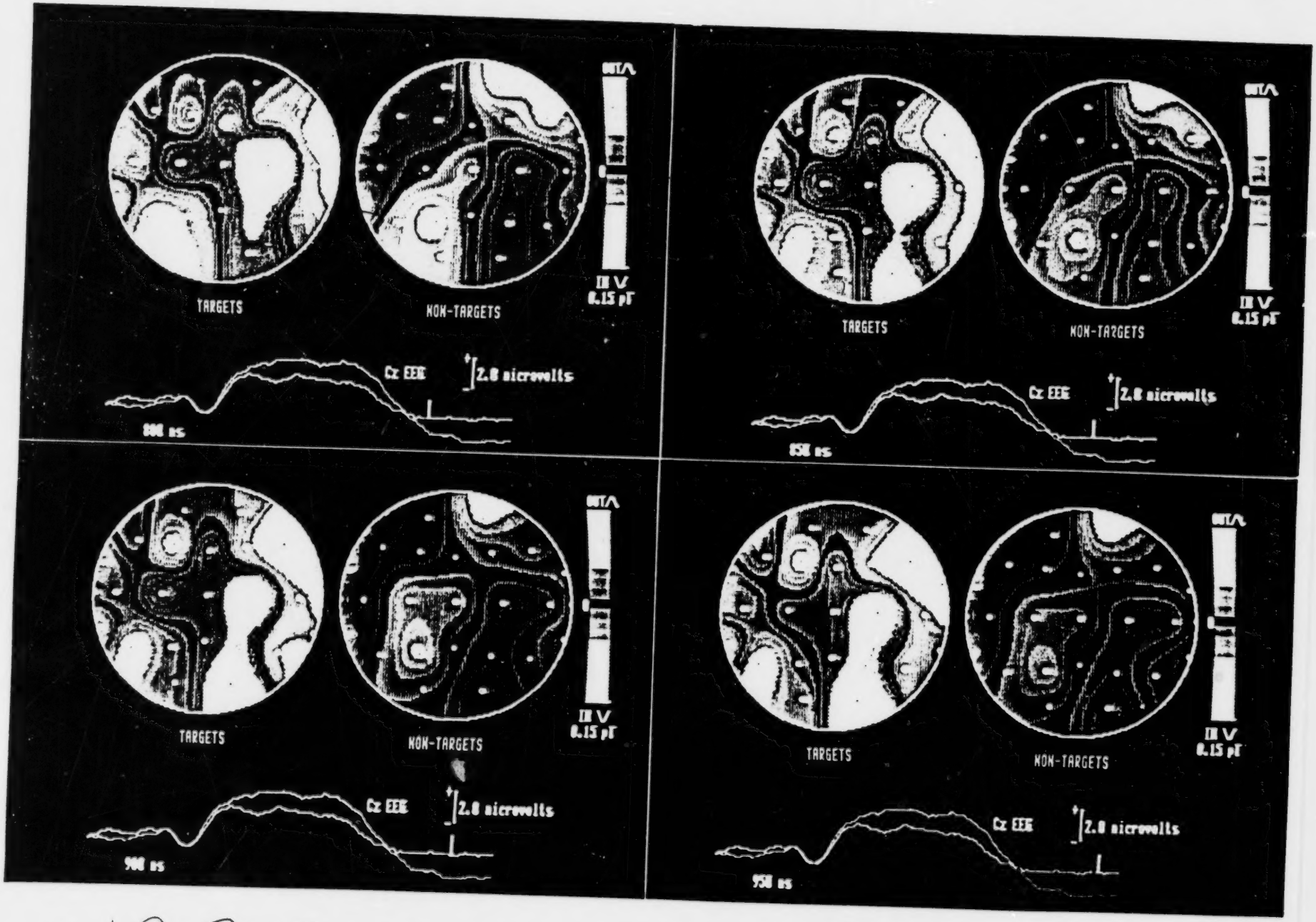
TARGETS
NON-TARGETS
II V
0.15 pT
Cz EEG
2.8 microvolts
908 ms
TARGETS
NON-TARGETS
II V
0.15 pT
Cz EEG
2.8 microvolts
858 ms
TARGETS
NON-TARGETS
II V
0.15 pT
Cz EEG
2.8 microvolts
908 ms
TARGETS
NON-TARGETS
II V
0.15 pT
Cz EEG
2.8 microvolts
958 ms

Figure 9. The following photographs show colour-coded isofield contour maps of MEG activity during the 1 second trial for target and non-target stimuli. Blue shades indicate fields coming out of the head and red shades indicate fields entering the head. The maps are shown as equidistant projections of the head surface with the vertex as the center of the map and recording positions indicated by white dots. Maps are shown for each 50 millisecond interval of the 1 second epoch. Below each map is the EEG (Cz) grand average for target (red) and non-target (blue) stimuli with the cursor bar at the corresponding point in time.
Colour images of the 3-dimensional head model used to position the biogradiometer (first page, upper left) are shown from three perspectives: top view (left), posterior view (upper right), and left lateral view (lower right).
Subject M. B. .

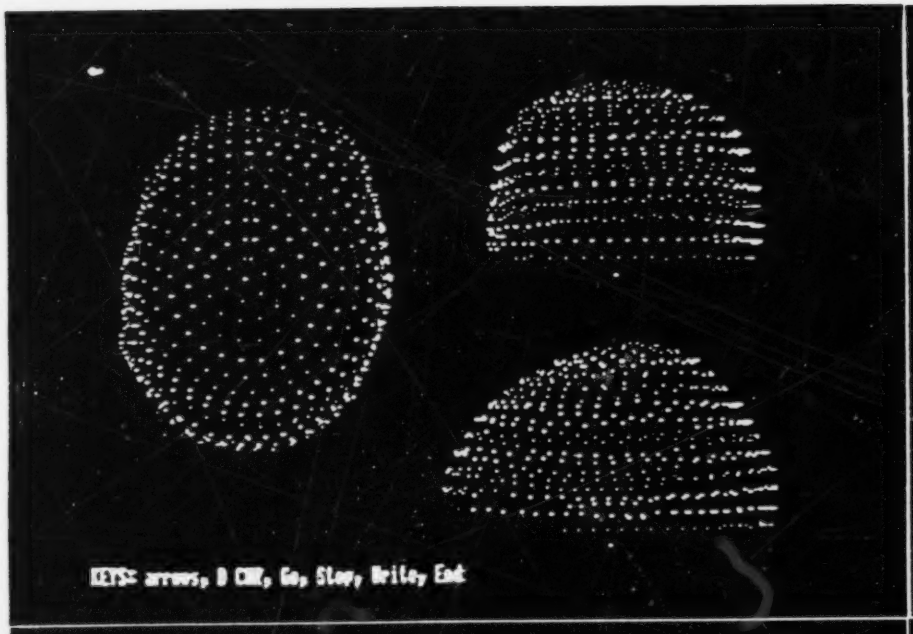
KEYS: arrows, B CHK, Go, Slow, Write, End

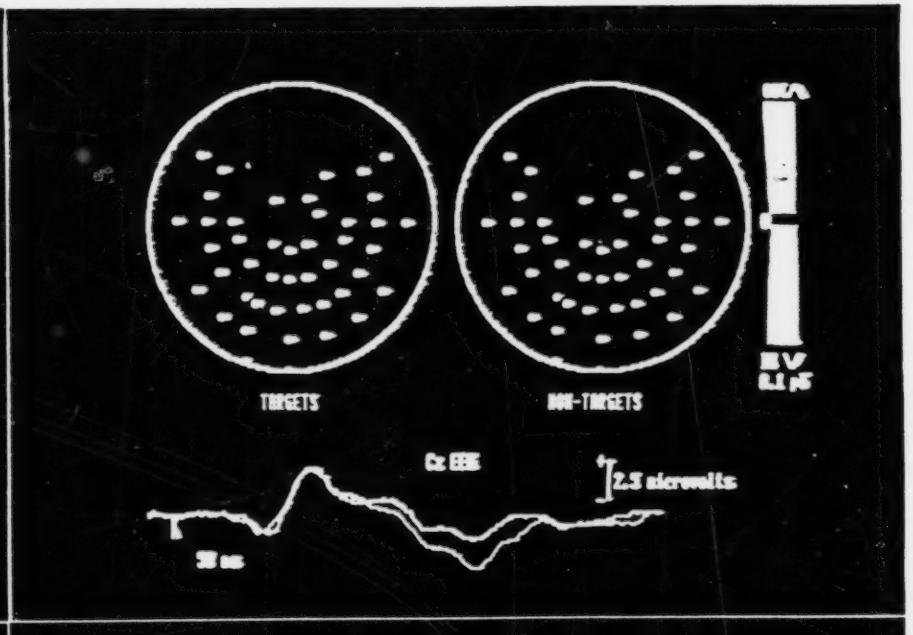
TARGETS
NON-TARGETS
Cz EEG
2.5 microvolts
300 ms

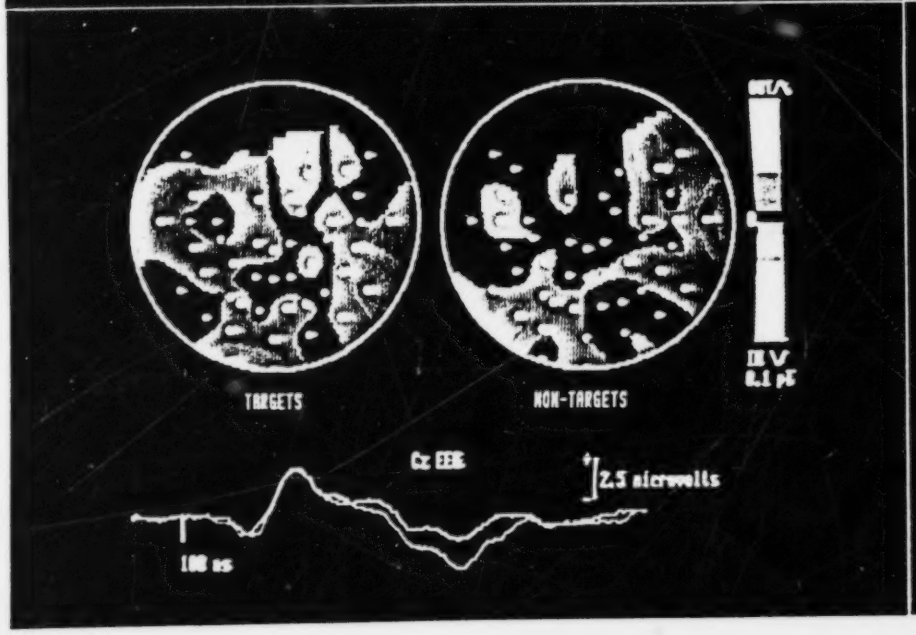
TARGETS
NON-TARGETS
Cz EEG
2.5 microvolts
100 ms

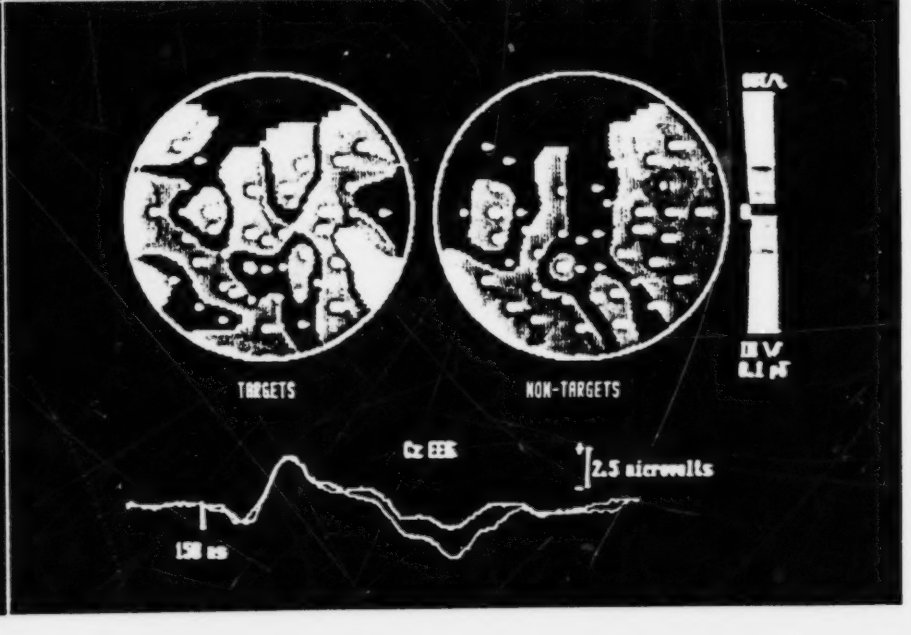
TARGETS
NON-TARGETS
Cz EEG
2.5 microvolts
150 ms

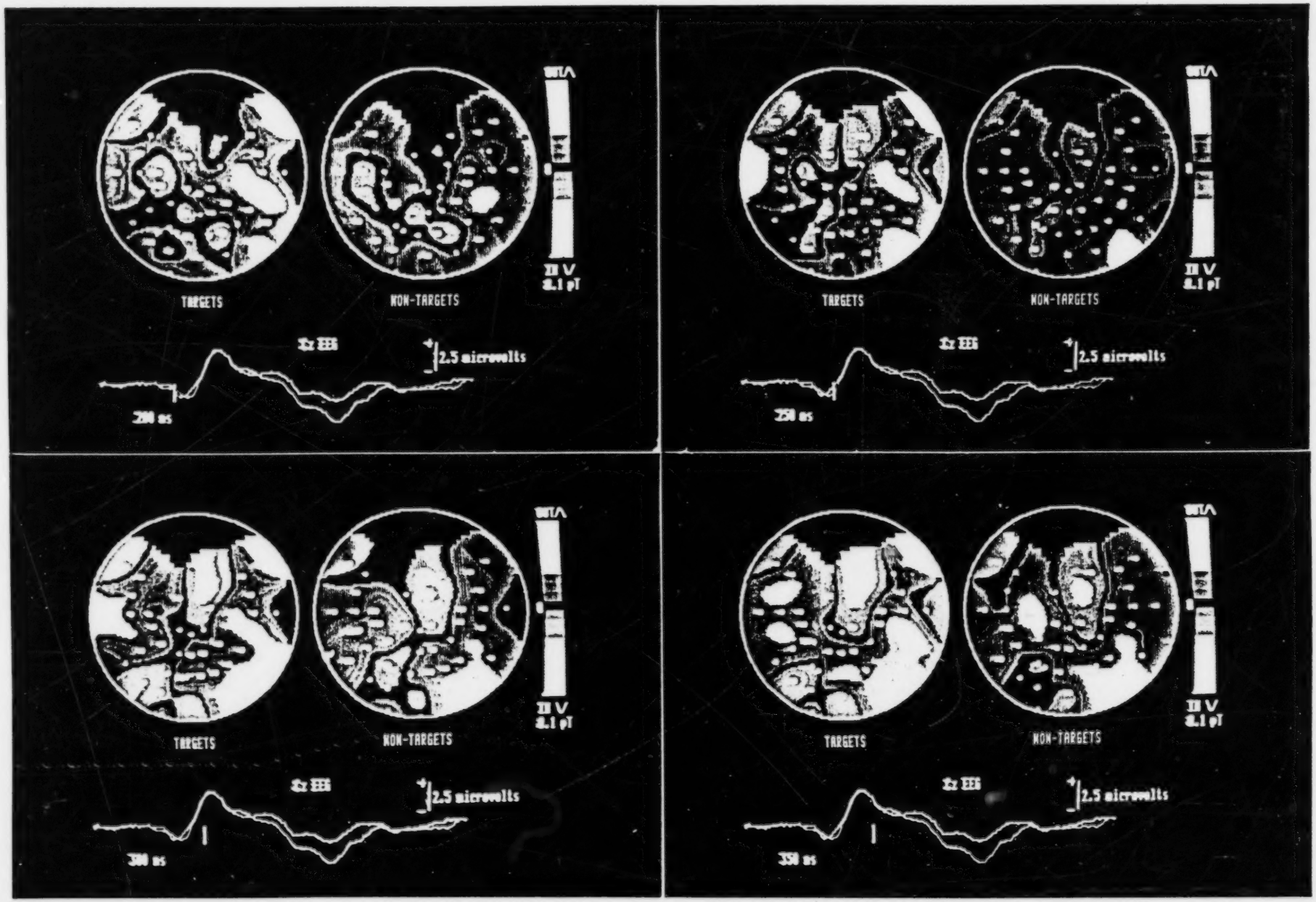
TARGETS
NON-TARGETS
11 V
8.1 pT
Cz EEG
2.5 microvolts
200 ms
TARGETS
NON-TARGETS
11 V
8.1 pT
Cz EEG
2.5 microvolts
250 ms
TARGETS
NON-TARGETS
11 V
8.1 pT
Cz EEG
2.5 microvolts
300 ms
TARGETS
NON-TARGETS
11 V
8.1 pT
Cz EEG
2.5 microvolts
350 ms

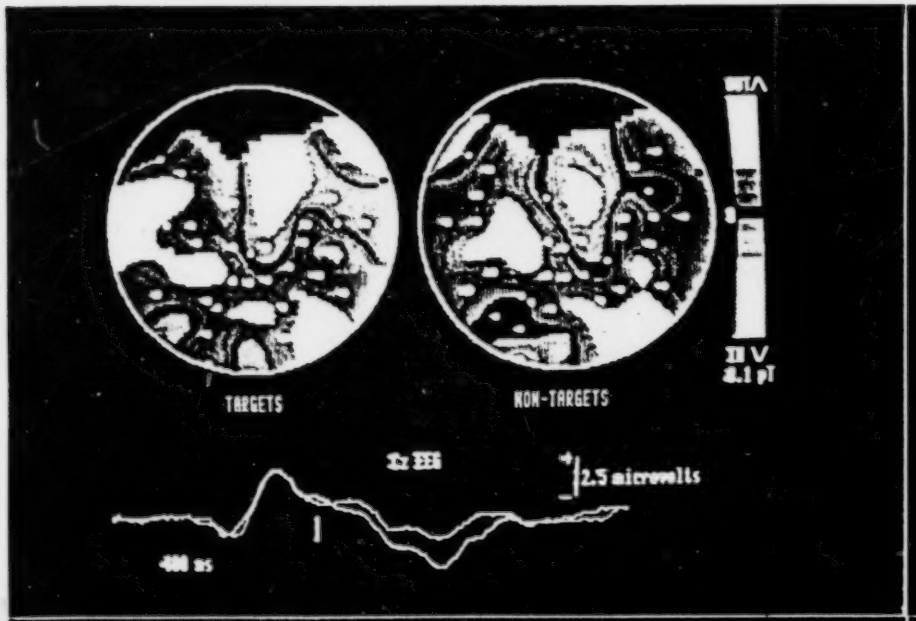
TARGETS
NON-TARGETS
2.5 microvolts
400 ms

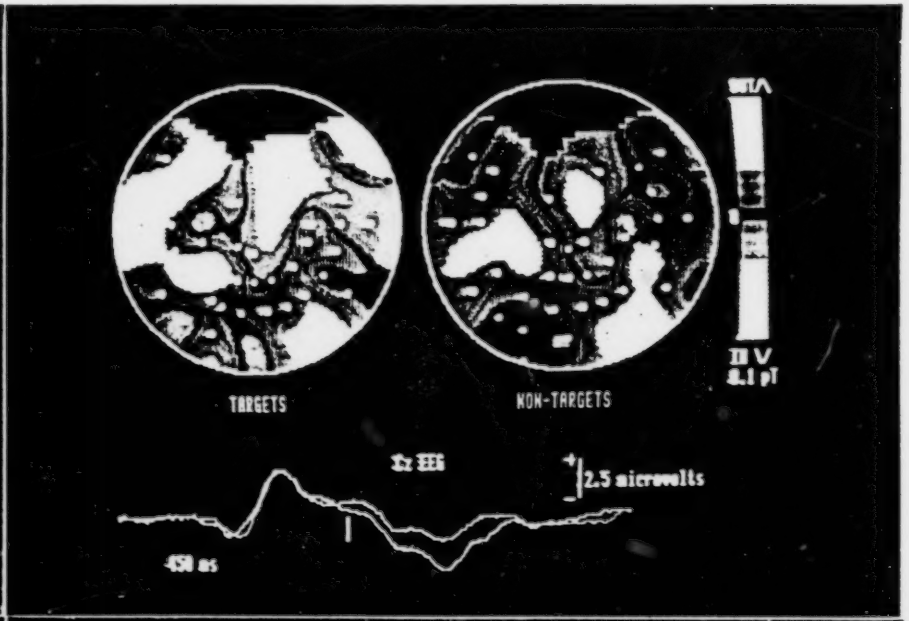
TARGETS
NON-TARGETS
2.5 microvolts
450 ms

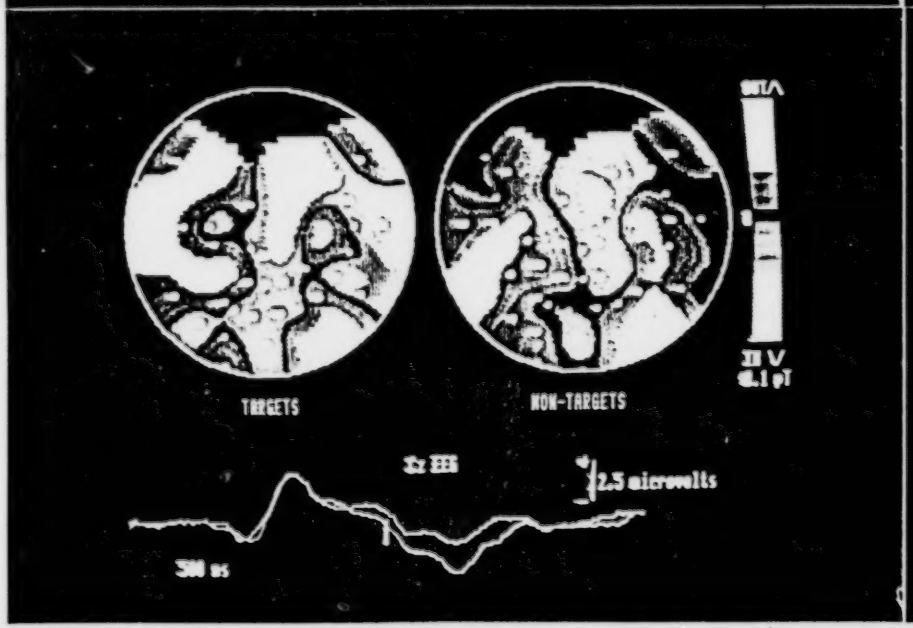
TARGETS
NON-TARGETS
2.5 microvolts
500 ms

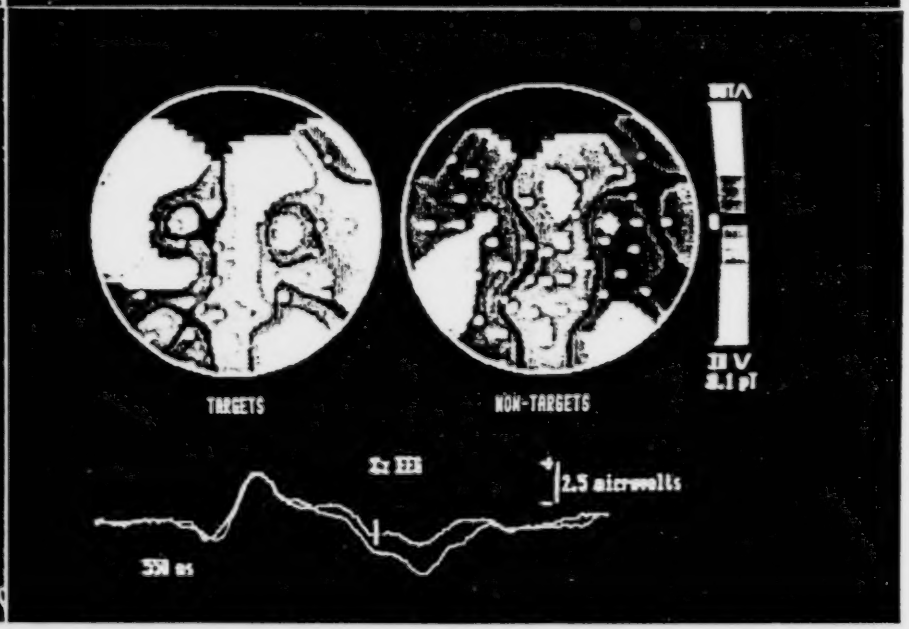
TARGETS
NON-TARGETS
2.5 microvolts
550 ms

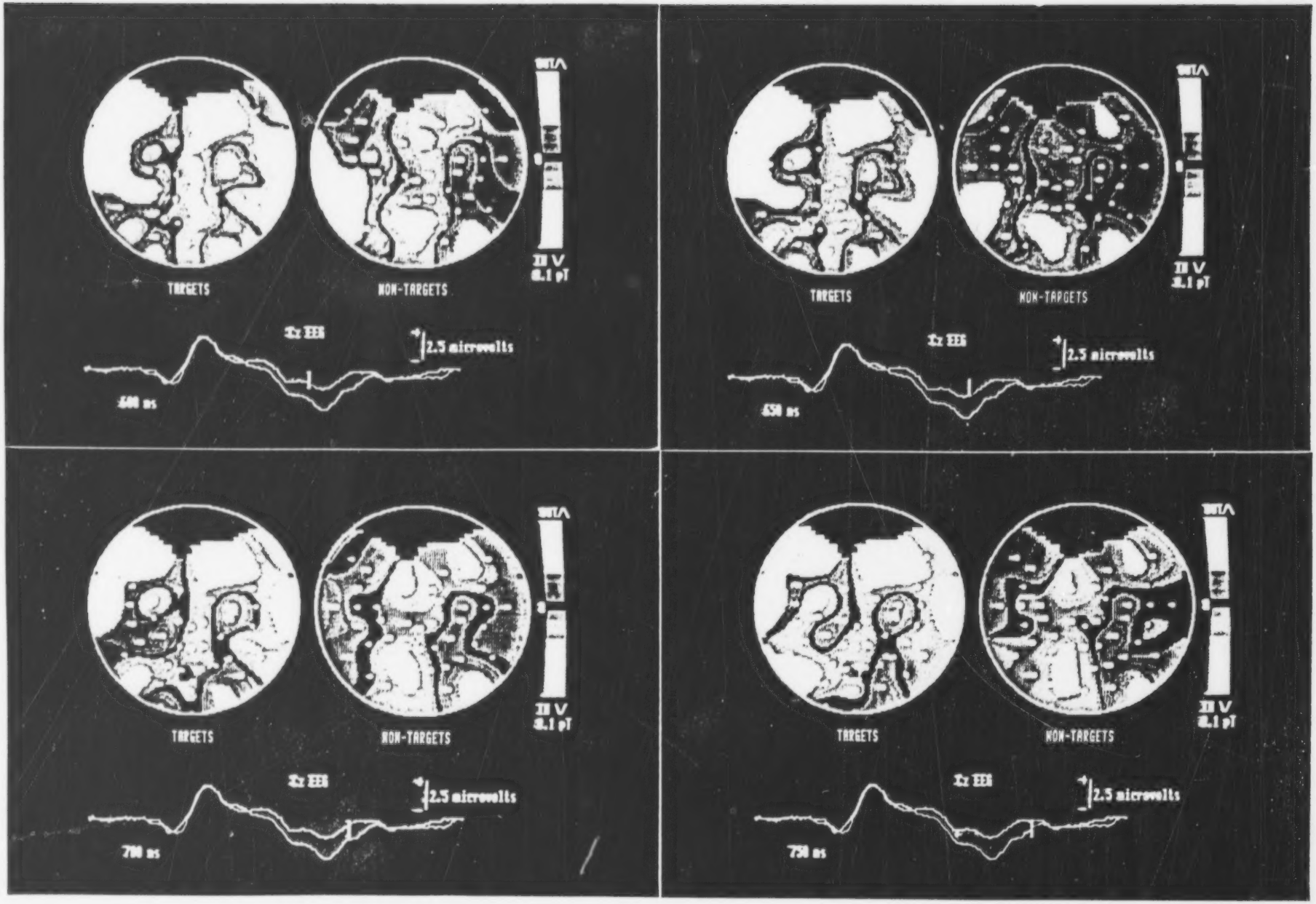
TARGETS
NON-TARGETS
2.5 microvolts
600 ms
TARGETS
NON-TARGETS
2.5 microvolts
650 ms
TARGETS
NON-TARGETS
2.5 microvolts
700 ms
TARGETS
NON-TARGETS
2.5 microvolts
750 ms

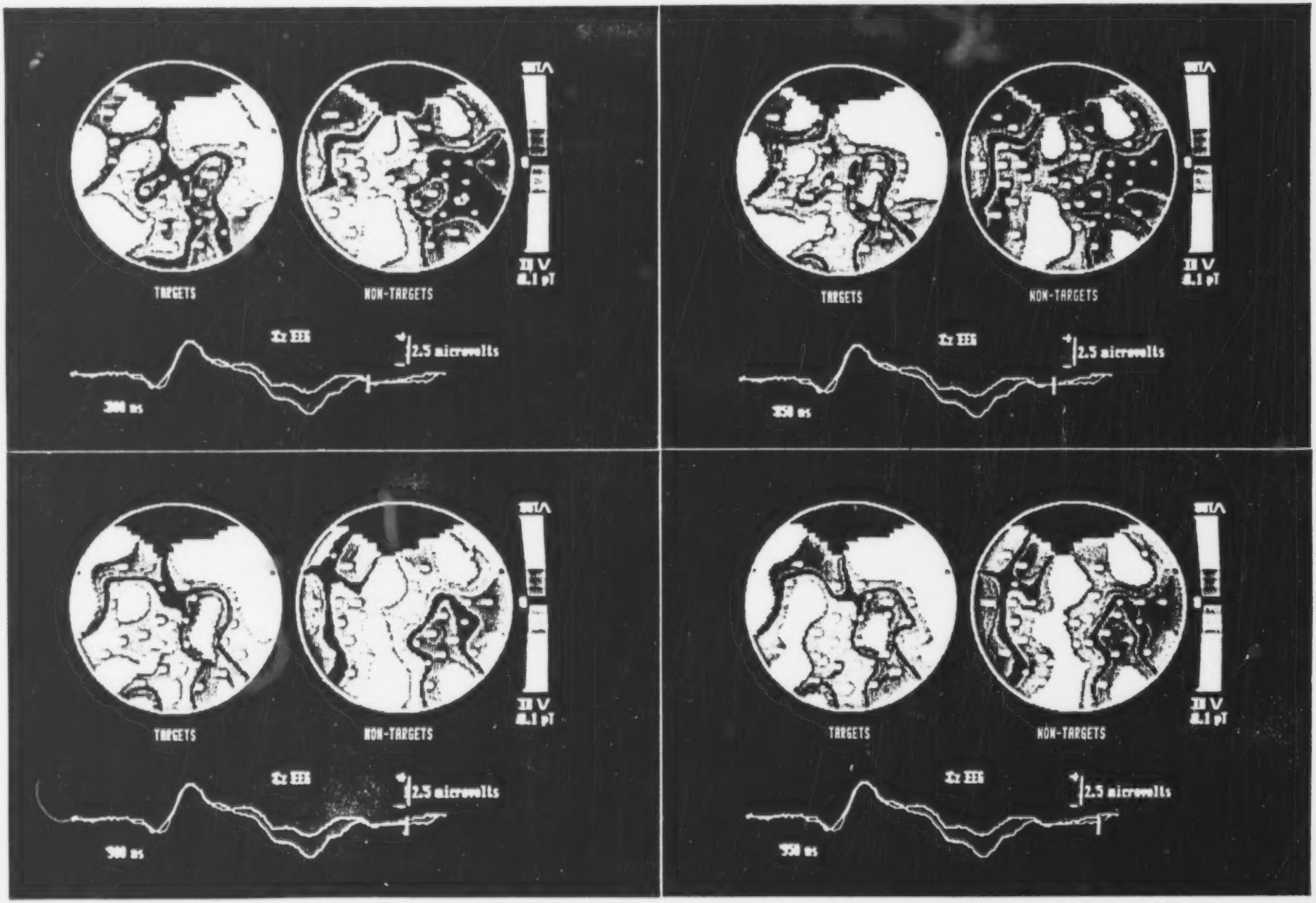
TARGETS
NON-TARGETS
2.5 microvolts
TARGETS
NON-TARGETS
2.5 microvolts
TARGETS
NON-TARGETS
2.5 microvolts
TARGETS
NON-TARGETS
2.5 microvolts

APPENDIX I

Magnetic Localisation of Intracranial Dipoles

MAGNETIC LOCALISATION OF INTRACRANIAL DIPOLES: SIMULATION WITH A PHYSICAL MODEL

H. Weinberg, P. Brickett, F. Coolsma, and M. Baff

Brain Behaviour Laboratory, Department of Psychology,

Simon Fraser University, Burnaby, B.C., V5A 1S6 (Canada)

Running title: MAGNETIC SOURCE LOCALISATION

Address for proofs:

H. Weinberg

Brain Behaviour Laboratory, Department of Psychology,

Simon Fraser University, Burnaby, B.C., V5A 1S6 (Canada)

Instruction for printers:

Figures: All the figures were designed to fit within one column width except for Figs. 6 and 7 (colour, 20 x 25 cm). These two figures were designed to be printed sideways, each on a full page, with the caption printed underneath (in vertical lines). Our preference is that they appear on facing pages. Figure 4 might not be legible if reduced to one column, as submitted. If for Fig. 4 part (c) were printed under part (b) it could appear on one column with less reduction.

Greek: The text of this paper contains five lower-case Greek letters, which are written as follows - mu (μ), phi (ϕ), theta (θ), omega (ω), and pi (π).

Keywords: Source localisation; magnetoencephalogram; dipoles; modelling.

Is this page necessary?

An important reason for a growing interest in the measurement of magnetic fields of the brain is the possibility of accurate localisation of the sources responsible for electrical changes known to be associated with both normal and pathological states of the brain (reviewed in Williamson et al. 1983). Using the simplifying assumptions that the neural generator can be modelled as a current dipole and that the head can be approximated as a sphere, the dipole location can be computed which best accounts for the observed data (Romani et al. 1985). Accurate localisation is made possible because magnetic fields are not attenuated or distorted by the various tissues of the head, a major problem for the analysis of electrical potential measurements obtained from the scalp (Plonsey 1981). Examples of recent studies which successfully employed this technique include magnetic localisation of an epileptic focus which was found to agree well with the site of a lesion appearing in CT scans (Chapman et al. 1983). Magnetic localisation of sources of sensory evoked responses for either electrical stimulation of the different digits (Okada et al. 1984), or photic stimulation of different retinal areas (Mclin et al. 1983), has located dipole sources in areas consistent with the known somatotopic and retinotopic projections of these sensory systems.

However, given that it is impossible to precisely know the total pattern of current flow in the intact, functioning brain at any instant, it is also impossible to determine the amount of error in the source localisation and to compare different localisation techniques. Results of computer modelling (Cuffin 1982; Okada 1985) have important implications for this consideration, but the accuracy of localisation in these studies is determined by the assumptions used to develop the model. Other simulation studies in which the exact location of the source is known have

used physical models which represented either a flat surface (Snyder 1982), or, for application to cardiac studies, the human torso (Eskola and Malmivuo 1983).

For brain studies an important problem is how to accommodate the actual shape of the head in the dipole localisation procedure, as the spherical approximation has been found in some cases to cause significant errors (Ricci et al. 1985). Towards this end, the physical model used for the present study consists of a human skull filled with a conducting medium in which dipoles could be positioned in known locations. Similar physical models have been used by others in studies of the accuracy of source localisation based on electrical potential measurements applied to a spherical representation of the head (Schneider 1972; Henderson et al. 1975). Such use of surface-recorded potentials requires estimates of the electrical conductivity values for the intervening tissues of the head, which are not directly measureable, and which vary markedly for the brain, skull, and scalp. However, magnetic fields produced by current dipoles have been shown to be unaffected by spherically concentric changes in conductivity (Grynszpan and Geselowitz 1973). Given the advantages of magnetic recordings for source localisation, such a skull model should be useful for quantitative evaluation of different analysis methods. A brief description of the model and preliminary data have been published (Weinberg et al. 1985).

METHOD AND MATERIAL

Skull recordings

The head model consisted of a human skull filled with EKG Sol electrode cream which had a resistivity of 650 Ohm·cm (Fig. 1). All openings in the skull were sealed with wax, except for the foramen magnum which was closed with a rubber bung. Each current dipole was 22 mm in length, constructed from aligned ends of pairs of wires forming the top of a "T". The wires were insulated except at the ends which were capped with 1 mm spheres of solder. Three such dipoles, arranged to form an equilateral triangle and mounted on plexiglass tubing, were inserted into the skull through the foramen magnum and positioned 6 mm below the parietal bone. The posterior corner of the triangle was located at the vertex. The exact position of each dipole was later calculated with measurements made from radiographs. Dipoles were energised by electrically isolated constant-current sources which supplied a 45 Hz square wave current of 125 μA for EEG recording and of 70 μA for MEG recording. Recordings were made for each dipole energised individually and also for dipoles II and III energised simultaneously. Electrical potentials were recorded from GKASS gold cup electrodes attached to the skull with dental cement at the 10/20 international system locations and additional locations near the dipoles (Fig. 2). Linked reference electrodes were attached 15 mm above the external auditory meati; linked grounding electrodes were attached to the cheekbones.

Magnetic recordings from the same positions were obtained with a third order gradiometer manufactured by CTF Systems Inc. (Vrba et al. 1982). The diameter of the sensing coil of this instrument is 38 mm and the inter-coil separation is 55 mm. For each recording the skull was positioned on a

wooden gimbal so that the surface of the skull was normal to the vertically oriented gradiometer. Thirty-two 250 msec epochs of data were averaged, rectified about the mean, and integrated. The resulting values were used to construct isofield and isopotential contour maps of the whole scalp and a five times enlargement of the area near the dipoles. Details of the mapping techniques are included in Weinberg et al. (1985). The two-dimensional projection of the head illustrated in Fig. 2 is termed an azimuthal equidistant projection in cartography (Kellaway 1949), and has the property that equal arc lengths on meridians (through the pole at the vertex) are projected as equal distances.

Least-Squares Dipole Fitting

For the computations described below the coordinates of the 10/20 system and added locations on the skull were first measured with respect to a rectangular coordinate system. The origin was initially located in the horizontal plane determined by the nasion and the left and right preauricular points, on the vertical projection of the nasion-inion line at the perpendicular to the left preauricular point. After making various plots of the skull coordinates and also computing the least-squares estimate of the origin which best fits a sphere to the measured scalp locations, a more dorsal origin was located on the vertical axis at its intersection with the projection on the sagittal plane of the line connecting Fp and Oz.

The linear distance (R) from the origin to each recording position was calculated from the measured coordinates for that position. A distance of 12 mm was added to account for the distance between the sensing coil and

the bottom of the dewar. The two angles for azimuth and inclination, which together with R defined in spherical coordinates the location of each recording position, were the same as those used for the mapping projection.

The five parameters for a tangential current dipole: distance from the origin (b), dipole moment (Q), azimuth (ϕ), inclination (θ), and orientation (ω) were initially estimated using the peak-location method of Williamson and Kaufman (1981). For this method we used the largest of the two field strength values recoıded at the maximum and minimum positions, and the radius was taken as the mean of the two radii to these positions on the skull. For the iterative least-squares method, the technique used was based on the "Simplex" algorithm as described by Caceci and Cacheris (1984) and was programmed on a microcomputer. At each iteration, the dipole parameters were changed slightly and the magnetic flux density in the radial direction (Br) was predicted for each position using the following equation from Williamson and Kaufman (1981, equation 14) after the coordinate system had been rotated so as to position the dipole as shown in Fig. 3.

$$Br = \frac{\mu_0 Q}{4\pi d^2} \frac{\frac{b}{d} \cos\beta \sin\epsilon}{\left[1 + \frac{2bR}{d^2}(1-\cos\epsilon)\right]^{3/2}}$$

where Br is in units of newton per ampere-meter (N/A·m), also known as tesla (T); Q is in ampere meters (Am); μ_0 is a constant of proportionality for the permeability of free space, equal to $4\pi \times 10^{-7}$ N/A^2; R, b, and d are in meters; and d equals R-b.

At each iteration the sum of squared differences between the predicted and the measured Br values were calculated as an index of the remaining error for the dipole fit. Iterations were continued to minimize the error

until convergence was reached, normally requiring from two- to five hundred iterations.

Comparison of Different Procedures

The least-squares and peak-location methods were compared for three different conditions. First, for the "unisphere" model, the Br values from all the recorded positions were used to locate the dipole in the skull modelled as a single sphere of fixed radius, the value of the radius used being the mean of the measured distances from the origin to each of the 25 recording positions.

For the second condition the skull was modelled as a collection of 25 spheres, all centered on the origin, but with radii equal to the measured distance to each of the recording positions. This model was implemented by using for R in the equation above the radius at a recording position in calculating the predicted value of Br at that position. Figure 4 illustrates the measured distances from the origin to the 21 points of measurement in the horizontal, coronal, and sagittal planes. All 25 radii are in addition shown in a topographical map in Fig. 5. Positions on the skull are the same as in the whole-head diagram in Fig. 2. Red-yellow colors in this figure indicate a bulge in the skull, as seen in the parietal-occipital area, while blue-cyan indicate areas of the skull closer to the origin, as observed at temporal positions. One anatomical feature that can be visually appreciated from Fig. 5 is that although the skull shows strong left-right symmetry, the left hemisphere is slightly more prominent at parietal-occipital locations.

Finally, for the third condition, the relative sensitivity of the least-squares method to errors in peak location was investigated by excluding the two positions producing the maximum and minimum Br values. This approximates the effect of reduced density of sampling positions over the skull, which will on average correspondingly increase the error in the location of the peak and the measured Br value. Most of the published research in magnetic localisation has made use of rectangular grids of recording positions with separation distances of 2 to 4 cm (see reviews in Williamson et al. 1983). Ignoring the problem of fitting a plane to a curved surface, for a square grid with spacing S the maximum distance between the location of a peak within the grid and the nearest grid point is equal to $S/\sqrt{2}$. For the present study however, the positions were not sampled in a regularly spaced array. An equivalent measure was therefore derived from the distance of the peak locations calculated theoretically to the nearest recording position for each of the three dipoles. The average for the six values was .83 cm, corresponding to an equivalent grid spacing of 1.2 cm. To simulate a coarser grid spacing, data were discarded from the two recording positions for each dipole which showed the highest and lowest values (the peaks). The error in peak location for the remaining positions corresponded to an equivalent grid spacing of 3.9 cm. The "no peaks" condition was the use of the remaining 23 positions for localising each dipole using the peak-location and least-squares methods.

RESULTS

Topographical mapping

Figure 6 shows maps of the recorded electric and magnetic data for dipoles I, II, and III as well as the predicted Br values from the least-squares dipole fitting using the multisphere model. Results of the dipole-fitting are presented quantitatively in the next section. For the recorded data in Fig. 6 the maps showed that, as expected, a single dipole produced relatively symmetric fields. Consistent with the right hand rule, the line connecting the magnetic field extrema was perpendicular to the dipole axis. The electrical field shown in Fig. 6 was rotated 90 degrees with respect to the magnetic field. Maximum positivity and negativity of the electrical field were located over the positive and negative poles of the dipoles, respectively. These results were what would be expected for a single dipole (Cohen and Cuffin 1983).

For the maps of the predicted data, the arrow position indicated the least-squares dipole localisation. In general, the difference between the actual and predicted dipole position was not very great, the most noticeable error being that for dipole I. For the predicted maps, although the absolute amplitudes were not very accurate, as reflected in the difference in scale, the general shape of the predicted and recorded fields were quite similar.

Figure 7 presents maps for two different combinations of dipoles II and III; II+III (top) and II-III (bottom), in which for the latter the polarity of dipole III was reversed. Maps are shown for both recordings done with the two dipoles simultaneously energised and also for the calculated sum (II+III) or difference (II-III) of the data presented in Fig. 6. The measured and calculated fields in Fig. 7 were nearly identical

in both general shape and absolute amplitude. Small differences were also more easily found for the electric data than for the magnetic data, e.g. at position Pz for II-III. The similarity of the measured and constructed maps indicates that the recordings are reliable and also that, as predicted by theory, magnetic as well as electric fields from independent sources add linearly.

Comparing the two combinations, the field for II-III appeared very similar to that for a single dipole, whereas the field for II+III was more asymmetrical in shape and showed an extended distribution of the outward-going (blue) magnetic flux.

For the predicted maps, the numbers on the figure indicate whether one or two dipoles have been used to model the recorded data. The two dipole maps have been calculated by adding or subtracting the predicted values for dipoles II and III shown in Fig 6. The single dipole maps show the predicted values for the single equivalent dipole which best fits the two-dipole data. The location of the single equivalent dipole was similar for both II+III and II-III combinations, but the dipole orientation was quite different.

Comparing the maps of the predicted and recorded values, the two-dipole solution, as should be expected, appeared quite similar to the recorded data. The single dipole solution predicted the data for II-III quite well, but for II+III the extended distribution of emergent flux could not be duplicated with a single dipole.

Quantitative dipole measures

Table I includes the actual values for all five parameters of each dipole and the estimates calculated by the least-squares method for the multisphere model. Of the five parameters, Q was consistently found to be underestimated, which was to be expected since we had not corrected for the effects of the relatively large diameter of the sensing coil and its relatively small distance to the other coils of the gradiometer (Cuffin and Cohen 1983). Other errors were more difficult to account for, the largest being that for the azimuth of dipole I, which resulted in the dipole being localised to the left of its actual position, as shown in Fig. 6.

The last two columns in the table provide summary measures of how well the parameters of each dipole have been estimated. The first of these is a function of the criterion which was minimized by the Simplex algorithm for the dipole fitting procedure. That criterion is the sum of the squared differences between the observed Br values and those values calculated for a dipole with the parameters as estimated. The ratio of this criterion and the sum of squares of observed values gives the proportion of error relative to the original data (%SS). This error measure, which can also be expressed as the percentage of variance not accounted for by the model, was larger for dipole I than for dipoles II and III.

Although this error measure can be used to establish how well a particular model fits different sets of data, there are similar problems as with other least-squares methods in that increasing the number of parameters in the model or decreasing the number of positions will tend to increase the goodness of fit. For example, if there are only five positions measured, a dipole can always be found which accounts for 100% of the data. This criterion was therefore not appropriate for a comparative evaluation of the peak-location method or the goodness of localisation for

the reduced number of positions when the peaks had been discarded.

The last column in Table I gives a different error criterion, the three-dimensional (3D) location error. This is the distance between the center of the physical dipole and the point in space determined by the predicted parameters b, β, and θ. The other two parameters, which determine the dipole moment and orientation, have no influence on this value, but these parameters are of less importance than those which determine location. The location error was also greatest for dipole I, while the mean location error for the three dipoles was 3.5 mm.

The 3D location error measure was used to summarize the relative accuracy of the single dipole fits for the least-squares and peak-location methods applied in the three experimental conditions. Figure 8 presents these data graphically. By far the largest error occurred for the peak-location method in the "no peaks" condition, i.e. for which the maximum and minimum positions had been discarded and the equivalent grid spacing increased from 1.2 to 3.9 cm. The least-squares method, on the other hand, showed no increase in error when the peaks were discarded, and actually the error was slightly less for each of the three dipoles. The suspected reason why the least-squares method did so well with less data was that the Br value at a peak could not be accurately measured with a relatively large sensing coil, so a proportionally larger measurement error was made at the peak than at other parts of the field. Therefore, when the peak positions were discarded the dipole parameters were estimated more accurately.

For the unisphere model for which a constant radius was used equal to the mean of the 25 radii, the least-squares and peak-location methods did about equally well. For the multisphere model the peak-location method

using the radius equal to the average radius of the maximum and minimum positions resulted in about the same error as that found for the unisphere model, but the least-squares method showed the best accuracy for the multisphere model.

Two dipole combinations were investigated for dipoles II and III because this pair is oriented symmetrically with respect to the recording locations and also because almost 98% of the variance for both dipoles II and III was accounted for by a single dipole model. Approximately the same percentage of variance was accounted for by a two-dipole solution for the combinations II+III and II-III (Table II). The two-dipole fits were computed by simply adding or subtracting the predicted Br values for the single dipoles. A single-dipole model fit to the data for II+III showed approximately 8% error, but this figure was only 2% for the combination II-III. This shows that when current flow was in the primarily posterior direction (Fig. 7, bottom right), the resulting field pattern was virtually indistinguishable from that produced by a single dipole. The field for II+III however was significantly different from that for the best fitting single dipole ($F(5,20) = 10.2$, $p < .001$).

The suspected reason for the difference in the single dipole fit for the two combinations is related to the relative dipole orientation. The orientation angles (ω) of dipoles II and III differ by 126 degrees, but for the combination II-III subtracting dipole III is equivalent to addition after a 180 degree phase shift. This results in an orientation difference of only 60 degrees and more similarity to a single dipole.

DISCUSSION

For the purpose of testing localisation procedures, the advantage of using a physical skull model rather than either a computer simulation or an intact, functioning head is that although the problems of data recording are similar to those encountered when recording from subjects, the actual nature and location of the source is known. The original intention prior to the beginning of this research was to show that magnetic recordings could be made which corresponded to those predicted from physical theory. Initial results indicated qualitative agreement with theory. Further research was then done to quantitatively compare different localisation methods and to investigate one approach to the problem of the non-sphericity of the head.

Our results indicate that the least-squares localisation method, although requiring more computational effort, does have as a major advantage over the

peak-location method the benefit that less recording positions are necessary for accurate localisation of a dipole source. Furthermore, the multisphere model was also found to partially accommodate for the anatomical shape of the head and to increase the accuracy of source localisation, with only a minor addition to the computational procedure.

Other sources of error which we are presently investigating include the gradiometer sensing coil diameter and coil separation distance, the difference between the normal and radial magnetic components, and also the length of the dipole.

The skull model has been found to be useful for investigations related to head shape, but it is not a realistic model for other problems, such as the effects of non-concentric inhomogeneities due to different tissues in the head. Ideal for such a study would be patients with intracerebral electrodes implanted for recording purposes. Smith et al. (1983) recorded potentials from the scalp produced by the dipoles formed by energising the implanted electrodes using currents too small to result in tissue damage but which were large enough to be sensed with a biomagnetometer.

Generally speaking, the task of source localisation requires answering two questions, i.e., what is the nature of the source, and where is it located? Although the present study relates primarily to the second question, understanding the nature of sources is at least as important. The concept of the current dipole has proven useful as a means of making source localisation possible, but it is not an adequate representation of the complexity of anatomical structures.

Future work is planned with the skull model which will employ more realistic source configurations. Results from these and other studies may hopefully lead to more sophisticated localisation methods and a better understanding of the field patterns recorded from the brain.

SUMMARY

Current dipoles energised by isolated sources were located in known positions inside a human skull filled with an electrically conductive medium. Maps of the measured electrical and magnetic fields confirmed the predicted relationships between those fields for both single and multiple

dipoles. Two methods of dipole localisation were compared: the peak location method which used only the locattions of the maximum and minimum recorded values, and a least-squares iterative method which found the parameters for a dipole such that the sum of squared differences between the recorded and predicted data was minimized. Also, in an attempt to account for some of the error due to the non-sphericity of the head, the measured distance from the centre of the skull to each recording position was used in the dipole calculations. This last technique resulted in the smallest three-dimensional location error (averaging 3.5 mm) for the least-squares method, even when no recording positions were near the actual field extrema and the peak-location method therefore produced much greater error. Combinations of two dipoles were also investigated for which the magnetid field maps appeared similar to those for a single dipole and comparisons were made to determine how well single and double dipole models could account fot the recorded data.

Résumé

Localisation magnétique des dipôles intra-craniales: simulation avec un modèle physique. Des dipôles de courant energisés par des sources électriques isolées étaient situés à des positions connues en dedans dún crane humain remplit avec un intermediaire conductif. Des cartes topographiques des champs magnétiques et électriques mesurés confirmaient la relation entre ces deux champs pour des dipôles simples ainsi que pour des dipôles multiples. Deux méthodes étaient comparées: la methode de localisation de crête quin'emploit

que les positions des valeurs enregistrees maximum et minimum, et une methode iterative aux carrees minimises qui determine les parametres d'un dipole de maniereace que le total des differences au carre entre les valeurs enregistrees et celles prevues soit minimise. De meme facon, en tentant de rendre compte de la non-sphericite de la tete, la distance mesuree du centre du crane a chaque position d'enregistrement etait employee dans le calcul des parametres des dipoles. Cette technique resultait en la plus la methode des carres minimises, meme qu'aucune des positions d'enregistrement etait situee aupres des extremes actuels du champ, et par consequent la methode de localisation de crete produisait une erreur plus grande. Des combinaisons de deux dipoles etaient aussi recherchees pour lesquelles les cartes topographiques de leurs champs magnetiques ressemblaient celles pour un dipole simple et comparaisons etaient faites pour determiner quelle mesure des modeles de dipoles simples et doubles pourraient rendre compte du champ magnetique.

The authors wish to thank Drs. J. Vrba and R. Harrop for helpful discussion, DR. M. Low for the radiography, and H. GAbert for technical assistance. This study was supported by N.S.E.R.C., N.R.C., Minstry of Trnasport, D.S.S. of Canada, and the Science Council of B.C.

REFERENCES

Caceci, M.S. and Cacheris, W.P. Fitting curves to data. Byte, 1984, 9(5): 340-362.

Chapman, R. M., Romani, G. L., Barbanera, S., Leoni, R., Modena, I., Ricci, G. B. and Campitelli, F. SQUID instrumentation and the relative covariance method for magnetic 3D localization of pathological cerebral sources. Lett. Nuovo Cimento, 1983, 38: 549-554.

Cohen, D. and Cuffin B. N. Demonstration of useful differences between magnetoencephalogram and electroencephalogram. Electroenceph. clin. Neurophysiol., 1983, 56: 38-51.

Cuffin, B. N. Effects of inhomogeneous regions on electric potentials and magnetic fields: Two special cases. J. Appl. Phys., 1982, 53: 9192-9197.

Cuffin, B. N. and Cohen, D. Effects of detector coil size and configuration on measurements of the magnetoencephalogram. J. Appl. Phys., 1983, 54: 3589-3594.

Eskola, H. and Malmivuo, J. Optimizing vector magnetocardiographic lead fields by using a physical torso model. Il Nuovo Cimento, 1983, 2D: 356-367.

Grynszpan, F. and Geselowitz, D. B. Model studies of the magnetocardiogram, Biophys. J., 1973, 13: 911-925.

Henderson, C. J., Butler, S. R. and Glass, A. The localization of equivalent dipoles of EEG sources by the application of electrical field theory. Electroenceph. clin. Neurophysiol., 1975, 39: 117-130.

Kellaway, G. P. Map Projections. Methuen, London, 1949.

Mclin, E., Okada, Y. C., Kaufman, L. and Williamson, S. J. Ketinotopic map on the visual cortex for eccentrically placed patterns: First noninvasive measurements. Il Nuovo Cimento, 1983, 2D: 410-419.

Okada, Y. C. Discrimination of localized and distributed current dipole sources and localized single and multiple sources. In: H. Weinberg, G. Stroink and T. Katila (Eds.), Biomagnetism: Applications and Theory. Pergamon Press, New York, 1985: 266-272.

Okada, Y. C., Tanenbaum, R., Williamson, S. J. and Kaufman, L. Somatotopic organization of the human somatosensory cortex revealed by neuromagnetic measurements. Exp. Brain Res., 1984

Plonsey, R. Generation of magnetic fields by the human body (theory). In: S. N. Erne', H. D. Hahlbohm and H. Lübbig (Eds.), Biomagnetism. Walter de Gruyter, Berlin, 1981: 177-205.

Ricci, G. B., Leoni, R., Romani, G. L., Campitelli, F., Buonomo, S. and Modena, I. 3-D neuromagnetic localization of sources of interictal activity in cases of focal epilepsy. In: H. Weinberg, G. Stroink and T. Katila (Eds.), Biomagnetism: Applications and Theory. Pergamon Press, New York, 1985: 304-310.

Romani, G. L. and Leoni, R. Localization of cerebral sources by neuromagnetic measurements. In: H. Weinberg, G. Stroink and T. Katila (Eds.), Biomagnetism: Applications and Theory. Pergamon Press, New York, 1985: 205-220.

Schneider, M. R. A multistage process for computing virtual dipolar sources of EEG discharges from surface information. IEEE Trans Biomed. Eng., 1975, 19: 1-12.

Smith, D. B., Sidman, R. D., Henke, J. S., Flanigin, H., Labiner, D. and Evans, C. N. Scalp and depth recordings of induced deep cerebral potentials. Electroenceph. and clin. Neurophysiol. 1983, 55: 145-150.

Snyder, U. K. Neuromagnetism: A short theoretical and experimental study. M.A. thesis, 1982, Dalhousie University.

Vrba, J., Fife, A. A., Burbank, M. B., Weinberg, H. and Brickett, P. A. Spatial discrimination in SQUID gradiometers and 3rd order gradiometer performance. Canadian J. Phys., 1982, 60: 1060-1073.

Weinberg, H., Brickett, P., Coolsma, F. and Baff, M. Topography of simulated MEG and EEG generated by multiple intracranial dipoles. In: H. Weinberg, G. Stroink and T. Katila (Eds.), Biomagnetism: Applications and Theory. Pergamon Press, New York, 1985: 273-277.

Williamson, S. J. and Kaufman, L. Magnetic fields of the cerebral cortex. In: S. N. Erne', H. D. Hahlbohm and H. Lübbig (Eds.), Biomagnetism. Walter de Gruyter, Berlin, 1981: 353-402.

Williamson, S. J., Romani, G.L., Kaufman, L., and Modena, I., (Eds.), Biomagnetism: An Interdisciplinary Approach. Plenum Press, New York, 1983.

TABLE I

Single dipole fits for individual dipoles.

	Dipole parameters (actual, estimated)					Error measures	
Dipole	b(mm)	Q(uAm)	ϕ(deg)	θ(deg)	ω(deg)	%SS	3D(mm)
I	80, 78	1.5, 1.4	2.1, 15	14, 15	265, 270	4.0	5.1
II	80, 82	1.5, 1.4	334, 334	7.0, 8.0	145, 154	2.1	2.3
III	80, 80	1.5, 1.3	34, 37	8.5, 6.3	29, 31	2.1	3.1

TABLE II

Single and double dipole fits for two dipole combinations.

	Single equivalent dipole fit						Two dipole fit
Dipoles	b(mm)	Q(uAm)	ϕ(deg)	θ(deg)	w(deg)	error %SS	error %SS
II+III	80	1.9	357	1.9	98	7.6	1.7
II-III	82	2.0	1.2	4.9	176	2.0	2.4

FIGURE CAPTIONS

Fig. 1. Radiograph showing location of dipoles and connecting wires in the skull. The inset at upper right is a tracing identifying the dipoles.

Fig. 2. Schematic diagram of the dorsal surface of the skull showing the 10/20 system and the additional recording positions located just anterior of Cz, as indicated by the dots. The locations of dipoles I, II, and III are indicated by arrows in the five times enlargement of the central area.

Fig 3. Coordinate system used for the calculation of the radial magnetic flux density (Br) at point P. The XYZ axes are first rotated so that the dipole is in the position shown. This is the position for which the formula for calculating Br applies.

Fig. 4. Distance from the origin to the location on the skull for each of the 10/20 system electrode positions indicated, shown for (a) the horizontal, (b) the coronal, and (c) the sagittal planes. Dashed lines indicate positions for which no recordings were obtained. Unlabelled lines are added positions, close to the location of the dipoles.

Fig. 5. Isocontour map of the radius measurements. Values are presented as deviations from the mean radius, which was 92 mm. Each contour interval corresponds to 2 mm; maximum difference from the mean is 18 mm.

Fig. 6. Isocontour maps for dipoles I, II, and III (top to bottom). For each pair of maps, the whole head view is shown on the left and the 5 times enlargement is on the right, with recording locations as indicated in Fig. 2. For the maps of recorded electric and

magnetic data, the arrow indicates the actual dipole location and orientation, while for the predicted magnetic maps the arrow shows the result of the dipole fitting procedure. A dot indicates the dipole centre; the length of the arrow represents the actual length of the wires in the skull. Color bars at bottom show polarity conventions, for which an upward-pointing arrowhead indicates that the magnetic field is emerging from the skull. For the six columns of maps from left to right, the amplitude range from black (zero) to white corresponds to 1.75 mV, 4.0 mV, 85 pT, 125 pT, 38 pT, and 60 pT, respectively.

Fig. 7. Maps for two dipole combinations II+III (top) and II-III (bottom). For maps of recorded data the label "M" signifies that the data were measured by recording with both dipoles simultaneously energised (for II-III the direction of current flow was reversed in dipole III); "C" indicates that the map was calculated from the data for dipoles II and III shown in Fig. 6 by adding or subtracting the two values at each position. Predicted maps are labeled with a number to indicate either a 1 or 2 dipole solution. Same calibration as in Fig. 6.

Fig. 8. Mean absolute error in 3D dipole location (mm). Peak location and least-squares methods are compared for three conditions: the unisphere head model, the multisphere model, and the multisphere model for which the positions yielding the maximum and minimum values have been discarded (no peaks).

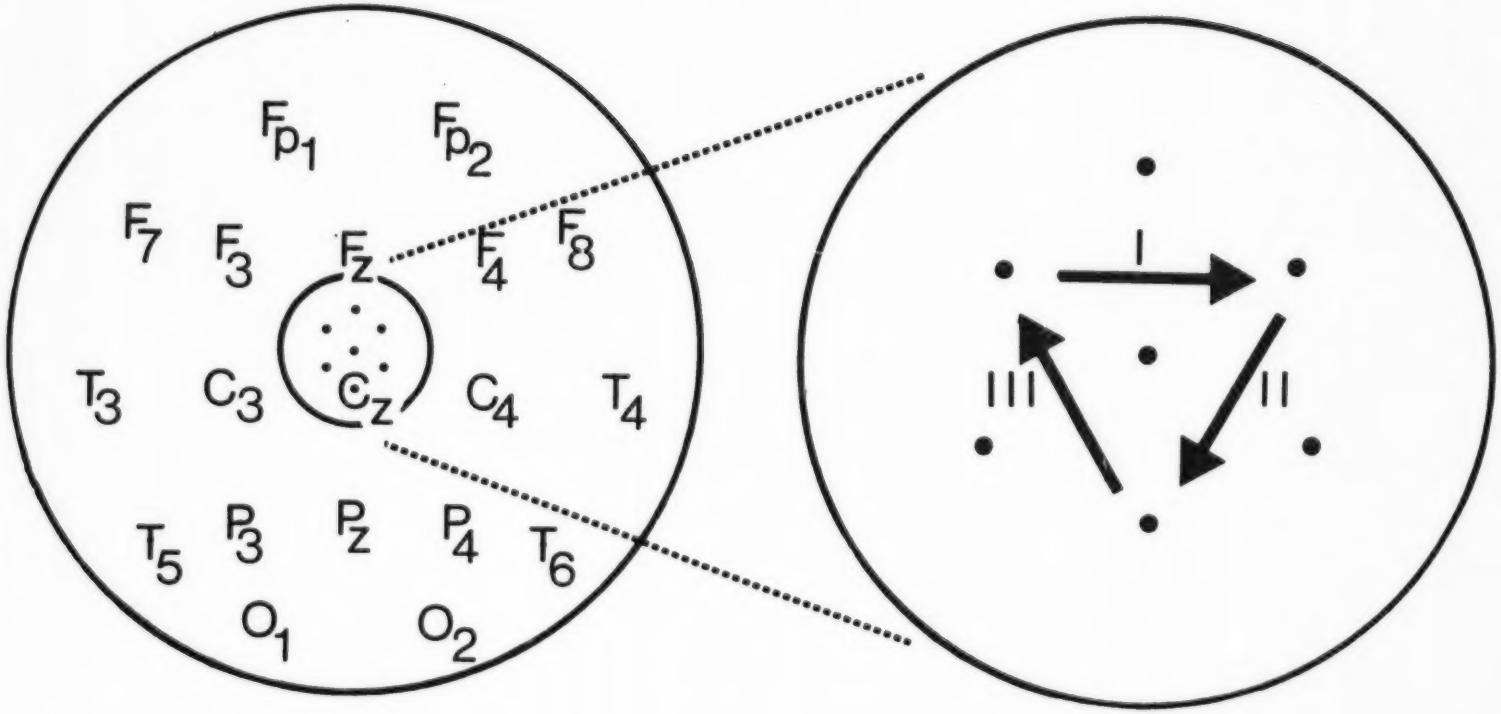
Fp1
Fp2
F7
F3
Fz
F4
F8
T3
C3
Cz
C4
T4
T5
P3
Pz
P4
T6
O1
O2
I
II
III

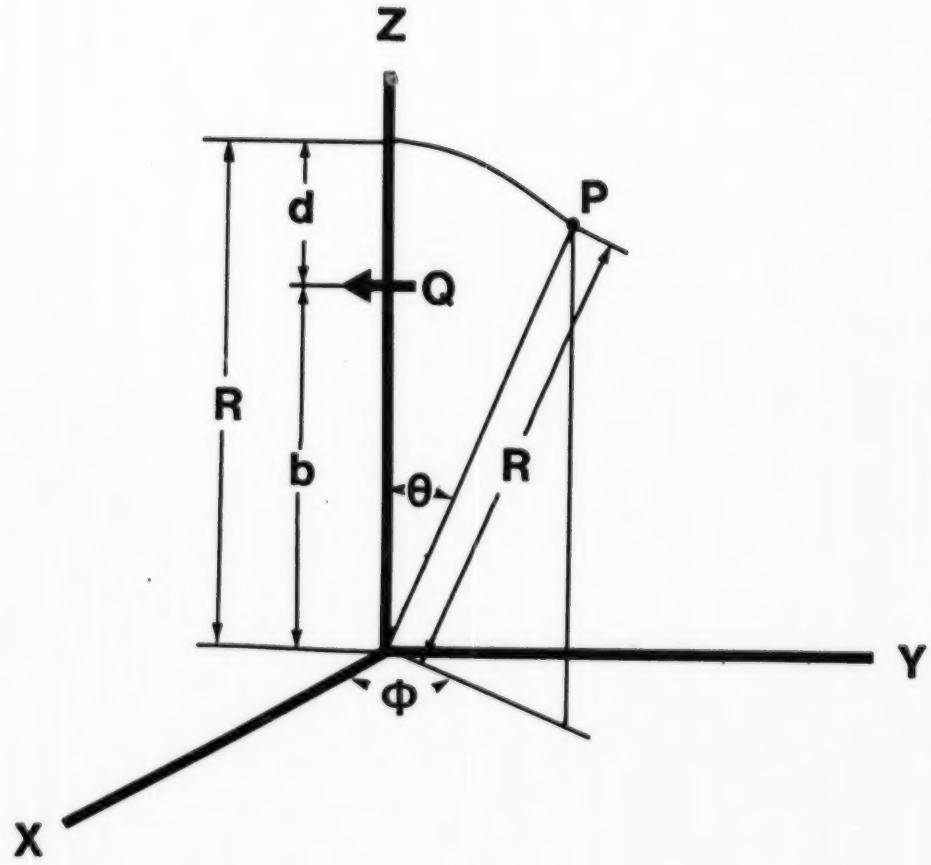
Z
d
P
Q
R
b
θ
R
Y
Φ
X

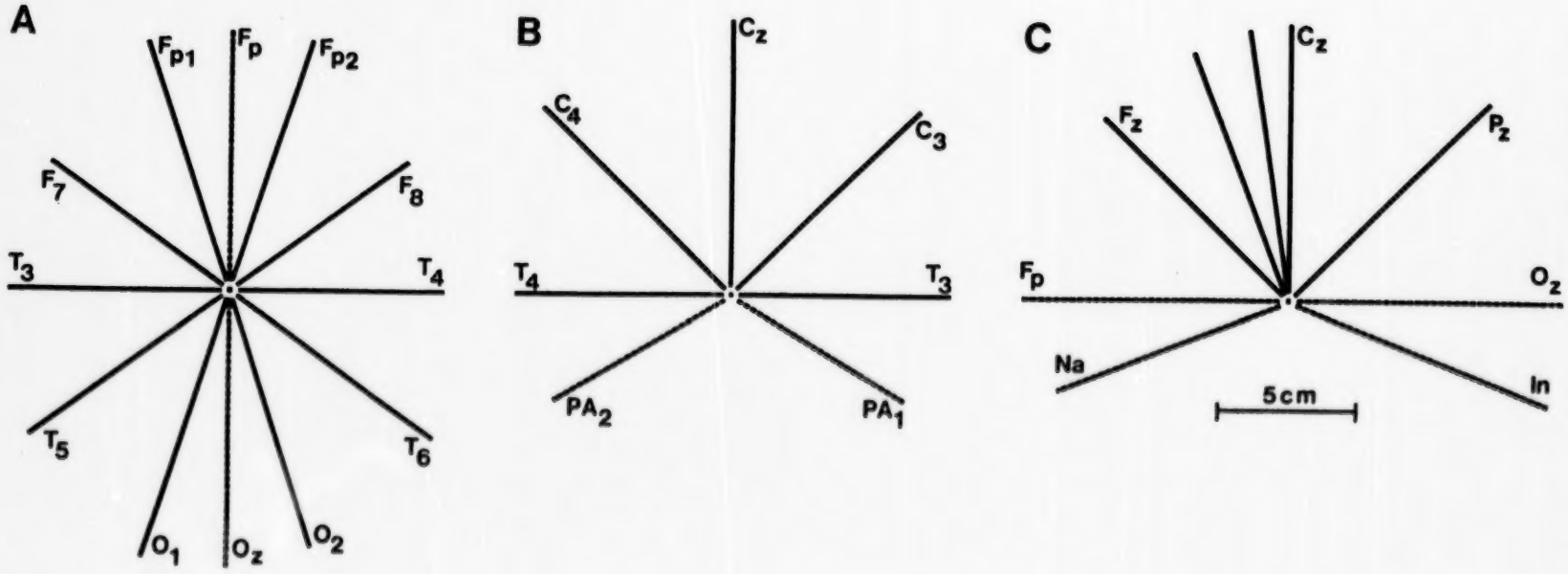
A
F_{p1}
F_p
F_{p2}
F_7
F_8
T_3
T_4
T_5
T_6
O_1
O_z
O_2
B
C_z
C_4
C_3
T_4
T_3
PA_2
PA_1
C
C_z
F_z
P_z
F_p
O_z
Na
In
5cm

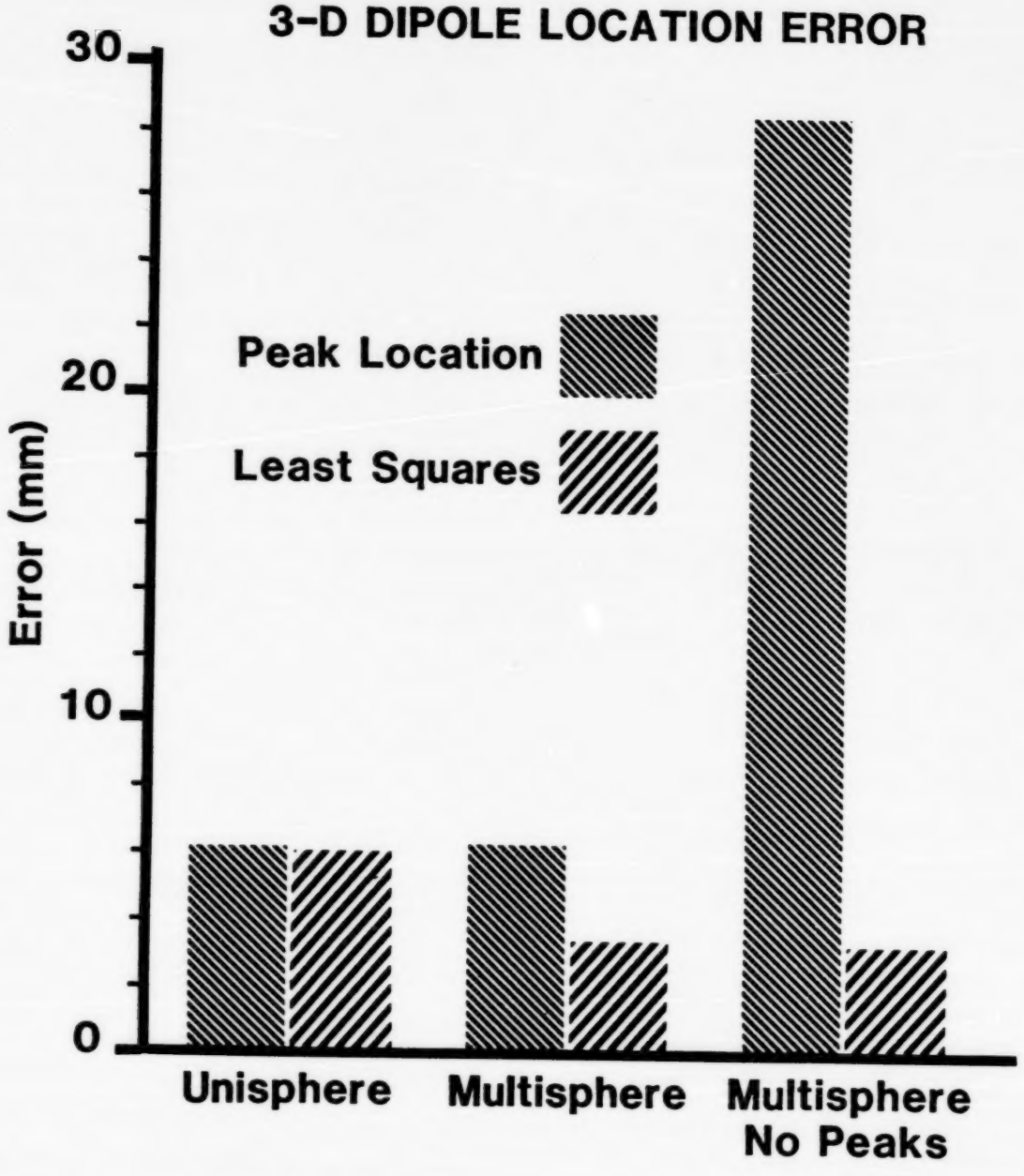
3-D DIPOLE LOCATION ERROR
30
20
10
0
Error (mm)
Peak Location
Least Squares
Unisphere
Multisphere
Multisphere
No Peaks

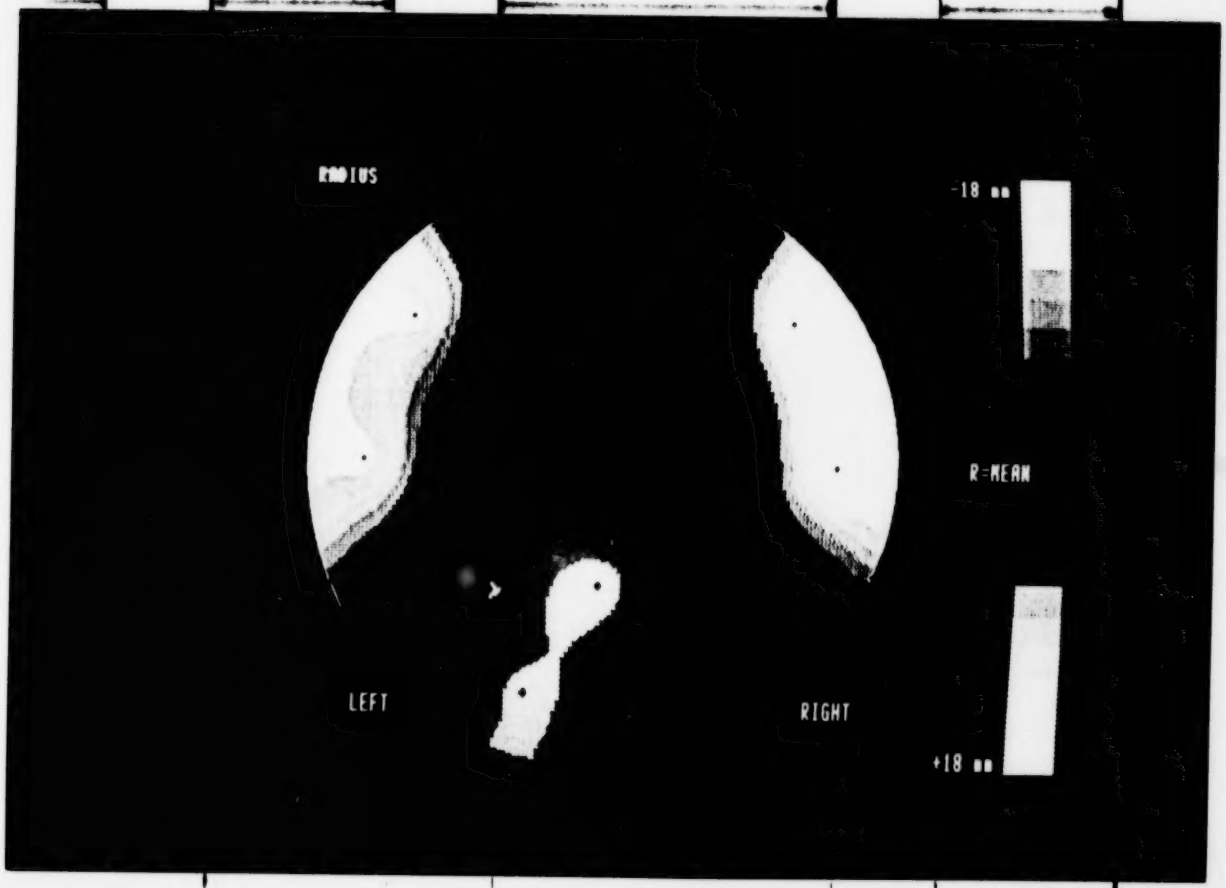
RADIUS
-18 mm
R=MEAN
LEFT
RIGHT
+18 mm

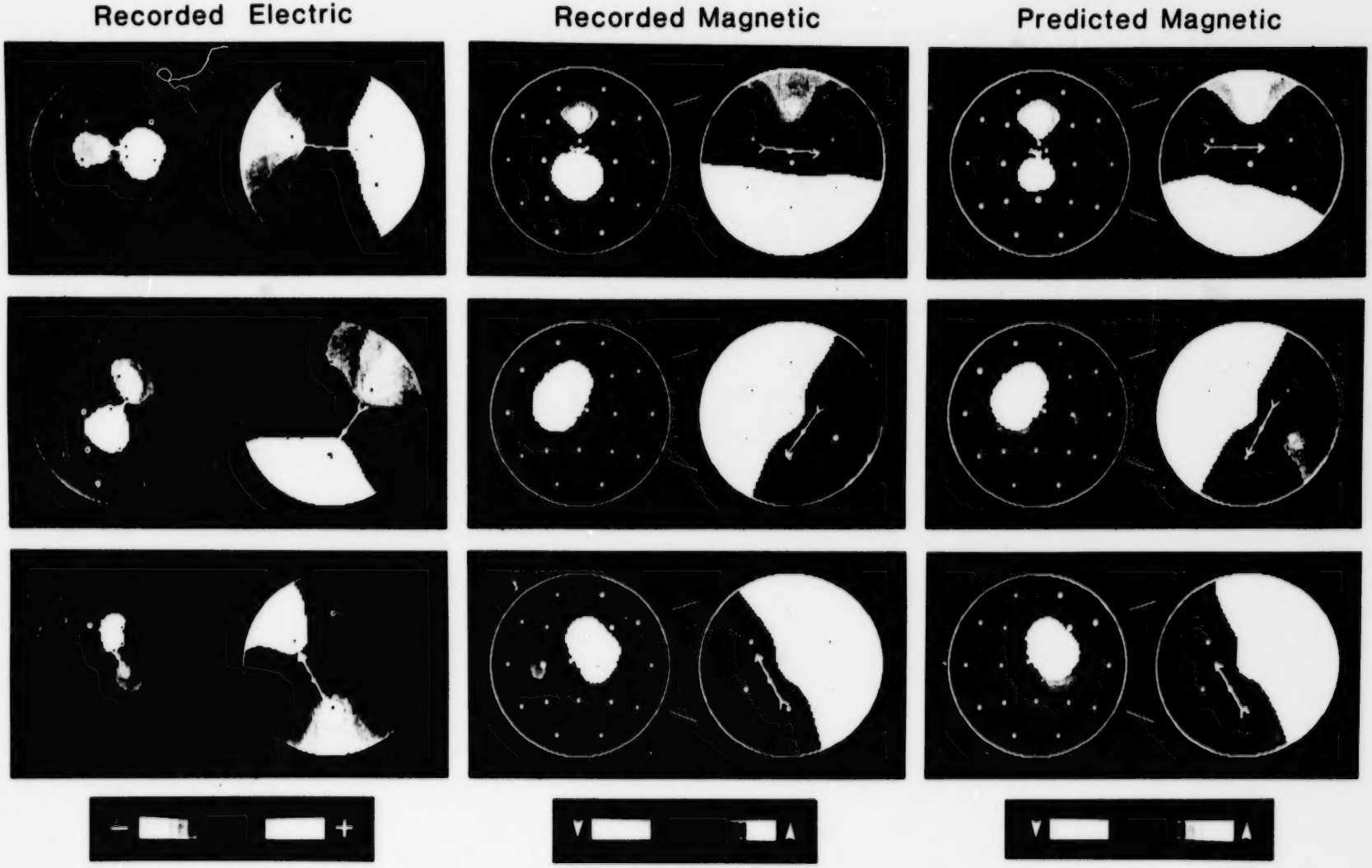
Recorded Electric
Recorded Magnetic
Predicted Magnetic
−
+

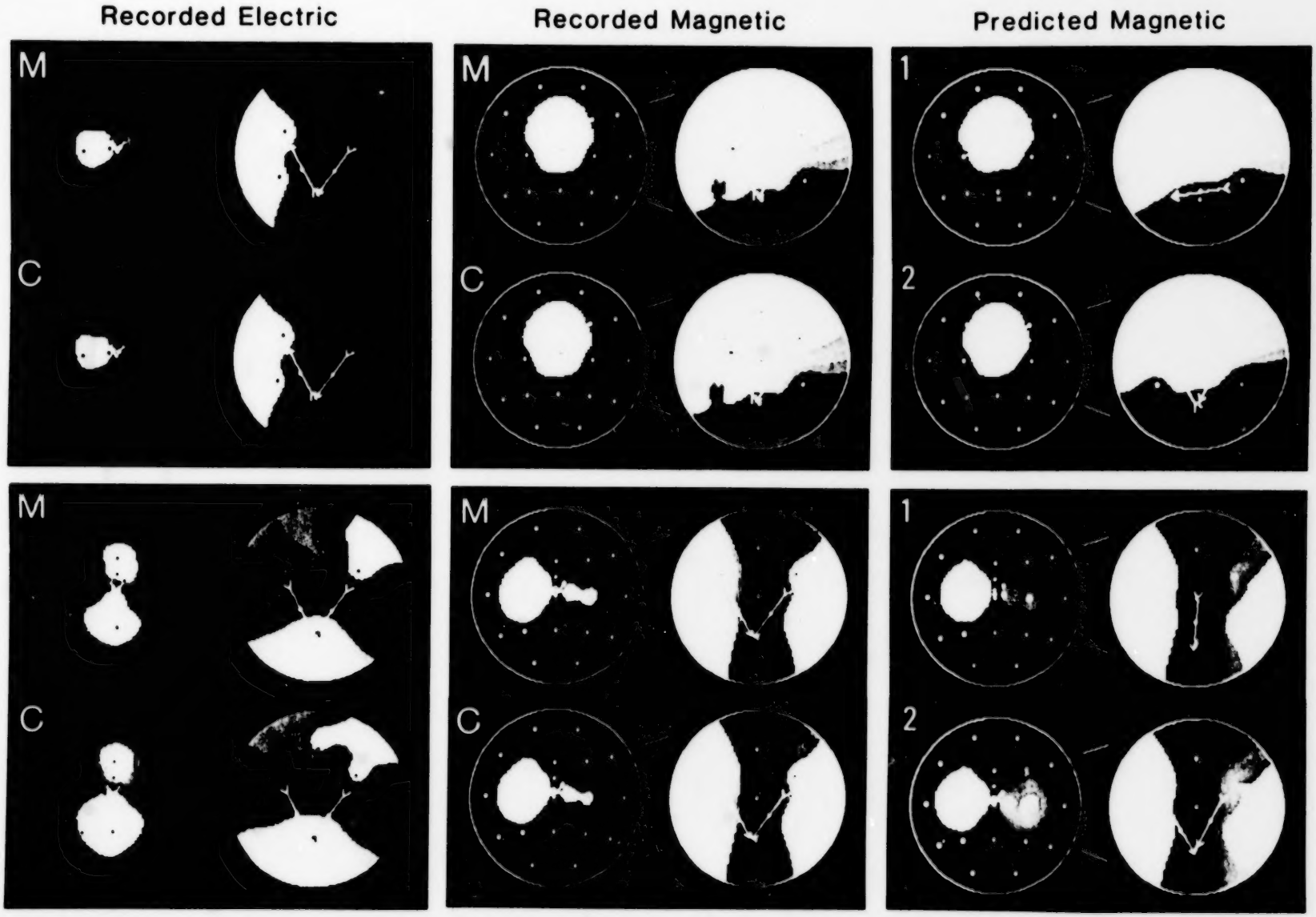
Recorded Electric
Recorded Magnetic
Predicted Magnetic
M
C
M
C
1
2
M
C
M
C
1
2

APPENDIX II

MEG in the Evaluation of Complex Neural Systems

IL NUOVO CIMENTO Vol. 2 D, N. 2 Marzo-Aprile 1983

Slow Magnetic Fields of the Brain Preceding Movements and Speech (*) (**).

H. Weinberg and P. Brickett

Brain Behaviour Laboratory, Simon Fraser University - Vancouver, Canada

L. Deecke and J. Boschert

Department of Neurology, University of Ulm - Ulm, West Germany

(ricevuto il 12 Novembre 1982)

Summary. — Magnetic fields of the brain were recorded preceding self-initiated finger, foot, toe movements, stimulus-triggered finger and toe movements, and speech. Slow magnetic-field shifts were found with morphology similar to coincident electrical potentials, but with very different distributions. Inferences from the data about localization of cerebral generators were discussed.

PACS. 87.40. – Biomagnetism (including magnetc ardiography).
PACS. 85.25. – Superconducting devices; superconducting magnets.

1. – Introduction.

Three different electrical potentials can be recorded preceding voluntary motor acts, the Bereitschaftspotential (BP), premotion positivity (PMP) and the motor potential (MP). The BP starts about 1 s prior to the onset of muscle

(*) Paper presented at the «IV International Workshop on Biomagnetism», held in Rome, September 14-16, 1982.

(**) These studies were supported by grants from the B.C. Research Council and N.S.E.R.C. of Canada.

contraction and reaches an amplitude of $(-5 \div 10)\,\mu V$ with finger movements. Prior to unilateral movement, the precentral BP becomes asymmetrical in the later fore period giving way to a contralateral preponderance of negativity (CPN) about a half-second prior to the movement, sometimes earlier. The BP is followed by a further bilateral smaller potential, the premotion positivity, PMP, with an onset time of about 90 ms and a typical distribution over the parietal cortex and the fronto-central midline. Only the third potential, the negative motor potential, MP, is unilateral with unilateral movement, *i.e.* restricted to the contralateral precentral motor cortex starting about $(50 \div 60)$ ms prior to the onset of the contraction as defined electromyographically [1,2].

The CNV is a negative baseline shift in the electroencephalogram (EEG) occurring between a ready signal and a following stimulus which signals the performance of a behavioural response [3]. When the response is a motor movement, some of the elements of the BP, MP and PMP are superimposed on the later components of the CNV. However, the CNV has a different brain topography than the MP, PMP or BP. The CNV has two components; an early component related to arousal and orientation to the ready signal and a later component related to the information processing related to the imperative stimulus which signals the response [4]. KATILA *et al.* [5] observed magnetic fields preceding foot movements in the period of approximately 250 ms. These were probably the last stages of the BP and included the MP. OKADA *et al.* [6] also showed a shift in the magnetoencephalogram (MEG) preceding finger movements triggered by a stimulus with a random intertrial interval and occurring approximately 100 ms before the movements. DEECKE *et al.* observed MEG shifts 1 s before finger movements [7]. WEINBERG *et al.* reported initial evidence of magnetic fields associated with the CNV [8]. The intent of these studies was to see if MEG components can be recorded which are initiated at the same time as the BP and CNV and to investigate their comparative morphology and topology.

---

[1] L. DEECKE, B. GROZINGER and H. H. KORNHUBER: *Biol. Cybernetics*, **23**, 99 (1976).
[2] L. DEECKE, H. EISINGER and H. H. KORNHUBER: *Prog. Brain Res.*, **54**, 170 (1980).
[3] W. C. MCCALLUM: *Prog. Clin. Neurophysiol.*, **5**, 151 (1979).
[4] H. WEINBERG, H. MICHALEWSKI and R. KOOPMAN: *Neuropsychologia*, **14**, 87 (1976).
[5] R. HARI, A. ASTERVO, T. KATILA, T. POUTANEN, M. SEPPÄNEN, M. TUOMISTO and T. VARPULA: *Proceedings of the XVI Annual Conference of the Finnish Physical Society, August 16, 1982.*
[6] Y. OKADA, S. J. WILLIAMSON and L. KAUFMAN: in *Proceedings of VI Congress on Event-Related Slow Potentials of the Brain, Chicago 1981* (New York, 1983).
[7] L. DEECKE, H. WEINBERG and P. BRICKETT: *Exp. Brain Res.*, **48**, 144 (1982).
[8] H. WEINBERG, P. A. BRICKETT, J. VRBA, A. A. FIFE and M. B. BURBANK: in *VI Congress on Event-Related Slow Potentials of the Brain, Chicago, 1982* (New York, 1983).

2. – Method.

Magnetic fields were measured with an asymmetrical 3rd-order SQUID gradiometer (*). After a detailed analysis of the comparative performance of various spatial gradiometers, a novel 3rd-order spatial gradiometer was constructed. The analysis indicated that, for the practically achievable levels of common-mode rejection (relative to field, first and second spatial gradients), the 3rd-order gradiometer significantly improved noise rejection for noise sources located at intermediate distances of about (2÷30) m from the gradiometer ([10]). The instrument was designed to function in an urban environment and with moderate levels of white noise of about (30÷40) fT r.m.s./Hz$^{\frac{1}{2}}$ and an increased rejection of $1/f$ noise in comparison to that of a 2nd-order gradiometer. The measured level of white noise was about (30÷50) fT r.m.s./Hz$^{\frac{1}{2}}$ and the onset of $1/f$ noise was about 0.5 Hz. The gradiometer sensing coil diameter was 3.81 cm and the baselines were 5.5 cm each. The flux transformer gain was 270 pT/φ_0.

For studies of finger movements the subject sat in a nonmagnetic chair, fixated on a designated point and performed self-paced volitional flexions of the right finger. The surface electromyogram (EMG) served as the trigger and was bipolarly recorded from the right superficial flexor digitorum muscle. EEG recordings were taken from vertex (*Cz*) according to the International EEG 10-20 System. The electro-oculogram (EOG) was recorded from the lower orbital ridge. EEG and EOG were referred to a linked mastoids reference. For all MEG recording positions the sensing coil of the SQUID gradiometer was positioned normal to the head. MEG, EEG, EOG, EMG and head movements were recorded with a Siemens Mingograph (band width (0.03÷15) Hz, EMG (5÷70) Hz) and averaged by using a PDP 12 laboratory computer. A total of 256 points was sampled over an epoch of 3 s, 2.25 s of which were sampled prior to the response. Artifact-contaminated trials were rejected on line by the experimenters. For the BP preceding speech sampling epochs were triggered with EMG electrodes located over upper and lower lips 1.5 cm lateral to the midline. Each word vocalized by the subject began with the letter « *p* ». For CNV recordings the warning stimulus (S1) was a 100 ms, 4000 Hz tone. This was followed after 1 s by a train of 14/s clicks (S2) which were terminated by the subject's response. The EMG defined the response and terminated clicks. The subject was instructed to respond as quickly as possible so that only a few clicks would be heard. The sampling epoch was triggered by the first click

(*) Manufactured by C. T. F. Systems Inc. 15-1750 McLean Avenue, Port Coquitlam, British Columbia, Canada V3C 1M9.

([10]) J. Vrba, A. A. Fife, M. B. Burbank, H. Weinberg and P. Brickett: *Can. J. Phys.*, **60**, 1060 (1982).

in S2, rather than by the response. The experimenter manually initiated each trial at intervals approximately the same as those previously recorded between movements in the BP experiments. The subjects were instructed to take a normal breath after each trial and to inhibit all movements during the S1-S2 interval.

Early experiments determined that head displacements resulting from movement-related vibrations translated through the body frame and from breathing were an important source of artifact. Therefore, the head displacement was measured to 0.1 mm with a mechanograph and recorded simultaneously with MEG and EEG. The convention adopted for these experiments was to show field lines out of the head as upward deflections in the MEG.

3. – Results.

Figure 1 shows the MEG recorded from an anterior/posterior distribution over the hemisphere contralateral to finger movements, from one position over the ipsilateral hemisphere and from two midline positions. The grand average of the EEG recorded from vertex is also shown. The figure demonstrates that a BP beginning as early as 1.2 s before the movement can be seen in the MEG. This early response coincided with the beginning of the BP. The MEG from *C3* is similar to that of *C4*, while the recording from *Pz* shows the same polarity as the MEG recorded from posterior positions of the contralateral hemisphere. From the figure it can also be seen that a reversal in direction of field lines of the BP occurs as the coil is moved from anterior to posterior positions. The reversal occurs over the central sulcus. *C3* MEG and *Cz* EEG are superimposed and show the same time course for the BP. Averages of EOG and SG (head movement strain gauge) show that eye movement and head displacement artifacts did not contribute to the slow shifts identified as the BP. Components occurring after the response are probably artifacts of head movements resulting from finger flexion. However, it is interesting to note that the first component occurring after the response also reverses in polarity as the sensor position is moved across the Rolandic fissure.

Figure 2 (left) shows the MEG recorded before plantar flexion of the right foot. The transverse distribution of the MEG over the central sulcus shows no reversal of field direction. However, there are clear slow magnetic-field shifts recorded over frontal, central and parietal midline regions. Field lines are directed into the head over all these locations. In contrast to the findings for finger and foot movements, a systematic exploration of MEG locations produced no reliable MEG slow shifts preceding toe movements (fig. 2, r.h.s.).

Data from the speech experiment shown in fig. 3 show large magnetic-field shifts preceding vocalization over the left frontal and left central positions,

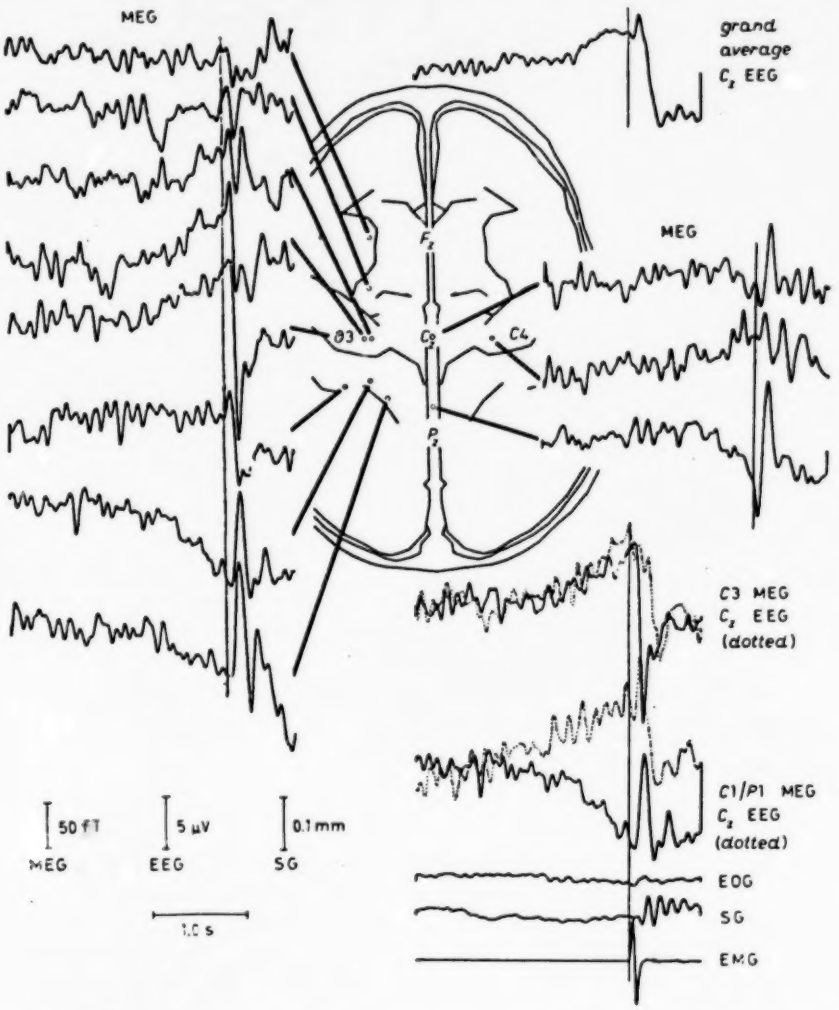

Fig. 1. – BP results for right-finger flexions from subject PB. Vertical line indicates onset of muscle activity. Each average computed from 80 trials.

directed out of the head. Shifts of opposite polarity are slightly left and right with respect to the vertex. Recordings from lateral positions of the right hemisphere show clear differences, the fields being directed into the head over the right hemisphere.

In the CNV paradigm magnetic fields preceding finger and toe movements were recorded, by using those movements as a response to S2. The data are shown in fig. 4. Large MEG shifts are found for the lateral left hemisphere posi-

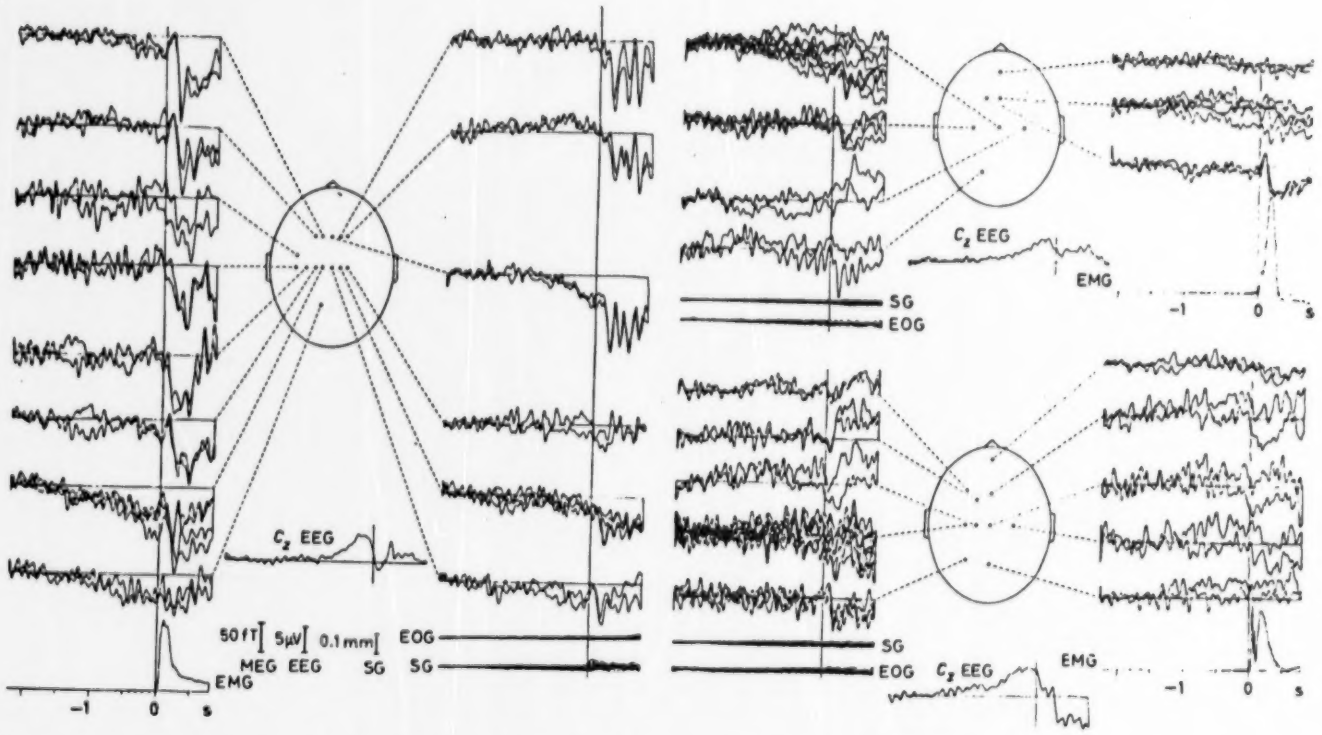

Fig. 2. – l.h.s.: BP results for plantar flexions of the right foot, subject LD; r.h.s.: BP results for right-toe flexions. Data from subjects LD (top) and PB (bottom). Superimposed averages of 40 trials.

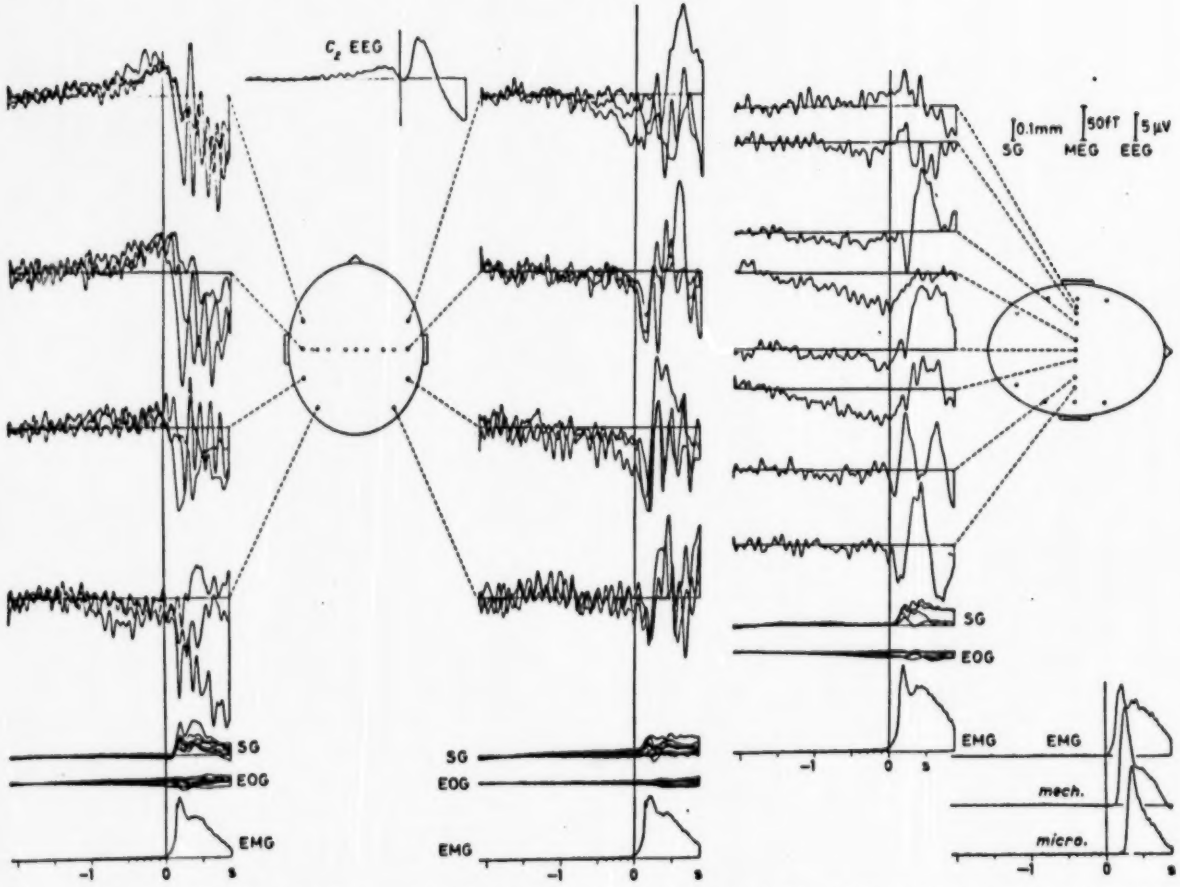

Fig. 3. – Results from vocalization of different words beginning with the letter *p*, subject LD. Superimposed averages of 80 trials.

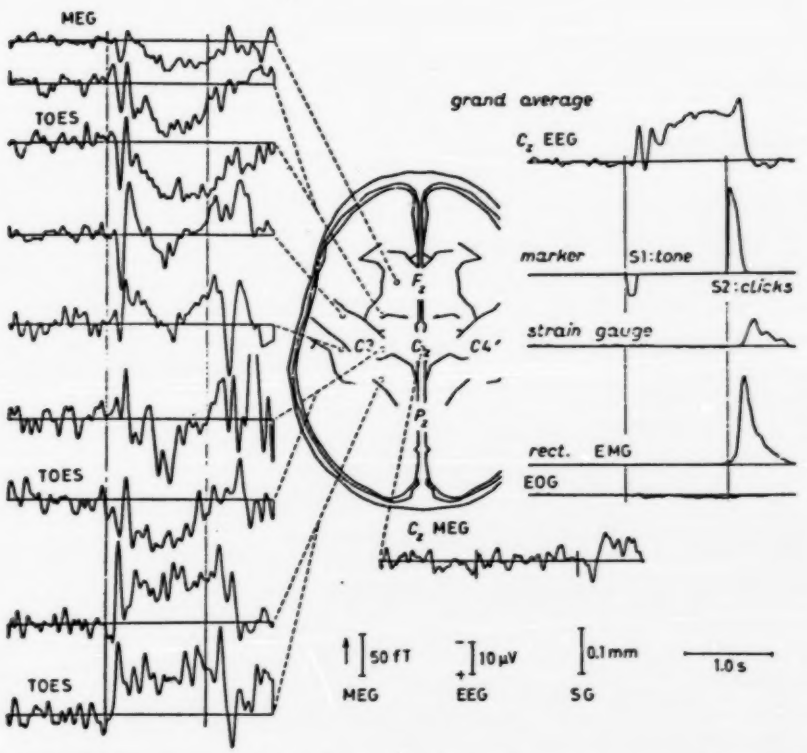

Fig. 4. – CNV results for subject PB. Vertical lines indicate the onset of the warning and imperative stimuli (S1 and S2). The response was either toe or finger movements, as shown.

tions, but no shifts are observed over vertex positions where the EEG has the largest amplitude. A polarity reversal in the slow shift is seen over the left parietal location compared with the left frontal locations. Lateral recordings also show a clear auditory evoked response. Recordings from lateral positions showed a MEG time course which was similar to that of the electrical change (CNV).

4. – Discussion.

The data demonstrate a slow change in the MEG occurring as long as 1.3 s before finger movements which can be identified with the BP. Unlike the electrical BP measure, there is a reversal of the readiness field recorded over positions anterior and posterior to the central sulcus. This suggests that

the source of the readiness potential is indeed in the precentral gyrus. If the assumption is made that these fields result from current dipoles, the direction of the fields measured indicates that the dipole could be oriented longitudinally along the precentral gyrus approximately in the location of the pyramidal cells projecting to muscles which control finger movements. The absence of a MEG shift preceding toe movements may be attributable to the fact that the pyramidal efferents controlling toe movements lie deep in the precentral gyrus along the mesial surface; perhaps too deep and too small for the sensitivity of our instrument. However, when toe movements are used as a response in a C[illegible]aradigm, there are large and reliable shifts of the MEG. The morphology of the electrical response at *Cz* is shown in fig. 4. The morphology and the polarity of the CNV, when measured as an electrical-potential change, are similar when recorded from the positions over which the MEG was recorded. The MEG morphology when measured posterior to *C3* is very similar to the electrically recorded CNV. However, as the recording positions for MEG move anteriorly, a polarity reversal in the early period of the shift occurs, whereas the polarity of the later shift does not, *i.e.* there appears to be a biphasic response. This occurs before both toe and finger movements. These data suggest that there are at least two generators influencing the CNV in anterior positions, one responsible for the early shift and one for the later shift. This is consistent with other EEG evidence which suggests that early components of the CNV are related to orientation and arousal, and the later components to response preparation. The fact that a BP was not found for toe movements even though a CNV paradigm which used toe movements as the response resulted in a slow MEG shift preceding the response adds weight to the inference that the constellation of CNV and BP generators is not identical. Our data relative to foot movements show a reversal between central and frontal regions, but the data are not as clear as those seen with finger movements, although there is a clear shift of field lines into the head preceding the movement. Both toes and feet have relatively small representations on the precentral and postcentral gyrus and this may contribute to the reduced effectiveness of localization with our system.

The data showing slow magnetic-field changes preceding speech are particularly interesting. In general, it is difficult to see clear lateralization of the EEG preceding speech. The coil positions from which the reversals were recorded were anterior and considerably posterior to Broca's area. Broca's area is known to be the motor site associated with speech in most people who are strongly right handed. Our intention is to systematically explore this result in right- and left-handed persons to determine if the MEG can identify the speech hemisphere. If the MEG can be used to identify the speech hemisphere, without the use of a Wada test (injection of Sodium Amytal into internal carotid arteries), it could be a useful clinical technique.

● RIASSUNTO (*)

Sono stati registrati i campi magnetici del cervello che precedono i movimenti autonomi delle dita della mano, del piede e delle dita del piede stesso, i movimenti delle dita della mano e del piede causati da uno stimolo e la parola. Sono stati trovati lenti spostamenti dei campi magnetici con morfologia simile ai coincidenti potenziali elettrici, ma con distribuzioni molto diverse. Si discutono le deduzioni ottenute dai dati sulla localizzazione dei generatori cerebrali.

(*) *Traduzione a cura della Redazione.*